

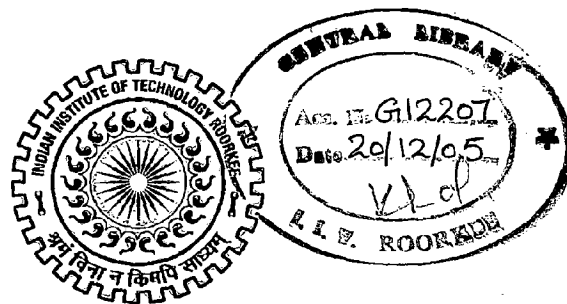
**THE INFLUENCE OF SEISMIC LOAD IN SLAB
AND EMBANKMENT OF CONCRETE
FACE ROCKFILL DAM**

A DISSERTATION

*Submitted in partial fulfillment of the
requirements for the award of the degree*
of
MASTER OF TECHNOLOGY
in
WATER RESOURCES DEVELOPMENT

By

FERDY FIRMANSYAH



**DEPARTMENT OF WATER RESOURCES DEVELOPMENT & MANAGEMENT
INDIAN INSTITUTE OF TECHNOLOGY ROORKEE
ROORKEE - 247 667 (INDIA)
JUNE, 2005**

CANDIDATE'S DECLARATION

I hereby certify that the work which is being presented in the dissertation entitled, **“THE INFLUENCE OF SEISMIC LOAD IN SLAB AND EMBANKMENT OF CONCRETE FACE ROCKFILL DAM”** in partial fulfillment of the requirement for the award of Degree of Master of Technology in WRD submitted in The Department of Water Resources Development & Management, Indian Institute of Technology Roorkee, India is an authentic record of my own work carried out during the period July 27th, 2004 till the date of submission under supervision of **Dr. Ram Pal Singh**, Professor, Dept. of WRD&M, IIT Roorkee and **Dr. B.N. Asthana**, Visiting Professor, Dept. of WRD&M, IIT Roorkee, India.

The matter embodied in this dissertation has not been submitted by me for the award of any other degree.

Dated : June 28th, 2005



(FERDY FIRMANSYAH)

This is to certify that the above statement made by the candidate is correct to the best of our knowledge.



(DR. B.N. ASTHANA)

VISITING PROFESSOR
Dept. of WRD&M, IIT ROORKEE
ROORKEE – INDIA, 247 667



(DR. RAM PAL SINGH)

PROFESSOR
Dept. of WRD&M, IIT ROORKEE
ROORKEE – INDIA, 247 667

ACKNOWLEDGEMENT

I would like to thank with my great honor to **Dr. Ram Pal Singh**, Professor of Dept. of WRD&M, IIT Roorkee and **Dr. B.N. Asthana**, Visiting Professor of Dept. of WRD&M, IIT Roorkee for their inspiration, guidance and correction for me during preparation and completion of this dissertation which was very valuable in enhancing my knowledge.

I express my sincere gratitude to **Dr. S.K. Tripathi**, Professor and Head of Dept. of WRD&M IIT Roorkee for extending various facilities during the course of this work, also thanks to all of Faculty Members of Dept. of WRD&M for providing sufficient knowledge for completion of this document. To all staff of Dept. of WRD&M who in one way or another extended their support, cooperation and provided facilities during course of preparation of this study. To all my fellows in Batch 48th WRD and 24th IWM for their cooperation, effort and sharing of valuable knowledge.

Special thanks to The Ministry of Settlement and Regional Infrastructure – Indonesia Government, my organization **PT. Indra Karya (Persero) Consulting Engineers** and the sponsor for giving the opportunity to study for Master of Technology (WRD) in Dept. of WRD&M – IIT Roorkee.

Ultimately, a special and sincerest thanks to Allah SWT for the blessing and, for my wife, my parents and my late father in law for their kindly supporting, encouragement and prayers throughout the duration of my study at Dept. of WRD&M.

Roorkee, June 28th, 2005


(FERDY FIRMANSYAH)

CONTENTS

	Page No.
CANDIDATE'S DECLARATION	i
ACKNOWLEDGMENT	ii
CONTENTS	iii
LIST OF TABLES	v
LIST OF FIGURES	vi
SYNOPSIS	vii
CHAPTER 1 : INTRODUCTION	
1.1. GENERAL	I - 1
1.2. PURPOSE	I - 4
1.3. SCOPE AND METHODOLOGY OF STUDY	I - 4
1.4. THE ORGANIZATION OF DISSERTATION	I - 5
CHAPTER 2 : DESIGN OF CONCRETE FACE ROCKFILL DAM	
2.1. INTRODUCTION	II - 1
2.2. DESIGN PRINCIPLES	II - 4
2.3. PLINTH (UPSTREAM TOE SLAB)	II - 7
2.3.1. General Requirement	II - 7
2.3.2. Geometry	II - 8
2.3.3. Foundations	II - 8
2.3.4. Stability	II - 11
2.4. EMBANKMENT	II - 12
2.4.1. Foundation Preparation	II - 12
2.4.2. Embankment Design	II - 13
2.4.3. Rockfill Properties	II - 14
2.4.4. Zoning	II - 15
2.4.5. Application of Water During Compaction	II - 16
2.4.6. Preparation of The Upstream Face	II - 16
2.5. CONCRETE FACE – DESIGN REQUIREMENTS	II - 17
2.5.1. Basic Design	II - 17
2.5.2. Cethana Face Details	II - 18

2.5.3. Evolution in Face Design	II - 22
2.6. PRELIMINARY DESIGN OF CFRD	II - 26

CHAPTER 3 : FINITE ELEMENT ANALYSIS OF CONCRETE FACE ROCKFILL DAMS

3.1. INTRODUCTION	III - 1
3.2. FINITE ELEMENT FORMULATION	III - 3
3.3. BASIC STEPS ON FINITE ELEMENT METHOD FOR LINEAR PROBLEMS	III - 4
2.3.1. Displacement Method	III - 4
2.3.2. Displacement Function	III - 5
3.4. STRESS - STRAIN RELATIONSHIPS	III - 5
3.5. EQUILIBRIUM EQUATIONS	III - 7
3.6. TYPICAL STRESS PATH	III - 7
3.7. CONSTITUTIVE LAWS	III - 9
3.7.1. Linear Elastic Analysis	III - 10
3.7.2. Power Law' Model	III - 11
3.7.3. Nonlinear Stress-Strain Behavior (Hyperbolic Model)	III - 12
3.7.4. K - G Model	III - 15
3.7.5. Elasto-plastic Model	III - 17
3.8. LAYERED ANALYSIS STIFFENESS OF THE SIMULATED LAYER AND COMPACTION STRESS	III - 18

CHAPTER 4 : ABOUT THE PROGRAMMES

4.1. PENTAGON3D	IV - 1
4.2. PENTMESH	IV - 2
4.2.1. Slice on PENTMESH	IV - 5
4.2.2. Creation of 3D Element that Use 2D Entity	IV - 5
4.2.3. Degenerate Elements	IV - 6
4.3. PENPRE	IV - 6
4.4. PENPOST	IV - 7
4.5. STEPS IN MAKING THE MODEL	IV - 8

CHAPTER 5 : RESULTS OF ANALYSIS

5.1. GENERAL	V - 1
5.2. DISCRETIZATION OF DAM SECTION IN MESH	V - 2
5.3. SIGN CONVENTION	V - 3
5.4. MATERIAL PROPERTIES	V - 4
5.5. ANALYSES PERFORMED	V - 5
5.6. GROUND MOTION FOR DYNAMIC ANALYSIS	V - 6
5.7. RESULTS OF ANALYSIS	V - 8
5.6.1. Case I: CFRD under Static Load Condition	V - 8
5.6.2. Case II: CFRD under Dynamic Load Condition	V - 10

CHAPTER 6 : DISCUSSION OF RESULTS

6.1. DISCUSSION OF RESULTS OF CASE I STUDY	VI - 1
6.1.1. Upstream Portion	VI - 1
6.1.1.1. Horizontal Displacement - U	VI - 1
6.1.1.2. Vertical Displacement - V	VI - 2
6.1.1.3. Horizontal Normal Stresses - σ_{xx}	VI - 2
6.1.1.4. Vertical Normal Stresses - σ_{yy}	VI - 3
6.1.2. Central Portion	VI - 3
6.1.2.1. Horizontal Displacement - U	VI - 3
6.1.2.2. Vertical Displacement - V	VI - 4
6.1.2.3. Horizontal Normal Stresses - σ_{xx}	VI - 4
6.1.2.4. Vertical Normal Stresses - σ_{yy}	VI - 5
6.1.3. Central Portion	VI - 5
6.1.3.1. Horizontal Displacement - U	VI - 5
6.1.3.2. Vertical Displacement - V	VI - 6
6.1.3.3. Horizontal Normal Stresses - σ_{xx}	VI - 6
6.1.3.4. Vertical Normal Stresses - σ_{yy}	VI - 7
6.2. DISCUSSION OF RESULTS OF CASE II STUDY	VI - 8
6.2.1. CFRD 50 m High	VI - 8
6.2.1.1. Slope 1V:1.30H at 0.1g to 0.5g Peak Acceleration	VI - 8
6.2.1.2. Slope 1V:1.50H at 0.1g to 0.5g Peak Acceleration	VI - 9
6.2.2. CFRD 100 m High	VI - 10

6.2.2.1. Slope 1V:1.30H at 0.1g to 0.5g Peak Acceleration	VI - 10
6.2.2.2. Slope 1V:1.50H at 0.1g to 0.5g Peak Acceleration	VI - 11
6.3. RATIO OF DISPLACEMENT UNDER STATIC LOAD	VI - 12
6.4. RATIO OF DISPLACEMENT UNDER DYNAMIC LOAD	VI - 13
6.4.1. CFRD with Slope 1V:1.30H	VI - 13
6.4.1.1. U_Displacements under Acceleration of 0.1g.....	VI - 13
6.4.1.2. V_Displacements under Acceleration of 0.1g.....	VI - 15
6.4.2. CFRD with Flatter Slope	VI - 16
6.5. ANALYSIS FOR CFRD WITH SINGLE STAGE OF RESERVOIR FILLING	VI - 17
6.5.1. CFRD 50 m	VI - 17
6.5.2. CFRD 100 m	VI - 18

CHAPTER 7 : CONCLUSIONS

7.1. CONCLUSION OF CASE I STUDY	VII - 1
7.2. CONCLUSION OF CASE II STUDY.....	VII - 2
7.3. GENERAL OBSERVATIONS	VII - 2
7.4. SUGGESTIONS FOR FURTHER STUDY	VII - 3

REFERENCES

BIBLIOGRAPHY

APPENDICES

LIST OF TABLES

	Page No.
Table 2.1 Zone Designation, Layer Thickness and Maximum Particle Size	II - 15
Table 2.2 Dam Embankment Performance Data	II - 22
Table 2.3 Criteria Adopted for Concrete Face Membrane Thickness ...	II - 23
Table 2.4 Face Concrete Data.....	II - 25
Table 5.1 Model Parameters of Duncan Model	V - 5
Table 5.2 Number of Stages for Each Concrete Face Rockfill Dam	V - 6
Table 5.3 Result of Analysis under Static Load	V - 9
Table 5.4 Result of Analysis under Peak acceleration of 0.1g	V - 10
Table 5.5 Result of Analysis under Peak acceleration of 0.2g	V - 11
Table 5.6 Result of Analysis under Peak acceleration of 0.3g	V - 12
Table 5.7 Result of Analysis under Peak acceleration of 0.4g	V - 13
Table 5.8 Result of Analysis under Peak acceleration of 0.5g	V - 14
Table 6.1 U_Displacement of CFRD 50 m in Static and Dynamic Condition	VI - 14
Table 6.2 U_Displacement of CFRD 100 m in Static and Dynamic Condition	VI - 14
Table 6.3 U_Displacement Ratio of CFRD 50 m to 100 m	VI - 14
Table 6.4 V_Displacement of CFRD 50 m in Static and Dynamic Condition	VI - 15
Table 6.5 V_Displacement of CFRD 100 m in Static and Dynamic Condition	VI - 15
Table 6.6 V_Displacement Ratio of CFRD 50 m to 100 m	VI - 15
Table 6.7 Ratio of U & V Displacements of CFRD 50 m	VI - 16
Table 6.8 Ratio of U & V Displacements of CFRD 100 m	VI - 16
Table 6.9 The generalized Increment of U & V Displacements for CFRD 50 m under Variation of Seismic Load	VI - 16

Table 6.10 The generalized Increment of U & V Displacements for
CFRD 100 m under Variation of Seismic Load VI - 17

LIST OF FIGURES

	Page No.
Figure 1.1 Details of typical concrete facing CFR Dams	I - 2
Figure 2.1 Feature of early concrete face rockfill dam design (ICOLD 1989a).....	II - 3
Figure 2.2 Current practice for zoning of CFRD constructed of sound Rockfill on a strong rockfill foundation (adapted from ICOLD 1989a)	II - 6
Figure 2.3 Toe slab design for a) Mangrove Creek Dam, b) Boondooma Dam (MacKenzie & McDonald 1985, Roger 1985)	II - 9
Figure 2.4 Toe slab design for c) Cethana Dam, d) Lower Pieman Dam (Fitzpatrick et la, 1985)	II - 10
Figure 2.5 Embankment zones in recent dam	II - 13
Figure 2.6 Crest wall arrangement	II - 14
Figure 2.7 Cethana dam face – Joint layout and details	II - 20
Figure 2.8 Lower Pieman Dam – Joint Layout and Details	II - 24
Figure 2.9 Nomenclature of CFRD	II - 29
Figure 3.1 Stress path for three types of rockfill dam	III - 8
Figure 3.2 Stress path for three points along a line normal to the concrete face of a hypothetical rockfill dam	III - 9
Figure 3.3 Finite element modeling of fill construction	III - 18
Figure 3.4 Effect of number of layers and compaction stress on settlement of a soil column	III - 19
Figure 5.1 Typical of concrete face Rockfill dam from downstream view	V - 1
Figure 5.2 The idealized meshing of CFRD model	V - 3
Figure 5.3 The concerned portion in analysis and sign convention	V - 4
Figure 5.4 Accelerograms recorded in Ofunato – Korea	V - 7
Figure 5.5 Result of seismic analysis using PENTAGON-3D	V - 8

Figure 6.1	Horizontal and vertical displacements of CFRD 50 m at different slopes	VI - 20
Figure 6.2	Horizontal and vertical displacements of CFRD 100 m at different slopes	VI - 21
Figure 6.3	Comparison between multi stages and single reservoir Filling stage of CFRD 50 m slope 1V:1.50H	VI - 22
Figure 6.4	Comparison between multi stages and single reservoir Filling stage of CFRD 100 m slope 1V:1.50H	VI - 23

SYNOPSIS

The objective of this study is to carry out the following:

1. To analyze the behavior of slab and embankment of concrete face rockfill dam under static load condition considering variation of slopes and dam heights.
2. To analyze the behavior of slab and embankment of concrete face rockfill dam under dynamic load condition using variation of peak accelerations at base of CFRD.
3. Conclusions are drawn concerning desirable slopes for concrete face rockfill dams under static load condition and under variation of seismic load.

Concrete face rockfill dam of height 50 m and 100 m, located in a narrow valley with slope of wall at 1V:1H, have been used for the analyses purpose. The typical section is shown in Figure 5.1. For both the height, the bottom width is fixed at 20 m. The dam has a water tight impervious layer placed on the upstream slope with a "cushion" layer of finer processed rockfill between the concrete face plate and the rockfill to provide uniform support for the face plate. Poorer quality rockfill has been used as secondary rockfill with zones of free draining rock incorporated to allow discharge of leakage. Should this occurs, as the rockfill is free draining, pore pressure do not develop in the dam and the upstream and the downstream slopes are commonly at the angle of repose of the rockfill. hence the slopes or the angle of repose of upstream and downstream dam faces are varied from 1V:1.30H; 1V:1.35H; 1V:1.40H; 1V:1.45H and 1V:1.50H to study the effect of slope on the behavior of dam under static and dynamic load condition. Free board is kept as 5 m. The soil foundation for dam is included in analysis up to depth of 15 m. The dams usually are situated in irregular shapes of valley but to reduce the size of the problem, the valley profile has been assumed symmetrical about the centre line of the valley and, therefore, only a half of the dam has been considered in the analyses.

The major findings of the present study are as follows:

○ **CFRD under static load condition**

The horizontal displacement of upstream, central and downstream portion toward the downstream direction from the beginning of construction to the last stage of reservoir filling, dam with slope 1V:1.50H is found minimum in both heights of 50 m and 100 m.

The vertical displacement at dam 50 m and 100 m high do not depict similar behavior of upstream, central and downstream portion. Maximum value has been found at different locations. For CFRD 50 m, slope 1V:1.50H has resulted in minimum displacement and for CFRD 100 m, slope 1V:1.30H has resulted in minimum displacement. In case of 100 m high dam, the results show settlement in upstream portion and heaving of crest and downstream portion. This indicates the necessity of flattening downstream slope.

The horizontal normal stress of upstream portion towards the downstream direction while stresses in central and downstream portion counter act it. Generally the slope is found to have insignificant in effect on these stresses.

The vertical normal stress of upstream, central and downstream portion in downward direction from the beginning of construction to the last stage of reservoir filling. The upstream portion has the maximum stress with all these slopes. This stress in central and downstream portion is found insignificant as compared to upstream portion. These stresses are found to increase in the ratio of the height of dam. Slope is found to have insignificant effect on the value of the stresses.

○ **CFRD under dynamic load condition**

The results have shown that in both heights of dam, the application of peak ground acceleration up to 0.5g has resulted into a maximum of 15% in the displacements and stresses over the static load values. This confirms the findings of other researchers that concrete face rockfill dam can safely stand by earthquakes.

CHAPTER I

INTRODUCTION

1.1. GENERAL

According to ASCE Rockfill Dam Symposium, 1960, a rockfill dam can be definition as "a dam that relies on rock, either dumped in lifts or compacted in layers, as a major structural element". Therefore, definition of Galloway (1939) which was used in an ASCE Symposium in 1939, a rockfill dam was defined as being composed of rockfill dumped loosely in position with an impervious face next to water, now become obsolete definition (1).

Rockfill dams are essentially of two types (1) :

- a) Earth-core type in which water tightness is obtained by a core of impervious material within the dam section. This can be sloping or central with rockfills in the shell on both sides. Problem associated with rockfill dams arise from excessive settlements of the rockfills under increasing weight of the fill, the process being rapid during construction and the first filling. These settlements may damage the impervious core due to excessive deformation.
- b) Face or impervious membrane type with an impervious membrane for water tightness placed on the upstream slope. Among the impervious face type of rockfill dams, the concrete face type is the most commonly used. Asphalt concrete is the next most frequently used impervious face, the use of granite, steel, timber and masonry being infrequent.

Concrete Face Rockfill Dam (CFRD) is one such type of the Impervious Face Membrane Rockfill Dam which in recent years became increasingly

popular with construction engineers in view of its many inherent advantages over "The Central Earth Core Type of Rockfill Dam".

A Concrete Face Rockfill Dam (CFRD) is constructed ideally of free draining rockfill, with a 'cushion' layer of finer processed rockfill or mortar between the concrete face plate and the rockfill to provide uniform support for the face plate.

The face is formed on the rockfill by slip forming, is reinforced and provided with construction joints and water stops to control cracking under the deformations induced by the water load. Poorer quality rockfill has been used, with zones of free draining rock incorporated to allow discharge of leakage. As the rockfill is free draining, pore pressure do not develop in the dam and the upstream and the downstream slopes are commonly at the angle of repose of the rockfill.

Rockfill (CFR) dams up to 160 m high are in service and larger dams are under construction. For dams less than about 20 m high, the cost of the plinth and setting up for faceplate construction usually makes concrete face rockfill uneconomical. CFR dams are particularly suited to construction in high rainfall areas, where placement of earthfill is impracticable and to sites with good rock foundations.

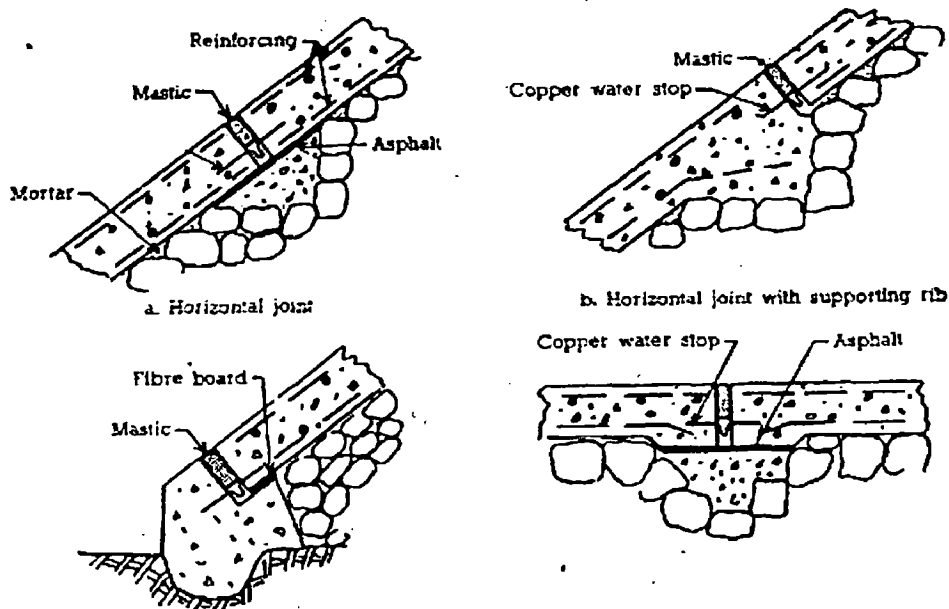


Figure 1.1 : Details of typical concrete facing CFR dams

The dam with an upstream impervious slab as CFRD has an advantage on a greater margin of safety against shear failure than any other type of earth or rockfill dam. Since cement has a very long life, it is an obvious watertight membrane on rockfill dams. Details of typical facing are shown in the Figure 1.1. The facing can be tied to the dam in two ways, either poured directly onto the rubble transition zone. A mortar bed is initially placed which penetrates into the rubble a few centimeters. This is immediately covered with the concrete to form a monolithic mass which extends into the rubble and is thus bonded to the dam. Or, ribs are placed in the bottom of the slab by forcing grooves in the facing. The ribbed support, however, is unnecessary if the bonding with the backing is effective.

Two types of facing have been used. One is a thin *monolithic slab* of concrete with no joints. It is sufficiently flexible to conform to movements in the backing without failure and the tensile forces are distributed by the reinforcements so that numerous small cracks develop rather than any major failures. The second type, used in most concrete faced dams, has a facing which consists of *monolithic slabs*, 10 to 30 sqm each. The concrete thickness is largely a matter of experience. Only nominal reinforcement is required, about 0.5% of concrete area in each direction. Water tightness is ensured by water stops.

Compared by earth core rockfill dam, for a given safety factor the embankment slopes of CFRD can be made steeper and the embankment volume smaller than for a dam with a core of rolled impervious earth or for a dam with vertical impervious membrane of manufactured material.

A significant question which has always raised concern about concrete face rockfill dams is their potential performance under earthquake shaking. Many engineers argue that the CFRD has the highest inherent conservatism of any of the commonly used earth or rockfill types against potential damage due to earthquake shaking. Therefore this study is conducted to analyze behavior of a CFRD during construction, reservoir filling and effect of earthquake shaking.

1.2. PURPOSE

The objective of this study is to carry out the following:

1. To analyze the behavior of slab and embankment of a concrete face rockfill dam under static load condition considering variation of slopes and dam heights.
2. To analyze the behavior of slab and embankment of concrete face rockfill dam under dynamic load condition using variation of peak accelerations at base of CFRD.
3. Conclusions are drawn concerning desirable slopes for concrete face rockfill dams under static load condition and under variation of seismic load.

1.3. SCOPE AND METHODOLOGY OF STUDY

First of all, this study will explain the design criteria of CFRD that has been used by construction engineers to accommodate the stability of rockfill embankment and also the ability of the concrete slab to withstand deformations to which they are subjected, although there is no rational criterion yet available for the design of such dams.

The method of analysis for design of a concrete face rockfill dam is described briefly. The analysis involves nonlinear material behavior for the rockfill and for bedding and transition layer, sequential construction and incremental reservoir loading to simulate the construction process and filling of reservoir. A study that has been done is to analyze the behavior of slab and embankment in concrete face rockfill dam during the period of construction and the filling of reservoir, then to determine the desirable slopes of dam under different levels of seismic load using three dimensional incremental non linear analysis. This study may not consider the time dependent creep.

Study has been limited to 50 m and 100 m heights of the dam. The dams are considered to be located in a narrow valley and fill material properties are modified from analysis of Yutiao Concrete Face Rockfill Dam, China (5).

1.4. THE ORGANIZATION OF DISERTATION

The study is presented in seven chapters. The contents of each chapter are briefly indicated below.

- Chapter 1 : Introduction of the problem scope and objective of study are described in this chapter.
- Chapter 2 : Design procedure of Concrete Face Rockfill Dam is briefly described in this chapter
- Chapter 3 : The finite element method and the method incorporating non-linearity of stress-strain relationship are described in this chapter
- Chapter 4 : A brief description of the PENTAGON3D program software of finite element for performing 3-D non linear sequential analysis of the dam is explained in this chapter
- Chapter 5 : The results of analysis are presented in this chapter
- Chapter 6 : The discussion of results are given
- Chapter 7 : Conclusions and suggestion for further study are given

CHAPTER 2

DESIGN OF CONCRETE FACE ROCKFILL DAM

2.1. INTRODUCTION

Prior to 1925, only eight rockfill dams were higher than 30 m, of which the Morena, Strawberry, and Swift Dams were the highest, about 45 m. All the eight dams were in the USA, mostly in California. In 1925, the 84 m high Dix river concrete face rockfill dam was constructed in Kentucky. Through the thirties a number of concrete face rockfill dams ranging from 60 to 90 m height were constructed, the highest being the 100 m high Salt Springs Dam.

The 1940s saw the continued use of concrete face dams and the beginning of high earth-core rockfill dams, namely : the 116 m high thick-central-core San Gabriel No. 1 dam in 1938, the 78 m high thin-sloping-core Nantahala dam in 1942, the 97 m high thick-central-core Watuga dam in 1948, and the 122 m high thin-central-core Mud Mountain dam in 1948.

Since 1950, the development of both the earth-core and concrete-face type of rockfill dams has been exceptionally rapid. Since 1950, concrete face dams have generally been of 30 to 75 m height, the highest being Paradela in Portugal at 110 m, Wishon and Courtright in California at 90 m and 97 m respectively and New Exchequer in California at 150 m. The New Exchequer dam uses a 95 m high existing gravity dam. Another recently constructed dam with concrete facing is the 110 m high Cethana dam in Australia (1).

The design of concrete face rockfill dam was (and is) mainly empirical, based on experience and judgement. The typical features of designs of CFRD until the late 1950's are shown in Figure 2.1.

The construction of concrete face rockfill dam, with several characteristics of upstream slab, has the advantage as follows :

- a) With a suitable drain behind it, the slab prevents seepage from entering the embankment and so eliminates probability of the development of pore pressures. Consequently, the embankment strength is higher and the margin of safety against shear failure is increased for both the upstream and downstream slopes (2);
- b) This dam has the greatest possible mass of embankment acting to resist the pressure of the water in the reservoir (2);
- c) Because the water pressure on the upstream slope, the total force exerted by the reservoir on the dam is directed downwards into the foundation with as great an inclination as possible. This is the optimum condition from the standpoint of stability of the foundation (2);
- d) Multi stage construction is feasible (3);
- e) Auxiliary work (tunnels, penstocks, spillways) are shorter as a result of steeper embankment slopes (3);
- f) The simplicity and speed of fill placement can reduce diversion requirements (3);
- g) Diversion capacity can be reduced by allowing overtopping during construction with downstream face protection, embankment stability analyses are not normally required (3);
- h) The embankment is suitable for wet weather placement (3);
- i) The embankment can be constructed with normal earth-moving equipment;
- j) Foundation clean-up requires no hand-work, except beneath and near the plinth(3);
- k) Grouting can be done in parallel with embankment construction (3);
- l) Slipforming provides a rapid and economical method of concrete face embankment (3).

Concentration on the concrete face rockfill dam in recent years can be attributed to the following combination of diverse factors which together resulted in this type of dam costing less than others :

- a) Dam sites with non-erodible rock suitable for sealing the concrete face to the foundation via a concrete plinth (upstream toe slab);
- b) An economic climate favoring the minimizing of labour and maximization of mechanized input in the execution of construction activities;

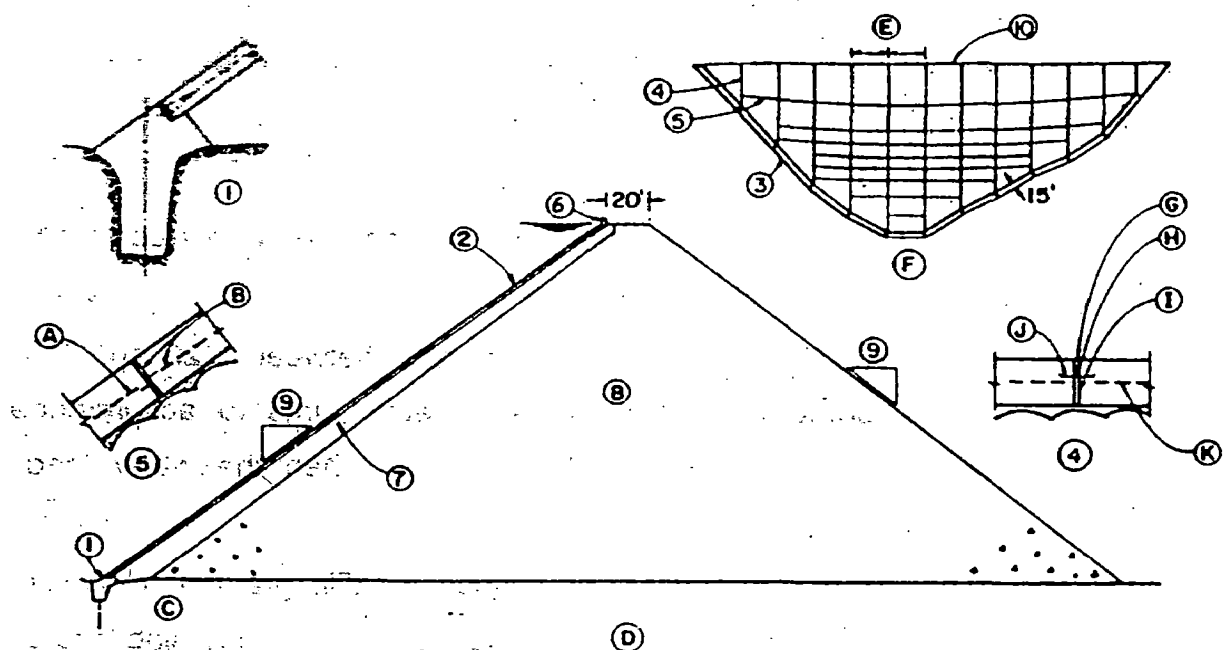


Figure 2.1 : Feature of early concrete face rockfill dam design (ICOLD 1989a). (1) Cut-off trench, (2) Concrete face, (3) Toe slab, (4) Vertical joint, (5) Horizontal joint, (6) Parapet, (7) Crane-placed large rock, (8) Dumped rockfill, (9) Slope, (10) Curved axis. (A) Reinforcement, (B) 1.9 cm redwood filler and Z waterstop, (C) Curtain grouting, (D) Cross section of dam, (E) 18 m (60 feet), (F) Elevation of face, (G) Mastic, (H) Premolded asphalt, (I) Compressible joint filler, (J) U copper, (K) Reinforcement. (at (7))

- c) Generally, a shortage of suitable low-cost core material for core type rockfill dams;
- d) High average rainfall imposing construction programming constraints and hence cost penalties on core construction as compared with an all-weather material such as rockfill;
- e) The advent of construction technology which through the use of compacted rockfill, ensured reliable performance in terms of safety and leakage for concrete face rockfill dams.

While the basic design philosophy remained largely unchanged over the years, extensive construction and performance experience introduced modifications resulting in increased economy. Design principles are discussed and the evolution of design procedure is presented for all major components of the dam.

2.2. DESIGN PRINCIPLES

ICOLD (1989a) describes the current practice for zoning of CFRD constructed of sound rockfill on a strong rock foundation. Figure 2.2 shows zoning of such a dam.

The dam consist of (4) :

Toe slab – A reinforced concrete slab cast on sound, low permeability rock to join the face slab to the foundation.

Face slab – Reinforced concrete, preferable between 0.25 and 0.6 m thick, with vertical, some horizontal and perimetric joints to accommodate deformation which occurs during construction and when the water load is applied.

Zone 2D – Transition rockfill, processed rockfill, grading from silt to cobble size. The transition provides uniform support for the face slab and acts as semi-impervious layer to restrict flow through the dam in the event that cracking of the faceplate or opening of joints occurs.

Zone 2E – Fine rockfill, selected fine rock which acts as a filter transition between Zone 2D and Zone 3A in the event of leakage through the dam.

Zone 3A – Rockfill, quarry run free draining rockfill placed in layers about 1 m thick. This zone provides the main support for the face slab and is compacted to a high modulus to limit settlement of the face slab.

Zone 3B – Coarse rockfill, quarry run free draining rockfill placed in layers about 1.5 to 2.0 m thick. Larger rock may be pushed to the downstream face. This zone is less affected by the water load than Zone 3B, so a lower modulus is acceptable. The thicker layers allow placement of larger rock.

Many dams include a concrete crest wall which reduces the quantity of rockfill required.

Many variations of this zoning are adopted to meet site conditions and the quality of construction materials available. In some dams, low permeability earthfill is placed upstream of the face (Zone 1A and 1B in Fig 2.2) to control leakage in the event of it leaking. The transition Zones 2D and 2E have been so designated in order to differentiate from Zones 2A, 2B and 2C used in earth and rockfill dams. There is no consistent terminology in use throughout the world.

When the design of Cethana Dam was in progress, no completely successful concrete face rockfill dam over 80 m high was in operation. Substantial leakage at such dams as Salt Springs, Courtwright, Parabela and New Exchequer, while not affecting their safety in any way, had tended to undermine confidence in the adequate performance of this type of dam. No analytical design was being carried out anywhere but some agreement on basic detail and methods was beginning to emerge.

Compacted rockfill had superseded dumped rockfill. Concrete plinths with grouted cut-offs were being simplified and were replacing the practice of blasted trench-type cut-offs.

Crane-placed rock faces were discarded and replaced by rolled selected fill and it was beginning to be filled with soft compressible materials.

An examination was made of the whole question of design in order to determine the best way of building a dam of this type. Important inferences are made as below :

- a) Large deformation of the face slab can result if it is constructed in stages as the embankment is raised;
- b) Strains in the concrete face are largely independent of its thickness and depend mainly on the movements of the rockfill; small in-plane deformation is associated with small normal deflection;

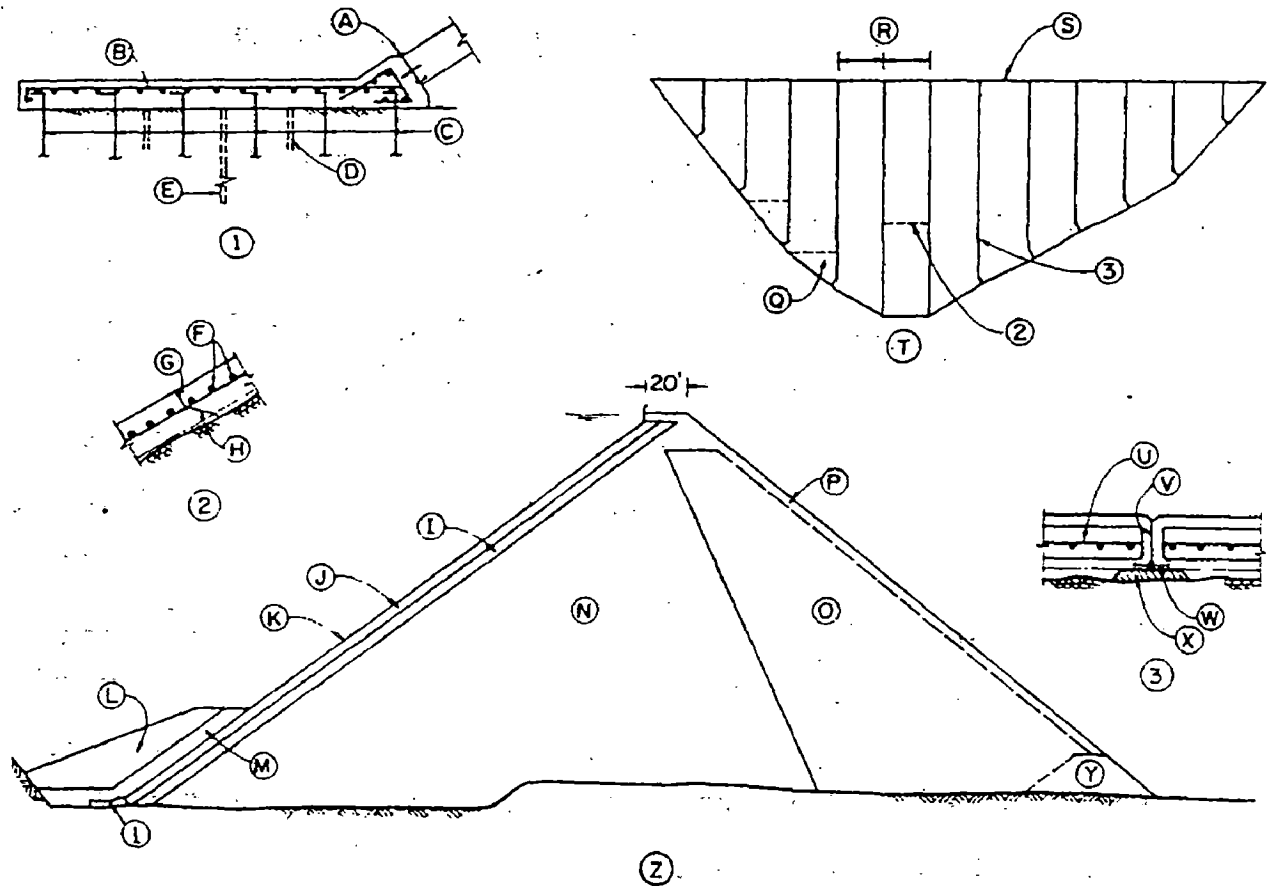


Figure 2.2 : Current practice for zoning of CFRD constructed of sound rockfill on a strong rockfill foundation (adapted from ICOLD 1989a at (7))

(1) Toe slab, (2) Horizontal Joint, (3) Vertical Joint. (A) Perimetric joint, (B) Steel reinforcement, (C) Anchor bars, (D) Consolidation grout holes, (E) Grout curtain, (F) Horizontal reinforcement, (G) With form, (H) Broom joint, (I) Zone 2E, selected small rock placed in the same layer thickness as Zone 2D, (J) Zone 2D, processed small rock, (K) Concrete face, (L) Zone 1B, random, (M) Zone 1A, impervious soil, (N) Zone 3A, quarry run rockfill or gravel fill, about 1.0m layers, (O) Zone 3B, quarry run rockfill or gravel fill, about 1.5 to 2.0m layers, (P) Available large size rock dozed to face, (Q) Starter slab, (R) 18 m (60 feet), (S) straight axis, (T) Elevation of face, (U) Horizontal reinforcement, (V) Surface painted with asphalt, (W) Copper waterstop, (X) Mortar pad, (Y) Zone 3D, plus 0.3 m rockfill, (Z) Section of dam.

- c) Strain in the concrete face generally are unlikely to be excessive for a dam of Cethana's height provided that correct technique of rock placing are used;
- d) As the majority of the face is in compression, joints between slabs can be reduced in number and soft filling material is to be avoided in the remaining joints.

From a) it was decided to almost complete the rockfill before commencing the concrete face. This in turn led to the adoption of slip forming and the general omission of horizontal joints. From b) the thickness of the concrete face was reduced to that judged adequate for impermeability and long

life. From c) and following Terzaghi, it was considered essential to wet the surfaces of all rockfill particles during placing and compaction. The purpose of this procedure was to reduce the rock strength, particularly at points of rock to rock contact, so that the maximum settlement possible would take place during compaction and own weight loading, prior to constructing the concrete face. And finally to satisfy d) plain butt joints were to be used for all joints in compression in order to limit the opening of joints at and near the parameter.

The only modification to these principles concerns a) where, following experience at Foz do Areia and Khao Laem Dams, construction of the face and rockfill in two substantially-equal stages is not now considered to be detrimental. It is apparent that relative down slope movement between the compacted rockfill and the concrete face, which must occur during staged construction, does not induce large compression loads in the concrete as was the case in dumped rockfill dams with crane-placed rock faces.

2.3. PLINTH (UPSTREAM TOE SLAB) ⁽⁹⁾

2.3.1. General Requirement

The principal purpose of the plinth is to provide a 'watertight' connection between the concrete face slab and the dam foundation. It is shaped to provide an apron or cap for foundation grouting operations and a surface in the plane of the face from which face-slab slipforming can start (see Fig. 2.3). On the downstream side of the plinth, it is important to maintain a minimum thickness of rockfill, or "cushion", between the underside of the face slab and the rock foundation. Compressive deformation of this rockfill under water load prevents any significant bending moments developing in the face slab adjacent to the plinth.

At Cethana, bend in the plinth alignment were minimized and located only at vertical joints in the face slab. This was done to avoid distress in case of large movements of the face slabs along the line of the plinth. To maintain a straight alignment across haul road benches and thereby avoid additional

bends, the plinth was carried across the haul road on mass concrete backfill which reached a considerable height on the inside of road.

After Cethana, where joint meter measurements showed conclusively that the perimetric joint opens when water load is applied, it was decided that these earlier restrictions were not entirely necessary. It is now the practice to locate only re-entrant, i.e. "inward" bends, at vertical joints in the face slab. At haul roads the plinth is now constructed across the road bench and up the both sections being completed prior to rockfill haulage to avoid interruption to rockfill placing.

2.3.2. Geometry

Apart from the apron, the basic shape of the plinth has changed little since Cethana. At Cethana the apron was made horizontal in a direction at right angles to the plinth reference line (see Fig. 2.4). For subsequent dams, in order to reduce the volume of plinth excavation, the apron was changed to horizontal in a direction at right angles to the dam axis so that the apron slope approximated the average abutment slope (see Fig. 2.3). Although excavation costs were reduced, concreting and grouting costs increased due to more difficult forming and access for drilling rigs. Reverting to the Cethana-type apron is being considered.

Other changes to the Cethana cross section are the reduction of the apron thickness from 450 mm to 300 mm and the increase in the slipform overlap (see Fig. 2.4) from 600 mm to a more generous 800 mm.

2.3.3. Foundations

Foundation rock should preferably be non-erodible; otherwise special measures are necessary to prevent piping and erosion.

Starting with Cethana a criterion was adopted for plinth width, or leakage path length, of 0.05 times the head for a sound rock foundation, or 0.10 times the head for a lesser quality foundation, with a minimum of 3.0 m.

This has proved adequate for all commissioned dams as evidenced by the small measured leakages.

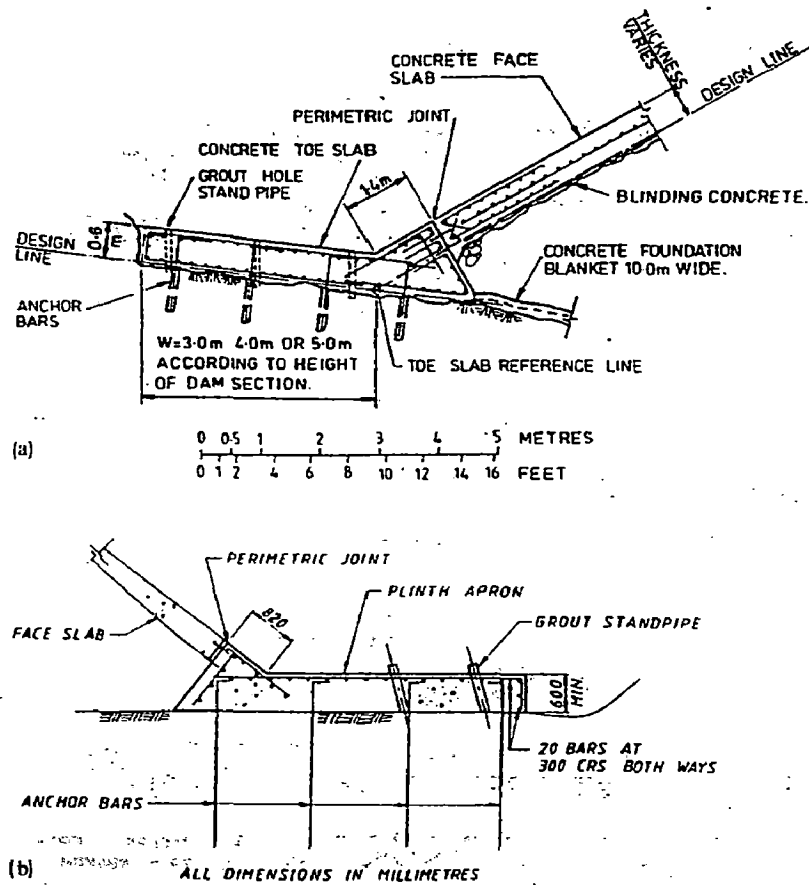


Figure 2.3 : Toe slab design for a) Mangrove Creek Dam, b) Boondooma Dam (MacKenzie & McDonald 1985, Roger 1985 at (6)).

The abutments along the approximate plinth lines are stripped and sluiced down to expose the in-situ rock. This enables the geology to be mapped and the plinth position to be sited with due regard to depth of weathering and major defects as well as the minimum excavation.

In all dams since Cethana the foundation rock under the plinth has been grouted with three rows of grout holes – shallow outside or “consolidation” holes and deep central “curtain” holes. At Cethana the curtain row was upstream.

The consolidation holes at Cethana were 8 m deep and at 3 m spacing. Primary, secondary and tertiary curtain holes were also provided at 3 m spacing but to a maximum depth of 0.5 times the head. Starting at Murchison Dam, this practice was changed with respect to the depth of the holes.

Consolidation holes now vary in depth from 5 m to 15 m depending on head. Curtain holes are generally drilled to a maximum depth of 0.33 times the head.

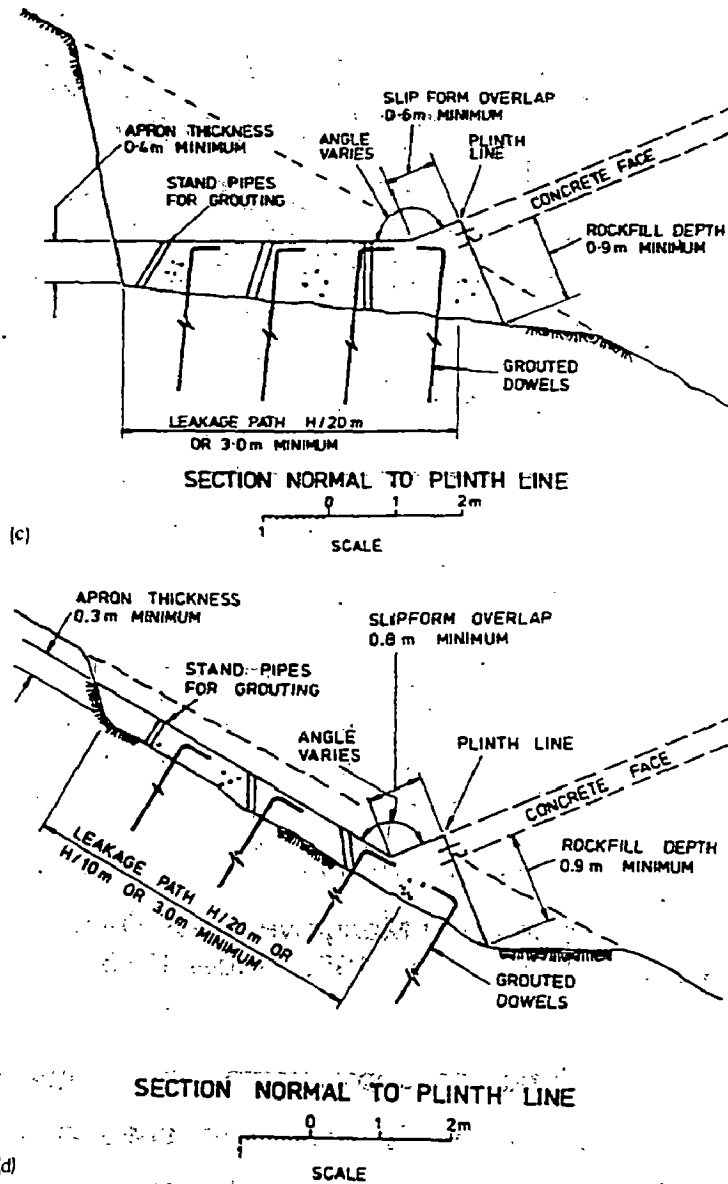


Figure 2.4 : Toe slab design for c) Cethana Dam, d) Lower Pieman Dam (Fitzpatrick et al, 1985 at (6)).

In all dams additional precautions are taken against leakage by covering areas of closely-jointed rock just upstream and downstream of the plinth with a layer of gunite and by excavating and backfilling with concrete any fault zones is generally to a depth equal to the width of the affected zone. This dental treatment is carried out upstream of the plinth wherever required

and is always extended downstream for about 6 m. A further distance downstream is covered with filter material if the infill is erodible.

Special measures were necessary at Lower Pieman Dam where the whole of the left abutment is amphibolite and schist which is highly to completely weathered to a depth of the 30 to 40 metres. Many joints, opened up to 20 mm to 100 mm by valley relaxation, are infilled with soft silty clay which is highly erodible. The residual rock is of doubtful erodibility. Instead of constructing a deep trench type cut-off under the plinth on the steep abutment, the hydraulic seepage gradient under the plinth was reduced to between two and three by constructing a reinforced-shortcrete blanket downstream of the plinth. To guard against piping of the joint infill material through cracks in the shortcrete, the blanket was completely covered with a double layered filter under the rockfill. The filter was extended to the downstream toe as an additional precaution against piping, into the zone 3A rockfill, of the foundation beyond the blanket.

Plinth foundations and indeed all dam foundation are inspected as a matter of policy of the authorized engineer. Rock Quality, defects and the optimum location and orientation of grout holes are all given detailed attention before approval is given for concreting to proceed.

2.3.4. Stability

In areas of foundation overbreak or where clay-filled planer joints provide potential sliding surfaces beneath the plinth, it is necessary to carry out a stability analysis for overturning and sliding.

Very little overbreak is needed to increase the overturning force substantially and cause the resultant to lie outside the middle third. No support is available from the face slab which pulls away from the plinth when the water load is applied. Some support is available from rockfill pressure on the downstream face of the plinth. Pressure meter measurements at Bastyan indicate this force is about 0.25 times the reservoir head acting on the

adjacent face slab. This stabilizing load is neglected where there is only a small amount of overbreak.

Uplift is assumed to act on 100% of the contact area with a linear distribution between full head at the upstream edge to tail-water, if any, at the downstream edge.

Once overbreak reaches 0.5 m the stability of the plinth is improved by widening the apron or by providing pre-stressing tendons or additional dowels.

2.4. EMBANKMENT

2.4.1. Foundation Preparation

Specification for foundation preparation under the embankment has remained essentially the same as at Cethana. The abutments downstream of the plinth are stripped of all superficial deposits to expose the high points of insitu rock or undisturbed residual clay. Any superficial material remaining between rock points is not likely to adversely affect embankment settlement. In the riverbed, alluvial gravels are allowed to remain except within a distance equal to 0.5 times head from the plinth. At the Lower Pieman Dam such gravels were found to have a modulus under embankment loading of approximately 200 MPa which is higher than for most compacted rockfills. Between the plinth and the dam axis, any overhangs are removed and battered back to permit efficient compaction of the rockfill against the abutment.

At both Mackintosh and Bastyan there is one long gradually-sloping abutment over the upper 20 to 30 meters height of the left and right banks respectively. Fluvio-glacial drift deposits, up to 12 m deep, covered each of these abutments and were allowed to remain in place under all of the embankment except for zones 2A and 2B. The occasional silt and fine sand lenses were covered with filter material.

2.4.2. Embankment Design

The lower slopes of upstream and downstream faces are at the angle of repose of free-draining rockfill (1 vertical to 1.3 horizontal, see Fig. 2.5) for all dams except Serpentine where the use of very fine rockfill made it prudent to adopt 1 vertical to 1.5 horizontal. However, within 10 or 15 meters of the crest, the upstream and downstream faces are steeped to as much as 1 on 1.25 to provide the crest camber required for water load settlement.

This section is intrinsically stable on a rock foundation provided massive leakage does not occur. As this is not expected with the plinth and face slab detail adopted, stability analyses are not usually carried out except for flow through rockfill cases during construction.

All dams since Mackintosh, except Tullabardine, have a reinforced concrete L-shaped retaining wall along the upstream side of the crest to reduce the volume of rockfill (see Fig. 2.6). At present the crest wall is standardized at 4.5 m in height, giving a 4.0 m high stem which is placed in a single lift. Higher walls, involving two lifts, are being considered for current designs.

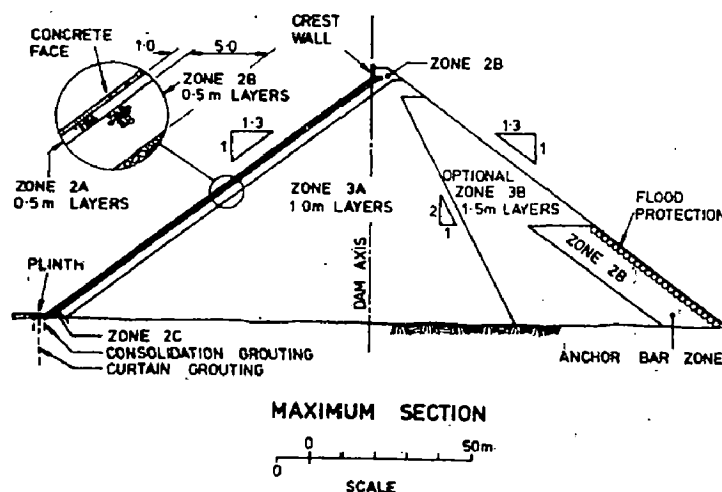


Figure 2.5 : Embankment zones in recent dam (6)

At the base level of the crest wall the width of the embankment is maintained at a minimum of 9.0 m to provide sufficient room for operating slipforming equipment. The resulting width of 4.9 m at the dam crest level is

sufficient for a single lane road and a protective railing on the downstream side.

2.4.3. Rockfill Properties

The basic requirement for the rockfill of a concrete face dam is that the settlement of the completed embankment under water load and long term creep effects is small enough not to cause damage to the face slab and its waterstops. An important practical consideration is that the rockfill can be quarried and placed in the embankment with a minimum of wastage and of construction inconvenience on the dam.

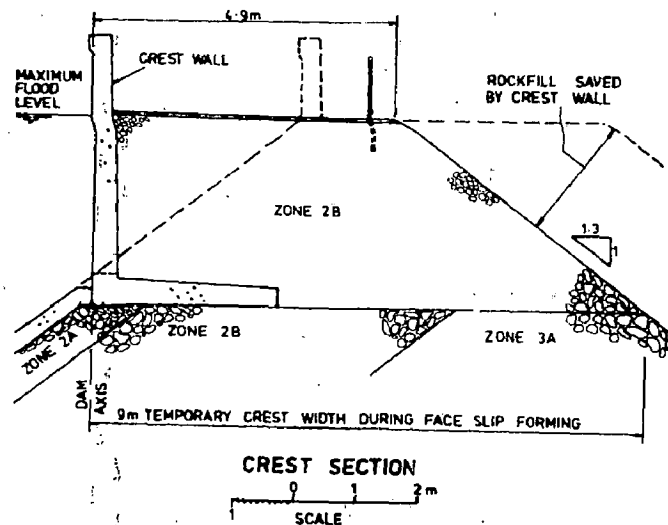


Figure 2.6 : Crest wall arrangement

It is preferable that the rockfill be free-draining, firstly to avoid the build-up of pore pressures during construction which would interfere with placing operations, and secondly to avoid the saturation of the downstream face of the dam in the event of gross leakage through the face slab.

In practice these requirements are met by well-graded rockfill, containing not more than a small percentage of weathered material, placed and compacted in layers about one meter thick.

At Cethana the rockfill was a hard quartzite which met all the requirements. However at some later dams, the ideal rockfill was not available locally and material of lesser quality was used out of necessity.

2.4.4. Zoning

Embankment zoning remains generally as at Cethana, although there has been some renumbering of the zones. Zone details are summarized in Table 2.1, and are shown in Figure. 2.5.

Note that currently the maximum sizes of 2B, 3A and 3B are equal to the layer thickness. Most of the other changes are due to rounding off as a result of conversion to the SI system.

Zone 2A acts as a bending layer for the face slab and its small size allows for accurate placing and trimming of the upstream face slope. It also acts as a semi-impervious barrier to restrict flow through the embankment during construction floods or in the event of leakage through the face slab in service.

Table 2.1 : Zone Designation, Layer Thickness and Maximum Particle Size

Zone Designation	Cethana Dam		Current Dams	
	Layer Thickness Before Compaction (m)	Maximum Particle Size, (mm)	Layer Thickness Before Compaction (m)	Maximum Particle Size, (mm)
2A	0.45	225	0.5	(200)* - 300
2B	0.45	375	0.5	500
2C	0.12	100	0.125	75
3A	0.90	600	1.0	1000
3B	1.35	900	1.5	1500

* within 500mm of the face

Zone 2B is a transition between Zone 2A and the Zone 3A rockfill. Filter grading rules are applied between 2A and 2B and between 2B and 3A to avoid any loss of face support during flood inflow or leakage. The 500mm maximum size of Zone 2B material makes it convenient for it to be placed around the flood protection anchor bars at the downstream toe of the dam.

Zone 2A is usually a processed material and, in view of its high cost, the horizontal thickness of the zone was reduced from 3 m to 1 m in the three most recent dams. At the same time the horizontal thickness of Zone 2B was increased from 3 m to 5 m to maintain the same total horizontal thickness of these two zones.

Zone 2C is a fine rockfill which is placed directly against the downstream face of the plinth where large rollers cannot reach. As a excessive settlement in this region could shear waterstops. Zone 2C is placed in thin layers and thoroughly compacted with hand-held mechanical tempers.

Zone 3A provides the principal support for the water load. The segregation which occurs during the spreading process on the dam is generally permissible (4), although on the Zone 2B/Zone 3A interface segregated material is removed.

Zone 3B permits the placing of larger rock with a wider grading. Because it is less highly stressed by the water load, some relaxation in rockfill quality is permitted. Although a Zone 3B is usually shown on the drawings and a grading envelope is specified, The Commission's construction engineers nearly always elect to place Zone 3A rockfill right across the dam for simplicity of control and to expand the working area, thus effectively eliminating Zone 3B.

2.4.5. Application of Water During Compaction

Except at Serpentine, where the rockfill was not free-draining, the rockfill specifications for all dams require a minimum percentage of water to be added to rockfill during placing and compaction. The amount of water which is added has varied from 15% of the volume of the rockfill at Cethana to 10% at the Mackintosh and 20% at Murchison. At Lower Pieman, as a significant economy measure, the usual monitors were dispensed with and the water was added to each loaded truck as it came onto the embankment.

2.4.6. Preparation of The Upstream Face

As each horizontal layer of rockfill is placed, the upstream face is trimmed to within plus 50 mm to plus 150 mm of the design plane, the positive tolerance is an allowance for subsequent face compaction.

At intervals of 25 m in slope length during the raising of the embankment, the face is compacted by rolling, primarily to minimize later face slab settlement under water load but also to provide a firm working surface during preparations

for the construction of the face slab. Any loosening of the working surface could itself lead to later settlement.

Present practice for compaction is to give four passes of a 10 tone roller without vibration, followed by four up-slope passes with half vibration (i.e. half centrifugal force) and then eight up-slope passes with full vibration. Before and during this compaction, the upstream face is thoroughly wetted. Backfilling of hollows during or after compaction is not permitted.

After rolling the surface is stabilized by spraying it with one coat of cationic bituminous emulsion at an application rate of approximately 1.75 liters per square meter. A second coat is applied if necessary. Before the emulsion breaks, its surface is dusted with fine sand. Apart from holding the compacted face intact the treatment protects the face from erosion during heavy rain.

At Cethana, face compaction trials with the vibrating roller prior to sealing with emulsion were unsatisfactory and eight passes with full vibration were specified to be carried out after sealing. Application of the Cethana procedure at Mackintosh proved completely unsatisfactory probably because the Zone 2A material here was much finer. Since then all compaction has been specified to be carried out prior to sealing.

2.5. CONCRETE FACE – DESIGN REQUIREMENTS

2.5.1. Basic Design

Wilkins, et al. (at (1)) suggested the following general design criteria governing design thickness, which was adopted at Cethana dam.

- i. Moment resistance is not relevant in determining the membrane thickness, because the membrane is uniformly supported against normal water load.
- ii. Under the action of normal water load, the slab is constrained to follow the rockfill strains in the plane of the face by the development of shear force between the underside of the slab and the rockfill so that the strain in the slab is independent of its thickness.
- iii. In the absence of determinant design criteria the slab thickness adopted may be judged to provide water tightness and durability.

Following the above basic principles, the design of the Cethana face slab was based on the following :

- a) Bending can be ignored because the face slab is uniformly supported on compacted rockfill and hydrostatically loaded;
- b) There are tensile and compressive strains in the plane of the face, caused by temperature changes in the concrete and deformation of the underlying rockfill under load; these strains are independent of the face slab thickness;
- c) The face thickness must be sufficient to permit thorough and uniform compaction of the concrete for strength and watertightness, to accommodate reinforcement and waterstops, and to ensure durability;
- d) The perimetric joint must be capable of allowing significant movement, during reservoir filling and long term settlement, without rupturing the waterstops;
- e) Areas of horizontal tensile strain require closer spacing of contraction joints and additional reinforcement.

2.5.2. Cethana Face Details

The adopted face thickness varies uniformly from 300 mm at the crest to 520 mm at the toe ($t = 300 + 0.002h$). The slabs were slipformed continuously from base to crest without horizontal joints, except for some slabs adjacent to the abutments. Details of the concrete slab used are given below.

Face Joints – The spacing of vertical joints (that is, those in the slope direction) was standardized at 12.2 m (actually 40 feet). This dimension was adopted after consideration of such factors as the weight of the slipform, the winch sizes, the method and rate of concrete delivery and the proportion of the total face area occupied by the remaining triangles.

Some additional vertical joints, midway between the main joint lines at 12.2 m spacing, were introduced in the area close to each abutment in the upper two-thirds of the face. Their purpose was to control possible crack spacing in this area in which horizontal tensile strains were expected to occur. These additional joints were not extended to the crest but were terminated on

horizontal contraction joints introduced for this purpose. The joint layout for Cethana dam is shown in Figure 2.7, together with details of the different types of joints which are described below.

Perimetric Joint – Dual waterstops were adopted here because the greatest joint movement was expected to occur at the perimeter and because the reservoir would never be drawn down during operation. The joints contain a soft but durable 12 mm thick timber filler to allow for rotation, shear and possible compression without spalling the concrete.

Vertical Contraction Joints – No joint filler was provided in order to reduce to a minimum movement of the slabs in the plane of the face. The dual waterstop system mentioned above was extended to the vertical joints in the tension areas close to each abutment. All others have only the copper waterstop on the underside.

Horizontal Contraction Joints – Timber filler was used to allow for any possible shear movement along the line of the joint.

Vertical Construction Joints – A central vertical construction joint was introduced in the triangular slabs adjacent to the plinth to enable a 6.1 m wide slipform to be used in this awkward section. This joint was waterstopped and terminated at a horizontal construction joint above which the 12.2 m wide slipform was used.

Horizontal Construction Joints – For ease of clean up, this joint was made normal to the face above the reinforcement and horizontal below it. No waterstop was required in this type of joint. Its main purpose was to act as a terminator for vertical construction joints; it was also to be used in the event of any enforced stoppage during slipforming.

Waterstops – The primary waterstop is of copper. The rubber waterstop in the perimetric joint (and in some vertical joints) is a safeguard against the possibility of a defect or rupture in the copper.

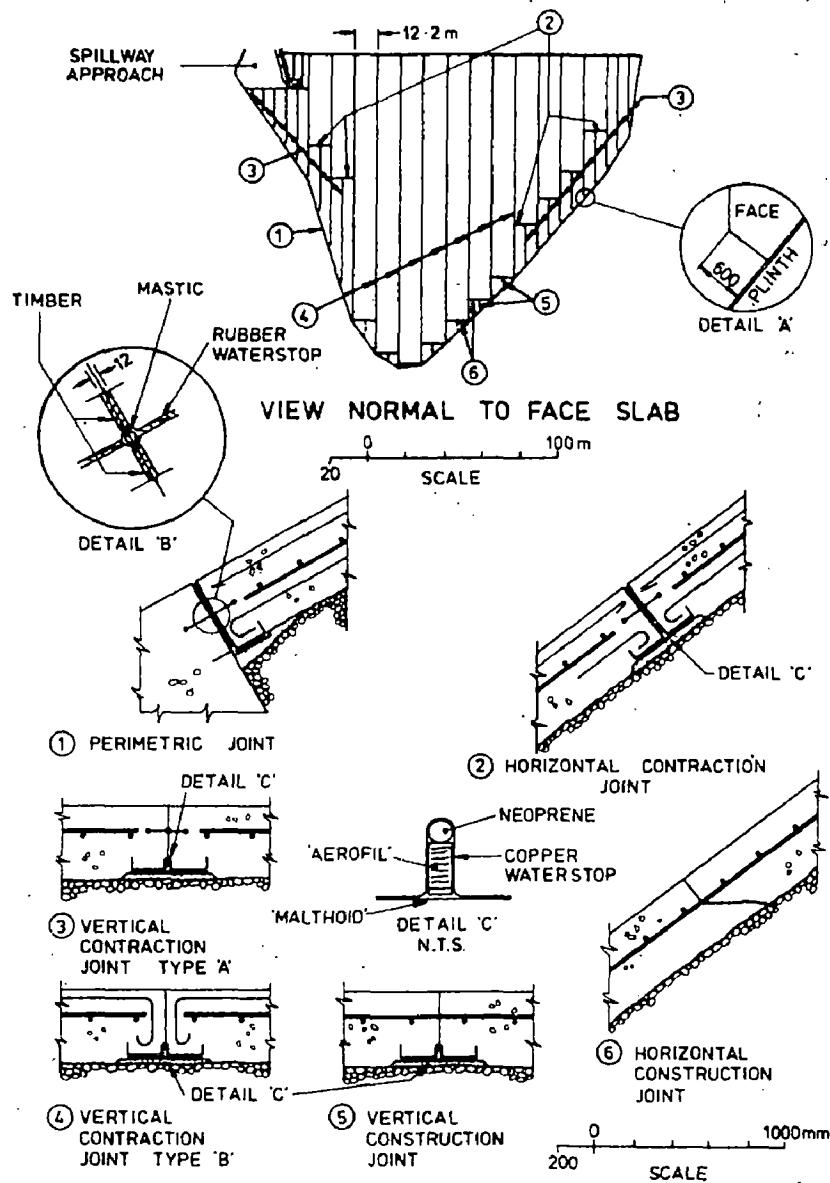


Figure 2.7 : Cethana dam face – Joint layout and details (at (6))

The W-shape of the copper waterstop was conceived and adopted primarily because concrete can be compacted more reliably around its upstanding legs than around the horizontal outstand of either Z-shaped or U-shaped waterstop. Also split formwork is not necessary for its installation. It was made with a high centre rib to permit quite large shear movement between adjacent slabs. To prevent external water pressure from squeezing the rib flat, it was filled with a solid continuous 12 mm diameter neoprene insert retained in place by a continuous strip of closed-cell polythene foam ("Aerofil") of rectangular section 16 mm by 32 mm. The waterstop was soft annealed after

forming to ensure maximum ductility in service. The waterstop is seated on a 400 mm wide strip of tar impregnated felt ("Malthoid").

Cement mortar pads were constructed beneath each joint to provide an even bedding surface for the copper waterstop and the joint formwork.

Natural rubber was chosen as the second waterstop because of its robustness and its ability to accept large deformations. All bends, crosses and tees were factory-made to suit specific locations; field joints were only permitted in straight sections of waterstop.

Face Reinforcement – The amount of reinforcement that should be used in a concrete membrane is somewhat arbitrary. Over most of its extent, the membrane will be in compression and one could possibly consider that no reinforcement is required at all. However, thermal and drying shrinkage will occur prior to filling the reservoir and the membrane must be reinforced to control cracking due to this cause.

In all American dams pre-dating Cethana, the steel area was 0.5% in each direction, based on the design thickness of the slab.

For Cethana face slab, 0.5% of S230 grade deformed bar was used in each direction, based on the design concrete thickness plus 100 mm, to allow for the unevenness of the embankment surface. The 100 mm allowance proved to be very close to the actual over-thickness achieved. However in expected tension zones close to each abutment, the horizontal steel was increased to control possible cracking of the concrete. The criterion used to determine the steel area here was that there should be sufficient steel to take the full water load transmitted to the steel by friction on the underside of the slab.

In addition, some light reinforcement was placed around the perimetric joint and at all vertical and horizontal contraction joints except those in tension areas. See Figure 2.7, joint types A and B. The purpose of this additional steel was to prevent possible spalling of slab edges

Concrete Curing – In order to minimize the effects of drying shrinkage on the long slab lengths, continuous curing with water was required right up to the

time reservoir filling commenced. Curing water could only be turned off for short periods to facilitate inspections and the installation of instrumentation.

2.5.3. Evolution in Face Design

While the Cethana basis of design remains largely intact, there has been some evolution with time and the principal changes are described below :

Face Thickness – In Table 2.2, there is a trend for a bigger face thickness to be used for progressively higher dams. For dams 40 m to 50 m high, a uniform design thickness of 250 mm was adopted in 1968; that thickness has now been used for dams up to 75 m high. For a 90 m high dam, a 300 mm thick face was adopted in 1980, and for a 120 m high dam being built in 1985, the face thickness varies from 300 mm at the crest to 420 mm at the toe ($t = 300 + 0.001h$). For comparison, the criteria adopted for concrete face slab thickness at some of the important dams are given in Table 2.3.

Table 2.2 : Dam Embankment Performance Data

Name of Dam	Maximum Height (m)	Crest Length (m)	Face Slopes		Rockfill Data				U/S Face Slab Thickness (mm)	Reinforcement each way (%)	Plinth Apron Width (m)	Remark
			U/S	D/S	Rockfill Type	Rockfill Density (ton/m ³)	Modulus Erc (Mpa)	Modulus Erf (Mpa)				
Wimot	35	138	1.33	1.33	Greywacke	2.2	115	180	250	0.7	1.8	
Cethana	110	215	1.3	1.3	Quartzite	2.1	145	310	300-620	0.5	3.0-5.3	$t = 0.3 + 0.002h$ mm (h = head in metres)
Paloons	38	159	1.33	1.33	Arg. Chert	2	75	115	250	0.6	1.8-3.5	
Serpentine	39	127	1.5	1.5	Quartzite	2.1	115	95	250	0.8	1.1-3.7	The nominal thickness of the plinth is 1.4 m
Mackintosh	75	465	1.3	1.3	Greywacke	2.2	40	95	250	0.5	3.6-4.6	
Tullabardine	26	200	1.3	1.3	Greywacke	2.2	80	170	250	0.5	3.0-3.7	
Murchison	94	200	1.3	1.3	Rhyolite	2.3	225	650	300	0.5	3.2-5.5	
Bastyan	75	430	1.3	1.3	Rhyolite	2.2	160	300	250	0.5	3.2-4.7	
Lower Pieman	122	380	1.3	1.3	Dolerite	2.3	160	no data	300-420	0.5, 0.4	4.0-7.0	$t = 0.3 + 0.001h$ mm (h = head in metres)

Erc = Modulus of deformation of rockfill during construction
 Erf = Modulus of deformation of rockfill during reservoir filling

Face Joints – For dams less than 30 m high, including the ends of higher dams, the adoption of 6.1 m wide slabs throughout has proved economic.

At Lower Pieman Dam (see Figure 2.8), the horizontal construction joint at the bottom of each 12.2 m wide slab has been changed to a contraction joint. There is evidence to suggest that this change will provide more freedom for thermal shrinkage and reduce face cracking.

Tabel 2.3 : Criteria Adopted for Concrete Face Membrane Thickness

Sl. No.	Name of Dam	Year of Construction	Height (m)	Criteria Adopted for Fixing The Membrane Thickness
1.	Cethana	1971	110	$t = 0.3 + 0.002xh$
2.	Kangoro Creek	1969	64	$t = \frac{0.305xh}{60.96} + 0.305$
3.	Lemolo-1	1954	36	$t = 0.3 + 0.005xh$
5.	Nozori	1956	44	thickness at bottom aqual to 1.5% of water head
6.	Paradela	1958	110	$t = 0.3 + 0.00735xh$
7.	Pindari Creek	1969	76	$t = 0.3048 + 0.0067xh$

Where, t = slab thickness normal to the face of dam in metres
 h = depth with relation to crest of dam in metres

Waterstops – The vertical joint openings in tension areas close to the abutments have proved to be quite small, and only one waterstop was provided here in all dams since Cethana.

On two dams 39 m and 26 m high, only one waterstop was placed in the perimetric joint, because very small movements were expected.

In a significant change, the W-shaped copper waterstop was replaced by 0.9 mm thick Grade 321 stainless steel of similar profile. The robustness of stainless steel is an asset during installation and, depending on metal prices, stainless steel can be cheaper than copper. Jointing consists of a lap joint fixed by spot welding, then sealed by tungsten-inert-gas welding, so that only one metal is involved.

The rubber waterstops in the early dams were made from natural rubber. Hypalon rubber was adopted in 1978 because it has greater resistance to oxidation and ozone attack which can occur above minimum operating level.

Face Reinforcement – Generally reinforcement was provided in each direction of not less than 0.5% of the concrete area including an allowance for overbreak. However, at Lower Pieman dam, the horizontal steel was reduced from 0.5% to 0.4% because no shrinkage cracks have been observed running in the slope direction. The bar sizes and spacings were determined at the base

The Influence of Seismic Load in Slab and Embankment of Concrete Face Rockfill Dam

of the dam where the slab is thickest and the same reinforcement mat was adopted throughout the face.

Grade 230S deformed bar was recently superseded in Australia by the higher yield grade 410Y deformed bar. 410Y reinforcement is being used in the face without any change in the steel percentage, in the hope of achieving better crack control.

The additional horizontal steel placed in tension areas at Cethana was not repeated in later dams because the measurements at Cethana shown the horizontal tensile strains are small.

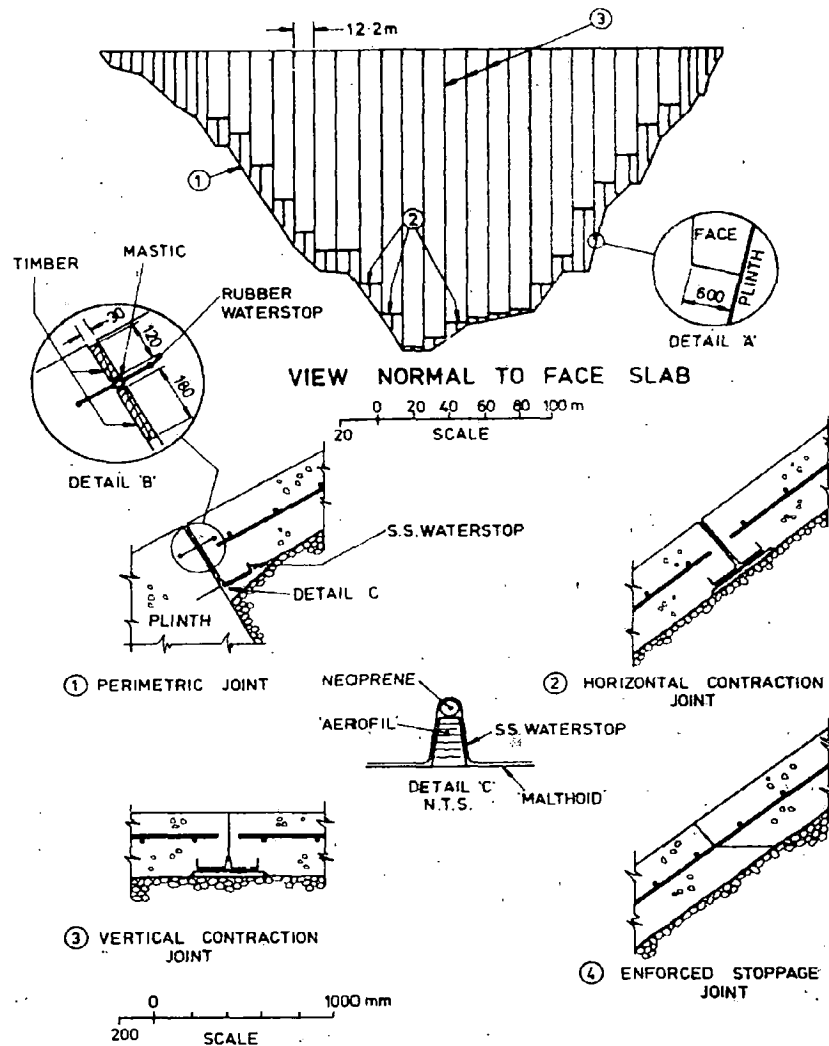


Figure 2.8 : Lower Pieman Dam – Joint Layout and Details

Irregularities in the rock foundation immediately downstream of the plinth can cause substantial variations in the depth of rockfill supporting the edge of face slab. Under water load, this uneven support will reduce bending stresses in the strip of face slab adjacent to the perimetric joint. Where necessary a second layer of reinforcement is added.

Face Concrete – The two concretes, for Cethana in 1968 and Lower Pieman in 1985, are compared in the Table 2.4 below.

The differences are not significant, the lower cement content and higher water cement ratio for Lower Pieman concrete merely reflect the use of crushed aggregates, whereas Cethana aggregates were mainly rounded gravels which have a weaker bond of paste to stone.

Replacement of cement with pozzolans has never been seriously considered because locally the cost of pozzolans is as expensive as cement.

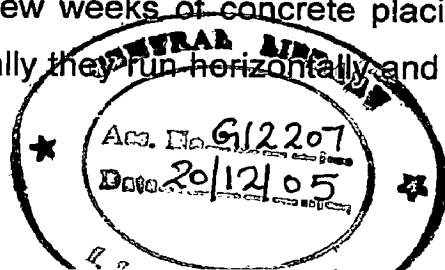
Table 2.4 : Face Concrete Data

No	Item	Cethana	Lower Pieman
1	Actual average strength (MPa)	40	40
2	Maximum aggregate size (mm)	40	40
3	Cement content (kg/m ³)	320 – 370	280
4	Water cement ratio	0.41 – 0.47	0.55
5	Slump (mm)	40	40

Concrete Curing – Continuous water curing from concrete placement to storage filling remains in force. Sometimes a substantial cost is involved, at Mackintosh dam, face construction and storage filling took 2 years and the water supply had to be relocated when storage filling commenced.

Interruptions to water curing are unavoidable, the installation of face instruments and power failures are examples. Nor can the runoff be allowed to impinge on fresh concrete. Generally interruptions are limited to a few hours.

Face Cracking – Few cracks have been seen in dams less than 50 m high. In higher dams, crack occur mainly in the longer slabs but not in every one. The cracks usually appear within a few weeks of concrete placing and are attributed to thermal shrinkage. Generally they run horizontally and extend



through the full depth and width of the slabs. Crack widths are commonly less than 0.1 mm and seldom exceed 0.2 mm.

Evidence of some closure and self-healing was observed there prior to reservoir filling and no treatment was applied. Whereas at Gethana several cracks occurred together in widely spaced groups, the pattern in recent dams consists of larger single cracks at 5 to 10 m spacing.

Only cracks 0.5 mm or wider are treated, normally by painting with a rubber-based compound ('Peratol'). The leakage through finer cracks is thought to be insignificant and indeed is expected to decrease with time due to closure, self-healing or clogging.

At Mackintosh dam, there was one exceptional crack up to 0.5 mm wide which crossed nine of the longest slabs about 1.5 m from the plinth. On investigation it was concluded that the trimming of the rockfill adjacent to the plinth, to provide local thickening of the slab, did not produce a gradual taper as intended but rather a sudden step, which concentrated restraint to thermal shrinkage of the slabs at this location. This crack was located in an area of tension under water load and was therefore likely to widen. To prevent leakage, the crack was covered with a 2 mm thick nylon-reinforced butyl rubber sheet followed by a 4 m depth of impervious backfill.

2.6. PRELIMINARY DESIGN OF CFRD

According to the above mentioned criterion, designing can be assigned as Sherard, Fitzpatrick et. al. recommendation (6).

A. CFRD 50 m high

The design of dam with data as follows:

High of Dam : 50 m (from the deepest river)

FRL : 45 m (head)

Hence :

PLINTH (UPSTREAM TOE SLAB)

- Apron thickness : min. 0.4 m (Ref. Cethana)
min. 0.3 m (Ref. Lower Pieman)
- Plinth width : min. 3.0 m
- (Leakage path) $H/20 = 45/20 = 2.25$ m (Ref. Cethana)
 $H/10 = 45/10 = 4.50$ m (Ref. Lower Pieman)
- Rockfill depth : min. 0.9 (General requirement)
(d/s face height)
- Slip form overlap : min. 0.6 m (Ref. Cethana)
min. 0.8 m (Ref. Lower Pieman)
- Consolidation Grouting : 8 m deep, spacing 3 m (Ref. Cethana)
5 m to 15 m depending on 'head' (much dams)
- Curtain Grouting : $0.5 \times h = 22.5$ m deep, spacing 3 m (Ref. Cethana)
 $0.33 \times h = 14.85$ m deep, spacing 3 m (Ref. Murchison & next generation)

EMBANKMENT

- Assume : Rockfill material met all the requirement
- Slope of U/S & D/S : 1 vertical to 1.3 horizontal (depend on requirement)

CONCRETE FACE

- Face thickness : $t = 0.3 \text{ m} + (0.001 \times 45) = 0.345 \text{ m}$
 $t = 0.35 \text{ m}$
- Parapet (crest wall) : using the recommended crest wall arrangement

B. CFRD 100 m high

The design of dam with data as follows:

High of Dam : 100 m (from the deepest river)

FRL : 95 m (head)

Hence :

PLINTH (UPSTREAM TOE SLAB)

- Apron thickness : min. 0.4 m (Ref. Cethana)
min. 0.3 m (Ref. Lower Pieman)
- Plinth width : min. 3.0 m
- (Leakage path) $H/20 = 95/20 = 4.75$ m (Ref. Cethana)
 $H/10 = 95/10 = 9.50$ m (Ref. Lower Pieman)
- Rockfill depth : min. 0.9 (General requirement)
(d/s face height)
- Slip form overlap : min. 0.6 m (Ref. Cethana)
min. 0.8 m (Ref. Lower Pieman)
- Consolidation Grouting : 8 m deep, spacing 3 m (Ref. Cethana)
5 m to 15 m depending on 'head' (much dams)
- Curtain Grouting : $0.5 \times h = 47.5$ m deep, spacing 3 m (Ref. Cethana)
 $0.33 \times h = 29.7$ m deep, spacing 3 m (Ref. Murchison & next generation)

EMBANKMENT

- Assume : Rockfill material met all the requirement
- Slope of U/S & D/S : 1 vertical to 1.3 horizontal (depend on requirement)

CONCRETE FACE

- Face thickness : $t = 0.3 \text{ m} + (0.001 \times 95) = 0.395 \text{ m}$
 $t = 0.4 \text{ m}$
- Parapet (crest wall) : using the recommended crest wall arrangement

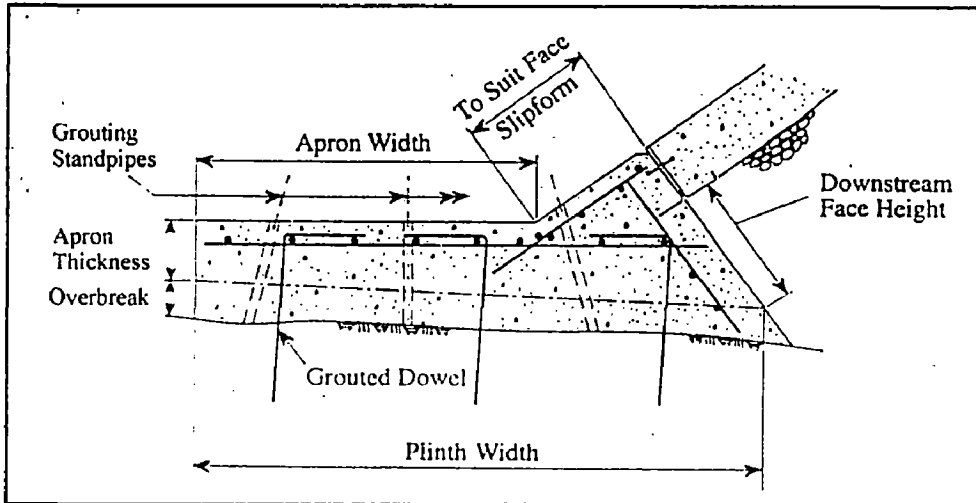


Figure 2.9 : Nomenclature of CFRD

CHAPTER 3

FINITE ELEMENT ANALYSIS OF CFRD

3.1. INTRODUCTION

Basically the concrete face rockfill dam consists of rockfill embankment faced with an impervious concrete slab. The rockfill embankment is generally provided with natural slopes and is inherently stable under all operating conditions. The shear strength of rockfill is thus generally not important for such type of dam.

The overall performance of the face membrane type of rockfill dam depends entirely on the compressibility of the embankment material and the ability of the membrane and its joints to withstand the deformation to which they subjected. The main problem in this type of dam is of cracking of concrete face resulting from high tensile strains and differential settlements.

In recent years the trend has been towards improving the deformation properties of the fill and this has been achieved by placing rockfill in thin layers and compacting with heavy vibratory rollers. The membrane is now constructed after the rockfill has reached virtually the crest level, this being done to preclude deformation of the membrane due to construction settlement.

Settlement of the rockfill can be minimized but not completely eliminated and so to avoid cracking in the impervious face membrane, it is desirable to give it the maximum possible flexibility so that it can follow the deformations without damage. If the settlement and in-plane movement of the face slab could be reliably estimated the joint layout would be properly designed instead of being provided in a more or less arbitrary manner.

Cracks do form in concrete, but if the stresses and strains in the membrane are accurately determined and tension zones properly located, then different alternative designs may be tested to ensure that tension in the concrete is within allowable limits, and then sufficient reinforcement may be provided at these locations, so that cracks are distributed as a pattern of hairline cracks by the reinforcement and are not harmful to the integrity of the concrete face membrane.

A comprehensive mathematical analysis which could correctly predict the prototype behavior of such type of a dam is not yet available. The design of concrete face is largely empirical, modification to design practice being made in the light of performance of each new dam.

Using finite element method as the analytical tool which available at present will lead to better understanding of actual stresses and deformations occurring within the dam section and face membrane.

The finite element analysis was carried out considering plane strain conditions and using a variety of isoparametric, numerically integrated curved parabolic elements. Thus while quadrilateral elements were used for the rockfill, joint elements for the concrete slab-rockfill and rockfill-foundation interface, specially device slender incremental elements were adopted to represent the thin-face membrane in the analysis.

The method of analysis was gradually developed from simple lift linear analysis to a more realistic analysis involving nonlinear material behavior for the rockfill and for the joint element at membrane-rockfill interface, sequential construction and incremental reservoir loading to simulate the construction process and filling of reservoir. Time dependent (creep) deformations of the rockfill were also considered and included in the analysis.

The finite element formulation which has been described in this chapter has been limited only on linear elastic analysis and non linear analysis.

3.2. FINITE ELEMENT FORMULATION

Most applications of finite element method in soil and rock mechanics have been made by adopting or suitably modifying formulation and programmes developed for structural and continuum mechanics. Three basic variation principles for stress analysis employed in structural mechanics are:

- i. The principle of minimum potential energy
- ii. The principle of minimum complementary energy and
- iii. The Hellinger-Reissner mixed principle

Displacements are adopted as primary unknown in the first case, stress are adopted as unknowns in the second case, and both displacements and stresses become primary unknown in the Hellinger-Reissner principle. Procedures based on the first and second and third principles are called the displacement, the equilibrium and the mixed methods, respectively. Often hybrid procedures have been developed in which some displacements or stresses within an element and some stresses or displacements on the boundary of the elements are adapted as primary unknown. The displacements procedure is most commonly employed in Geotechnical Engineering.

The displacements method offers a number of advantages over other methods. It is often more difficult to construct an approximate stress model that satisfies stress equilibrium than to construct a compatible displacement model. On the other hand, in the displacement method, the stresses are derived from computed (primary) displacement, hence the stress may not be as accurate and are often discontinuous across element boundaries. A majority of non linear formulation by finite element method have been written in terms of the displacements.

3.3. BASIC STEPS OF FINITE ELEMENT METHOD FOR LINEAR PROBLEMS

3.3.1. Displacement Method

In Finite Element Method, the structure is visualized as an assemblage of structural elements interconnected at a discrete number of nodal points. The behavior of the structure is studied by knowing the force-displacement relationships for individual elements, and which is defined by stiffness properties of the material. Writing in matrix form the relationship is given by as,

$$\{F\} = [K] \cdot \{\delta\} \quad (3.1)$$

where : $\{F\}$ = the force vector of equivalent loads acting at the nodal points

$[K]$ = the matrix of the stiffness properties of material

$\{\delta\}$ = the displacement vector of the nodal points

In the displacement approach, the total stiffness matrix is assembled for the continuum from the individual element stiffness and the unknown nodal displacements are solved using the known boundary condition and loads.

Thus at any point within the element, the displacement components are defined uniquely by the nodal displacements as,

$$\{u\} = [N] \cdot \{\delta\}^e \quad (3.2)$$

where : $[N]$ = the shape function defined by a suitable polynomial expressing displacement at any point in terms of its coordinates, the polynomial being known as displacement function or model

The strains are determined from the nodal displacements as,

$$\{\varepsilon\} = [L] \cdot \{u\} = [L] \cdot [N] \cdot \{\delta\}^e = [B] \cdot \{\delta\}^e \quad (3.3)$$

and the stresses from the strain as,

$$\{\sigma\} = \{\sigma_0\} + [D] \cdot [\{\varepsilon\} - \{\varepsilon_0\}] \quad (3.4)$$

where: $\{\sigma_0\}$ = the initial stress vector

$\{\varepsilon_0\}$ = the initial strain vector

$[D]$ = the elasticity matrix for the material

The matrix $[D]$ may be either for isotropic or anisotropic material approximately modified to include the nonlinear material behavior.

The choice of element shape and the displacement function is an important part of the finite element analysis and the accuracy of the results achieved depends in a large measure on these factors. In general higher order polynomial yields better results but it's taxing to computer as well as difficult to handle.

3.3.2. Displacement Function

A displacement function should satisfy the following three conditions,

- i. Continuity and compatibility of displacements between adjacent elements
- ii. Should include rigid body displacement
- iii. Should include constant strain state of the element

A general polynomial for the two dimensional displacement functions satisfying the above requirements is in the form of

$$f(x, y) = \alpha_1 + \alpha_2 x + \alpha_3 y + \alpha_4 x^2 + \alpha_5 xy + \alpha_6 y^2 + \dots + \alpha_m y^n \quad (3.5)$$

The constant term in this polynomial satisfies the requirement of rigid body displacement, whereas the linear terms satisfying the constant strain condition. In general higher order polynomial depends on the accuracy required in the problem. The constants are determined by solving a set of simultaneous equations obtained by substituting the coordinates of a node and equating the value to the nodal value.

Thus,

$$\{f\}^e = [C] \cdot \{\alpha\} \quad (3.6)$$

where: $[C]$ = the connection matrix between nodal values $\{f\}^e$ and undetermined parameter $\{\alpha\}$

3.4. STRESS-STRAIN RELATIONSHIPS

Supposes U and V be the displacement in X and Y directions respectively for a point within a two dimensional element. The strain vector at this point is given by,

$$\{\varepsilon\} = \begin{Bmatrix} \varepsilon_x \\ \varepsilon_y \\ \gamma_{xy} \end{Bmatrix} = \begin{Bmatrix} \frac{\partial u}{\partial x} \\ \frac{\partial v}{\partial y} \\ \frac{\partial v}{\partial x} + \frac{\partial u}{\partial y} \end{Bmatrix} = \begin{Bmatrix} \frac{\partial}{\partial x} & 0 \\ 0 & \frac{\partial}{\partial y} \\ \frac{\partial}{\partial y} & \frac{\partial}{\partial x} \end{Bmatrix} \begin{Bmatrix} u \\ v \end{Bmatrix}$$

$$= [L] \cdot \{u\} \quad (3.7)$$

The values of the derivatives of u and v in the above equation can be obtained by differentiating the displacement function adopted. Equation (3.7) will, thus reduce to equation (3.3) expressing the strain as the function of nodal displacements.

The stress-strain matrix for a three dimensional isotropic elastic continuum can be expressed in the matrix form as,

$$[D] = \frac{E}{(1+\nu)(1-2\nu)} \begin{bmatrix} 1-\nu & \nu & \nu & 0 & 0 & 0 \\ & 1-\nu & \nu & 0 & 0 & 0 \\ & & 1-\nu & 0 & 0 & 0 \\ & & & \frac{1-2\nu}{2} & 0 & 0 \\ & & & & \frac{1-2\nu}{2} & 0 \\ & & & & & \frac{1-2\nu}{2} \end{bmatrix} \quad (3.8)$$

In the case of plane strain problem, the strain in the z -directions vanishes ($\varepsilon_z = 0$). Applying this condition to equation (3.8), the relation for plane strain case reduces to

$$[D] = \frac{E(1-\nu)}{(1+\nu)(1-2\nu)} \begin{bmatrix} 1 & \frac{\nu}{1-\nu} & 0 \\ \frac{\nu}{1-\nu} & 1 & 0 \\ 0 & 0 & \frac{1-2\nu}{2(2-\nu)} \end{bmatrix} \quad (3.9)$$

On substituting the value of $\{\varepsilon\}$ from equation (3.3), and writing in matrix form, the equation reduces to,

$$\{\sigma\} = [D] \cdot [B] \cdot \{\delta\}^e - [D] \cdot \{\varepsilon_0\} + \{\sigma_0\} \quad (3.10)$$

3.5. EQUILIBRIUM EQUATIONS

The equilibrium equation is obtained by equating the virtual work done by the external forces to that done by internal stresses. Let the virtual displacement $\{\delta\}^e$ be applied to the nodes of an element causing virtual strain as $\partial\{\varepsilon\}^e$. Let $\{F\}^e$ be the nodal forces vector equivalent statically to the boundary stresses and distributed loads on the element. The equilibrium equation on the basis of principle of virtual work is,

$$[\partial\{\delta\}^e]^T \cdot \{F\}^e = [d\{\delta\}^e]^T \cdot \left[\int [B]^T \cdot \{\sigma\} dv - \int [N]^T \cdot \{b\} dv \right] \quad (3.11)$$

As the relation is valid for any arbitrary virtual displacement, this can be written as,

$$\{F\}^e = \int [B] \cdot \{\sigma\} dv - \int [N]^T \cdot \{b\} dv \quad (3.12)$$

Using the equation (3.10), the equation (3.12) can be written as,

$$\{F\}^e = \int [B]^T [D] [B] \{\delta\}^e dv - \int [B]^T [D] \{\varepsilon_0\} dv - \int [N]^T \{b\} dv \quad (3.13)$$

Here the term $[B]^T \cdot [D] \cdot [B] dv$ gives the stiffness of the element and the other terms are used to calculate the nodal loads due to initial strains, initial stresses and body forces. Expressing in terms of force displacement relationship, the $\{F\}$ can be expressed in nodal terms of nodal displacements by the equation

$$\{F\}^e = [K]^e \cdot \{\delta\}^e$$

A comparison with equation (3.13) gives

$$[K]^e = \int [B]^T \cdot [D] \cdot [B] dv$$

3.6. TYPICAL STRESS PATH

A great variety of stress path occurs in embankment dams (and their foundation). They are often accompanied by a large rotation of principal

stress and may be particularly complex during first reservoir impounding and subsequent operation. It is difficult to reproduce all these real stress paths, even using sophisticated laboratory equipment such as the hollow cylinder or true triaxial apparatus. Nevertheless, it is common to describe the behavior of fills using standards laboratory test. This is particularly so for rockfills.

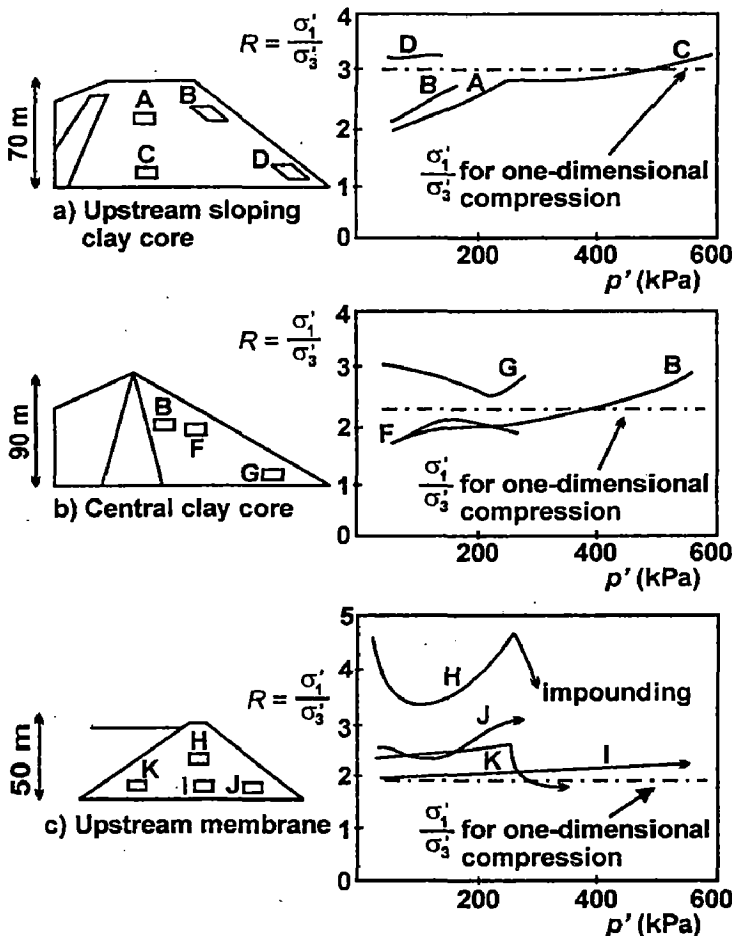


Figure 3.1 : Stress path for three types of rockfill dam

Because of their coarse nature, the tests have to be performed on large samples and are therefore expensive and laborious. Consequently, their number and types are limited. Sometimes both large triaxial and oedometer tests are performed for rockfills, but quite often only results from one of those two tests are available. Therefore, it is necessary to establish which of these is more representative to simulate rockfill behavior in an embankment dam.

It can be argued that the oedometer test, providing a constant stress ratio path,

$$R = \frac{\sigma_1}{\sigma_2} = \frac{1}{K_0}$$

can be better capture till behavior, at least during the construction stage. Although the principal stress ratio, R , is not ideally constant during dam construction, in most cases its values changes within relatively narrow limit and usually around the assumed $R = \frac{1}{K_0}$ value (Figure

3.1). That is why oedometer tests, with R typically between 2.0 and 3.0, give a reasonable prediction of overall rockfill dam behavior during construction.

However, in spite of this, triaxial tests should not be neglected. Apart from defining the rockfill strength envelope, these tests provide a useful insight into stress-strain properties of rockfills too. Also, due to lateral yield, the stress paths in the dam shoulders deviate from the K_0 line towards the strength envelope and can approach those imported by standard triaxial tests (Figure 3.2). It seems that, if rotation of principle stresses is ignored, the typical stress path during dam construction is somewhere between those imposed by oedometer and standard triaxial testing. Ideally, any constitutive model should predict the observed rockfill behavior in both oedometer and standard triaxial tests (if both types test are available). Then, it is reasonable to assume that rockfill behavior may be captured for any stress path in between.

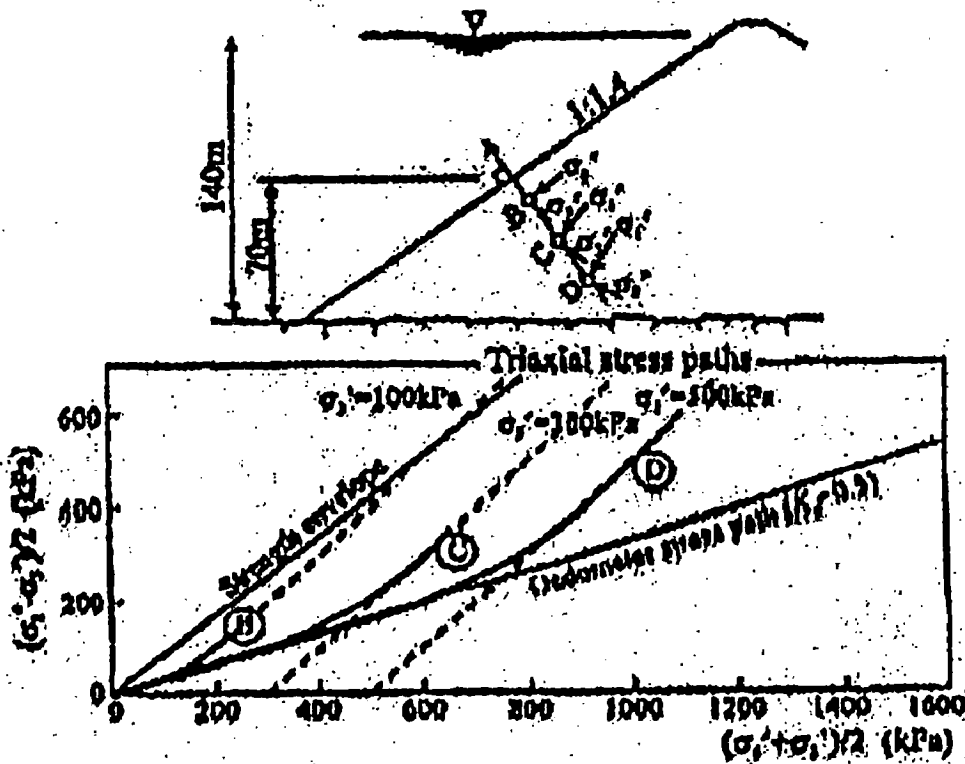


Figure 3.2. Stress path for three points along a line normal to the concrete face of a hypothetical rockfill dam

3.7. CONSTITUTIVE LAWS

It has been repeatedly shown that the most influential factor in the finite element analysis of embankment dams is the modeling of the stress-strain

behavior of the fill by an appropriate constitutive law. However, in spite of the diversity of the stress-strain relationship being used, reasonable agreement has usually been found when the results of finite element analyses (typically movements) have been compared with field observations. This is not surprising bearing in mind the fact that most of the analyses were done after the field measurement had been made.

A constitutive law (stress-strain relationship) is dependent upon many factors viz :

- i. Constitutional factors, which include the characteristics of the soil
- ii. Environment factors, which include the loading characteristics such as confining pressure

The constitutive laws can be broadly classified as follows.

3.7.1. Linear Elastic Analysis

Soils are far from being either linear or elastic. Nevertheless, because of simplicity, geotechnical engineers have often characterized the behavior of real soil using idealized models of linear isotropic elasticity. Reasonable results can only be obtained for conditions far away from failure, when a significant factor of safety operates. These conditions usually prevail in rockfill dams, and thus it is not surprising that linear elastic analyses have been successful in number cases.

Only two elastic constants are needed to characterize the stress-strain behavior of isotropic linear elastic materials. They are usually Young's modulus, E , and Poisson's ratio, ν . In order to obtain reasonable values of stresses and particularly displacements, it is essential to find the most suitable values of the above elastic constants. A 'constant equivalent compressibility' method for determination of Young's modulus using data from oedometer tests was proposed by Penman and Charles (1973). They showed that the internal distribution of vertical displacement during construction of a thick, broad layer (one dimensional condition) possessing self weight, can be predicted with little error by the use of constant Young's

modulus determined to give the correct final displacement of a point half-way up the complete layer.

Justo and Saura (1983) carried out a 3-D linear analysis of El-Infiernillo dam wherein the parameters E and ν used in the analysis were derived from the behavior during construction. The value of Young's Modulus E was found out from Oedometric modulus as described:

$$E = E_{oed} \frac{1 - \nu - 2\nu^2}{1 - \nu} \quad (3.14)$$

and the Poisson's ratio ν was estimated by the method used by Simmons (at Singh, 1991)

3.7.2. 'Power Law' Models

These models were developed in an attempt to fit the data from the oedometer test, which is sometimes the only available test for fills (e.g. rockfill). For granular materials, the relationship between volumetric strain, ϵ_v and axial stress, σ_a in a one dimensional compression test can be described by a power law of the form (Rowe at Potts and Zdravkovic, 2001):

$$\epsilon_v = C \left(\frac{\sigma_a'}{p_a} \right)^D \quad (3.15)$$

where p_a is atmospheric pressure in the same units as σ_a' , C , and D are dimensionless parameters. Skinner (at Potts and Zdravkovic, 2001) used the above relationship to derive the closed form solution for the settlement profile on the centre line of an embankment of height H constructed of rockfill of bulk unit weight :

$$s = \frac{C_1 \gamma^D}{D+1} \left[H^{D+1} - (H-h)^{D+1} - h^{D+1} \right] \quad (3.16)$$

where s is the settlement of a marker placed at a height h above the foundation and $C_1 = \frac{C}{p_a^D}$. Settlement in this case are treated as one dimensional and vertical effective stress is presumed equal to the overburden pressure (pore pressure is zero). The former results is under estimation of

settlements, the latter is an over estimation. The two effects are likely to be relatively small and compensating.

By differentiating equation (3.3), the expression for the tangential constrained modulus, E'_c , can be obtained. The tangential Young's modulus, E'_v , can be derived using the value of Poisson's ratio, ν , estimated from K_0 value (i.e.

$\nu = \frac{K_0}{(1 + K_0)}$) from elastic theory, where K_0 is related to the angle of shearing

resistance ϕ according to $K_0 = 1 + \sin \phi$, or determined directly from the

oedometer test as $K_0 = \frac{\sigma_r}{\sigma_a}$, by measuring the radial stress σ_r . If a constant

K_0 value is assumed (a frequently made assumption for soils), at least three model parameters are required to represent loading condition.

3.7.3. Nonlinear Stress-Strain Behavior

The relationships between stress and strain in soils are more complicated than the simple, linearly elastic ones described in previous section. The stress-strain relationship is being represented by a number of lines. Two general forms which are available for this purpose are tabular forms and functional forms.

Tabular Form :

The stress-strain results obtained from laboratory tests can be used directly in tabular form for finite element analysis as was done in case of Duncan Dam by Einstein, Krishnayya and Morgenstern (1972). For this, several points of the stress-strain curves are fed as input to the computer in the form of number pairs denoting stress and strain at these points, The material parameters E and ν are interpolated for the desired level of stress or strain by a suitable interpolation method, if it is on a single curve. If instead, there is more than one curve, as will be the case for materials whose stress-strain relationship is a function of the confining pressure; interpolation is done for the different

curves as well. The tabular form is cumbersome as it occupies a relatively large storage space in the computer.

Functional Form:

An obvious advantage of the use of the mathematical function is that, in contrast to the tabular form in which a number of data points are input, only a few parameters are needed to describe the curves.

The most widely used function for simulation of stress-strain curves in finite element analysis was formulated by Duncan and Chang (1970) using Kondner's (1963) finding that the plots of stress versus strain in a triaxial compression test is very nearly a hyperbola. The procedure uses Mohr Coulomb failure criterion and develops relationships for the tangent modulus and Poisson's ratio which may be expressed in terms of total or effective stresses. This model has been widely used (Botta et al. (1985), Kulhawy and Duncan (1972), Priscu, Stematiu and Dobrescu (1985) and Yasunaka, Tanaka and Nakano (1985) and is being briefly described below.

The tangent modulus E_t at a particular stress level is given by

$$E_t = (1 - mR_f)^2 E_i \quad (3.17)$$

where, R_f is the failure ratio defined as the ratio of the deviatoric stress at failure to the ultimate deviatoric stress given by

$$(\sigma_1 - \sigma_3)_f = R_f (\sigma_1 - \sigma_3)_{ult} \quad (3.18)$$

where σ_1 and σ_3 are the major and minor principal stresses respectively.

$m = \frac{(\sigma_1 - \sigma_3)}{(\sigma_1 - \sigma_3)_f}$ known as the mobilization factor and is defined as the ratio of the deviatoric stress $(\sigma_1 - \sigma_3)$ acting at any element to the failure deviatoric stress $(\sigma_1 - \sigma_3)_f$. E_i is the initial modulus of elasticity for a particular confining pressure. The value of E_i is defined by Janbu (at Singh, 1991) as follows:

$$E_i = Kp_a \left(\frac{\sigma_3}{p_a} \right)^n \quad (3.19)$$

where: σ_3 = the confining pressure

p_a = the atmospheric pressure expressed in the same unit as E_t

K = a dimensionless number termed the modulus number

n = a dimensionless exponent

Expressing the compressive strength and confining pressure in terms of Mohr-Coulomb failure criterion and using c and ϕ as strength parameters, the value of tangent modulus of elasticity can be expressed as:

$$E_t = \left[1 - \frac{R_f (1 - \sin \phi) (\sigma_1 - \sigma_3)}{2c \cos \phi + 2\sigma_3 \sin \phi} \right]^2 K p_a \left(\frac{\sigma_3}{p_a} \right)^n \quad (3.20)$$

in which c is the unit cohesion and ϕ is the angle of shearing resistance for the material. The expression for tangent Poisson's Ratio has been given by Kulhawy and Duncan (1972) as follows:

$$\nu = \frac{G - F \log \left(\frac{\sigma_3}{p_a} \right)}{(1 - d\varepsilon_a)^2} \quad (3.21)$$

$$\text{in which } \varepsilon_a = \frac{(\sigma_1 - \sigma_3)}{(E(1 - mR_f))} \quad (3.22)$$

where: G = value of initial Poisson's ratio ν_i , at one atmospheric pressure

F = reduction in initial Poisson's ratio for a ten fold increase in confining pressure

d = dimensionless parameter expressing the rate of change of ν , with strain

More complicated forms of Kondner's hyperbolic functions have been suggested Hansen (1963) as follows:

$$\left. \begin{aligned} (\sigma_1 - \sigma_3) &= \sqrt{\frac{\varepsilon_a}{(a + b\varepsilon_a)}} \\ (\sigma_1 - \sigma_3) &= \frac{\sqrt{\varepsilon_a}}{a + b\varepsilon_a} \end{aligned} \right\} \text{ and } \quad (3.23)$$

where a and b are constants analogous to a and b used in Kondner's equation.

Al-Hussaini and Radhakrishnan (at Singh, 1991) have extended the Kondner's hyperbolic form to develop non-linear octahedral stress-strain model in the form:

$$\tau_{oct} = \frac{\gamma_{oct}}{a + b\gamma_{oct}} \quad (3.24)$$

where a and b are analogous but not identical to a and b in the Kondner's relationship. τ_{oct} and γ_{oct} are octahedral shear and octahedral shear strain defined by

$$\left. \begin{aligned} \tau_{oct}^2 &= \frac{1}{9} \left[(\sigma_1 - \sigma_2)^2 + (\sigma_2 - \sigma_3)^2 + (\sigma_3 - \sigma_1)^2 \right] \\ \phi_{oct}^2 &= \frac{2}{3} \left[(\varepsilon_1 - \varepsilon_2)^2 + (\varepsilon_2 - \varepsilon_3)^2 + (\varepsilon_3 - \varepsilon_1)^2 \right] \end{aligned} \right\} \quad (3.25)$$

Relationship similar to those of Kulhawy and Duncan (at Singh, 1991) were developed as follows:

$$G_t = \left(\frac{1 - S_f \cdot \tau_{oct}}{\tau_f} \right)^2 G_i \quad (3.26)$$

where G_t is the tangent shear modulus, S_f is the shear ratio similar to the failure ratio defined by Kondner's (1963) and is given by

$$S_f = \frac{\tau_f}{\tau_{ult}} \quad (3.27)$$

G_i is the initial value of the tangent shear modulus given by :

$$G_i = C p_a \left(\frac{\sigma_3}{p_a} \right)^m \quad (3.28)$$

where C and m are pure numbers.

3.7.4. K - G Model

It was recognized a long time ago that modelling of soils in terms of the bulk modulus, K, and the shear modulus, G, had some advantages over the use of Young's modulus, E, and Poisson's ratio, ν .

This model was used by Domaschuk and Wade (1969) and Domaschuk and Valliappan (1975); $K_t - G_t$ models employed by Izumi,

Kamemura and Sato (1976). In comparison with the hyperbolic model, this model is simpler and only five parameters are required. For unloading an additional parameter is needed. As with the hyperbolic model discussed above, it seems that a good fit to both oedometer and triaxial test data cannot be obtained.

3.7.5. Elasto-plastic Model

It is well known that elasto-plastic stress-strain relationships are capable of modeling the behavior of real soils more closely. Taking into account the influence of stress path on soil behavior, elasto-plastic finite element analyses should provide a better prediction of stresses and especially movements in embankment dams. Unfortunately, in spite of the existence of different elasto-plastic constitutive models, these have not been widely used in practice. One reason might be considerable complexity of such analyses. Another can be found in the difficulties connected with testing of fill materials, especially rockfills.

Nevertheless, there have been attempts in the past to characterize the behavior of rockfill using elasto-plastic stress-strain relationships. The use of various perfectly elastic plastic models gave, essentially, an elastic solution as no (or only small) zones of plastic yielding were discovered. Significant factors of safety usually operate in rockfill dams and the modeling of plastic behavior at peak and post-peak, even with the inclusion of hardening or softening behavior, is unnecessary. Modeling such behavior is only of importance in special circumstances when a shear failure surface develops.

The inclusion of plasticity pre-peak has usually been associated with the modeling of dilatancy, i.e. the tendency of well compacted granular fills to increase, or soft clayey fills to decrease, their volume on shearing. There is both laboratory and field evidence that suggest that dilatancy is unlikely to occur widely in rockfill dams. Thus, the use of a complex elasto-plastic model to account for dilatancy alone is not warranted. However, the modeling of the plastic behavior pre-peak has another, more subtle advantage which concerns the patterns of deformation during yielding. Namely, in contrast to the elastic

strains which are dependent on the stress increment only, the plastic strains depend on the accumulated stress as well. The implication of this was clearly demonstrated by Naylor (at Potts and Zdravkovic, 2001) who analyzed the behavior during construction of a clay core embankment dam using two different constitutive models: 'variable' elastic and critical state elasto-plastic. He showed that the deformation behavior was sensitive to the type of model being used even though both models produce similar triaxial test stress-strain curves.

There exist a large variety of elasto-plastic models that have been proposed in order to characterize the stress-strain and strength behavior of soils. Most of them have been conceived from the concept of critical state soil mechanics. The Cam clay model and its various modifications have been increasingly used in the finite element analysis of various dams and embankments. Unfortunately, most of these applications were associated with embankments on soft ground where the overall behavior is usually governed by the soft material present in the foundation.

However, the suitability of critical state models to predict the behavior of till material is questionable. These models were originally developed for sedimentary clays. Compacted fills have a behavior pattern similar to that of sands. Thus, the elastoplastic constitutive models originally proposed for sands can better capture the behavior of compacted fills, even of clays. Rockfill can be considered as an extreme granular material.

Elasto-plastic models for sands usually separate the effects of consolidation and shearing. During consolidation deformations are governed mainly by crushing and yielding, of interparticles contacts. During shearing to high stress ratios deformations develop also due to sliding and rolling. To account for different plastic deformations during consolidation and shearing, so called 'double hardening' models have been proposed.

3.8. LAYERED ANALYSIS, STIFFNESS OF THE SIMULATED LAYER AND COMPACTION STRESS

Embankments are built up in relatively thin horizontal layers. Consequently, there will be a large number of layers during the construction of a large dam. The limitations of computer modeling require relatively thick layers to be used in the idealization (Figure 3.3).

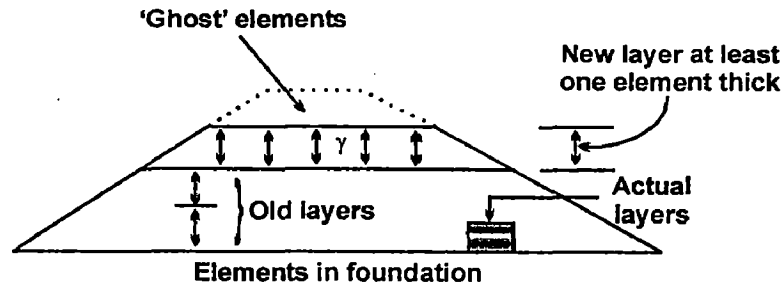


Figure 3.3 : Finite element modeling of fill construction

In the past, to provide an insight into the errors involved, the closed form solution of the incremental analysis was usually compared to the finite element 'layered' analysis using a one dimensional model which represents either a soil column or a fill of large lateral extent. It was concluded that as few as five layers is usually sufficient in embankment dam analyses if a nonlinear constitutive model is employed. However, the implication of this finding if an elastoplastic model is employed, has not been considered. It will be shown below that significant errors can occur if the layers are too thick when the effects of compaction are modeled, even the case elastic constitutive models (linear or nonlinear).

The effect of compaction is to increase horizontal stresses in a layer as further fill is placed. This effect typically becomes in-significant when 3 to 5 m of fill has been placed. Construction of a new layer is essentially performed by a gravity 'turn on' analysis. For a broad fill, the vertical stresses are equal to the overburden pressure, whereas the horizontal stresses are determined by the value of K_0 input by the user.

To provide an insight into the effect of modeling compaction stresses in a 'newly' constructed layer on the settlement profile during dam construction, a finite element 'layered' analysis using a one dimensional mode, (no lateral

strain) can be performed. A 50 m high soil column is constructed in four, ten and twenty layers respectively. The fill is modeled using the Lade's hardening model with the parameter values derived for the Winscar sandstone rockfill. In the first set of analyses the horizontal stresses in a 'newly' constructed layer were determined by the value of Poisson's ratio $\nu = 0.45$ leading to

$$K_0 = \frac{\nu}{1 - \nu} = 0.80.$$

In the second set of analyses the horizontal stresses were reduced to be equal to $K_0 = 0.25$ times the calculated vertical stresses, where $K_0 = 0.25$ is a typical K_0 value predicted by the idealized, single element oedometer test on the sandstone rockfill using the Lade's double hardening model (Kovacevic at Potts and Zdravkovic, 2001).

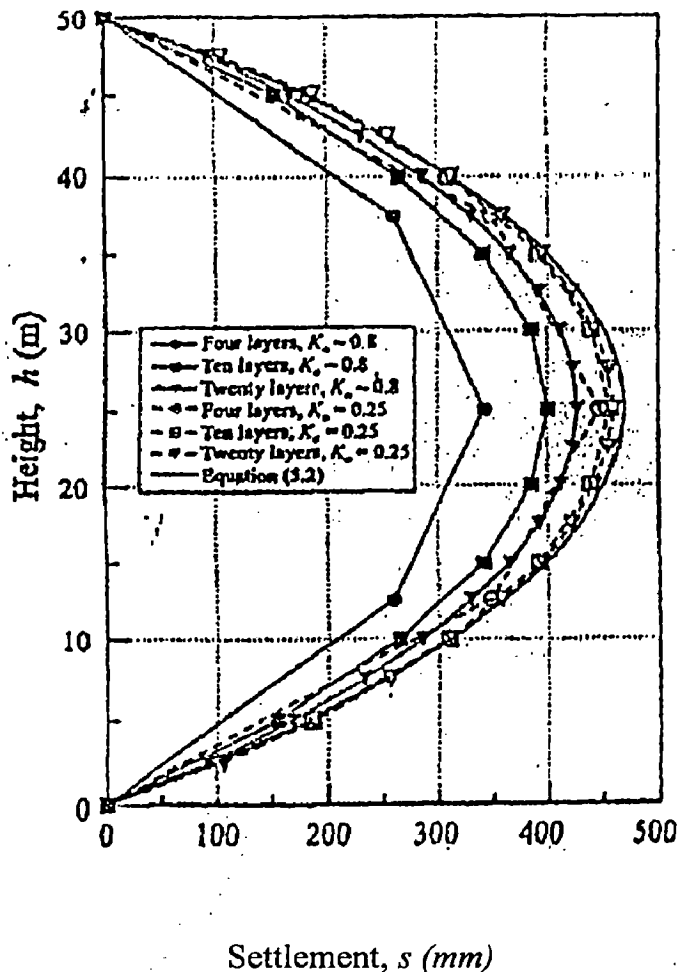


Figure 3.4. Effect of number of layers and compaction stress on settlement of a soil column

The results of this exercise are presented in Figure 3.4. It can be seen that the second set of analyses (broken lines with open symbols) predicts settlements profiles which are nearly independent of the number of construction layers used. This is not so when the higher horizontal stresses due to

compaction were modeled as in the first set of analyses (full lines with shaded symbols). However, the larger the number of layers employed, the more the settlement profile approaches to that predicted by the second set of analyses.

Although the one dimensional model (no lateral strain) is a good approximation of dam construction (at least in the central portion of the dam), and therefore is very useful in determining the optimum number of layers in the finite element analysis, it is important to recognize the particular influence of the stiffness of the new layer in two dimensional analysis. This is due to the difference in bending between one 'thick' simulated layer in finite element analysis when gravity is suddenly applied, and progressively occurring bending of several 'thin' layers in the field. It was recognized that some stiffness between zero and the full in-place stiffness would make the finite element layer equivalent to the real situation, and some work has been done in this respect for both linear and nonlinear elastic materials. Bearing in mind the complexity associated with modeling of compaction stresses (and, in the case of clayey fills, initial suctions), no attempt has been made to include these consideration in the example reported. Consequently, a negligible stiffness assigned to the layer of elements during construction results in an overestimate of deformation in the underlying layers. The effects of this when fills are modeled as elasto-plastic material is unknown, but is likely to be small.

CHAPTER 4

ABOUT THE PROGRAMMES

4.1. PENTAGON3D

PENTAGON3D finite element analysis software, which is developed by Emerald Soft P.E. South Korean, enables users to perform the following tasks:

1. Build computer models of geotechnical structures
2. Apply operating loads or other design performance conditions
3. Study physical responses, such as deformation level and stress distributions

The PENTAGON3D program has a comprehensive Graphical User Interface (GUI) that gives users easy, interactive access to program functions, commands, documentation, and reference material. The users use the GUI for virtually all interactive PENTAGON3D work. The GUI provides an interface between users and the PENTAGON3D program, which commands drive internally. Each GUI function – a series of picks resulting in an action – ultimately produces one or more PENTAGON3D commands that the program executes and records on the input history file. An intuitive menu system helps users navigate through the PENTAGON3D program.

The PENTAGON3D program is organized into three basic levels:

1. PENTMESH
2. PENPRE
3. PENPOST

The PENTMESH level acts as a gateway into and out of the PENTAGON3D program. It is also used for certain global program controls such as build the model, input and clearing the database, loading or stages, and

solve the FEM data with the main processor, Frontdbx. When users first enter the program, they are at the PENTMESH level. At the PENPRE level, the model including data input from PENTMESH level are verifying. The boundary condition and the sequence of construction could be easily checked to find out the errors. The PENPOST is the level to evaluate the results of a solution.

The program, which is permitted to be used for limited version only by the developer, is feasible to cope with 700 elements of 8-noded isoparametric hexahedral and 1500 nodes. The program has been executed on PC PENTIUM III – 1000 MHz.

4.2. PENTMESH

PENTMESH is the preprocess program of PENTAGON3D system. These provide the full graphical user interface to complete the analysis model including the geometry, the material properties, the boundary condition and the construction stages etc. The screen of PENTMESH is categorized with two groups in the main menus. The one group is mainly used to form and to display the entities in the workspace. The entities mean the nodes and the elements. The elements are composed with the quadratic, the frame, the truss, and the spring element types. The menus are : (1) Edit Menu (2) Model Menu (3) Mode2 Menu (4) Delete/Select Menu (5) Display Menu (6) Set Menu (7) MeshGen Menu (8) Layer Menu and (9) Misc Menu. The other menu group is mainly used to do the works except forming the entities, they are: (1) File Menu (2) View Menu (3) FEM Menu and (4) Help Menu.

A short description about the functions of the various menus following:

1. Edit Menu: The menu for copy and paste the points and the elements
2. Model Menu: This menu specifies the mouse mode to a certain mode (or state). Once users choose a mode, the mode is effective until another mode is selected. The menu contains: Zoom Mode, Select Points, Deselect Points, Relive Points, Add Points, Move Points, Select Elements (Within Box), Deselect Elements, Pan and Distance between Two Points

3. **Mode2 Menu:** This menu specifies the elements used on the model and generate the meshing on the geometrical plane. The menu contains: Add Quad3 Elements, Add Quad4 Elements, Add Truss2 Elements, Add Spring Elements, Add Frame2 Elements, Find Nodal Coordinate, Add Point from 2 Points, Add Point from 3 Points, Add Point from 3 Points Arc, Point L0 – Point S0 – Point L1 – Point S1, Add Quad6 Elements, Add Quad8 Elements and Moving Line Node
4. **Delete/Select Menu:** The menu is used to delete the points and the elements, which are selected. The menu contains: Select All Active Points, Select All Active Elements, Deselect All Points, Deselect All Elements, Delete Selected Points and Delete Selected Elements.
5. **Display Menu:** The display Menu controls the screen display by the view scaling and the view translation. With the various menu lists, users can choose the preferred view by selecting the viewing items, refreshing the window, displaying entire model, displaying the reduced model, displaying previous screen scale, and translating the model. The menu contains: Display Toggle, Redraw, Redraw All, Zoom Out, Pervious View, View Up, View Down, View Left, and View Right.
6. **Set Menu:** The Set Menu specifies the various settings for the modeling environment. The menu contains: Analysis range, Coordinate Resolution, Entity Toggle, Entity Capacity, Entity Scale, Entity Color, Print Offset/Scale, Background Color, Save Time Interval, Options, Grid Size for Node Numbering, and Set Star Number of Entities for Save Process.
7. **MeshGen Menu:** In MeshGen Menu, there are sub-menus to create the finite element geometry. Users can generate elements and nodes, mirror the mesh, copy the mesh, rotate the mesh and so on. The menu contains: Generate Quad4, Generate Truss2, Generate Spring, Generate Frame2, Mirror Elements, Add a Point, Add (Generate) Points, Copy Points, Move a Point, Move Points, Move Point onto a Circle, Rotate Points, Rotate Seq. No, Change Element Type, Smoothing, Generate Points From Background, Undo, Covert to Quad6 Quad8, and Renumber.

8. **Layer Menu:** In the Layer Menu, the layers are defined for the 3D mesh generation and boundary condition, the construction and loading conditions and so on. The number of input layers for each Layer Menu is limited to 300 and that of sub-layers is limited to 1500. The layer is defined for the selected nodes or elements. The sub-layer is created when some nodes or elements are selected. The menu contains: Coordinate Layer, Boundary layer, Add Element layer, Change Element layer, Remove Element layer, Calc Residual Force Layer, Prescribed Disp Layer, Gravity Force layer, Surface Force layer, Point Load Layer, Residual Force Layer, Prestress Layer, Prescribed Head layer, Review Bound layer, Point Flux layer, Surface Flux Layer and Temperature layer.
9. **Misc Menu:** In this menu, users can change the material number, boundary type, degenerate elements or other function which used to modify the element model. The menu contains: Material No, Mechanical Boundary, Arc layer, Degenerated Hexa Layer, Node Sublayer List, Element Sublayer List, Remove Unused Sublayer List, Load Function for Time History Analysis, Ground Motion Function for Ground Motion Analysis and Current Coordinate \leftrightarrow Slice Coordinate.
10. **File Menu:** The menu used for clears all the database of current project from memory, open the file, save the file or others function which is connected to arranged the file. The menu contains: New, Open, Save, save As, Import, Print, Print Preview, Print Setup, and Exit.
11. **View Menu:** In the View Menu, users can set the toolbar and the status bar to be displayed in the PENTMESH window, and users can view the model and the result in 3D in PENPRE and PENPOST respectively. The PENPRE and the PENPOST are executed by clicking the menu then another window will pop-up. The menu contains: Toolbar, Status Bar, 3-D Preview by PENPRE, 3-D Result by PENPOST, 3-D Preview by PENPRE without recreation FEM Data, 3-D Result by PENPOST without recreation FEM Data.
12. **FEM Menu:** This menu used to complete the FEM data such as analysis control, material properties or stages configuration. The menu contains:

Project ID, Analysis Type, Analysis Control, Material Property, Stage Configuration, Verify Stage/Layer, Set Work Space Property, save FEM Data, Analyze by Frontdbx with recreation FEM Data and Analyze by Frontdbx without recreation FEM Data.

4.2.1. Slice on PENTMESH

The real three-dimensional entities (elements and nodes) are created and specified in Layer Menu. The real three-dimensional entities are described and prescribed by combining the two dimensional entities with the concepts of slices. Here, the two-dimensional entities are just the ones which view on the PENTMESH work space which represents the two dimensional X-Y plane. And the slice represents the remaining z axis, after creating the multiple X-Y plane along to the minus (-) z axis direction, each X-Y plane is called the Slice. The slice 0 means the first X-Y plane, the largest z coordinate, and the Slice 1 means the second X-Y plane, the next largest z coordinate, etc. The slices are created in the Layer – Coordinate Layer Menu, in which the slices are created with assigning the z coordinate at each slice.

In view of the node connection, there are three element forms in PENTMESH work space, because the element is combined by linking the nodes. They are: (1) Quad4: consist of 4 node's links, (2) Quad8: consist of 8 node's links, and (3) Frame, Truss, Spring: consist of 2 node's link. Therefore, the elements can be created after nodes are created.

4.2.2. Creation of 3D Element that Use 2D Entity

Addition of three-dimensional element in PENTMESH is accomplished in 'Layer – Add Element Layer Menu'. The two-dimensional entity and three-dimensional shape for each type of added three-dimensional elements are the following. The example below is the case for adding 3D elements in one slice from 2D entity. If several slices are selected, 3D elements are added in the each selected slices. This study creates 3D 9-node solid elements using 2D

Quad4 element. Select 'Slice 3" in 'Applied Slice' column in the prior figure, then 3D 8-node solid elements are created between slice 3 and 4.

4.2.3. Degenerate Elements

This model is used to generate elements due to the shape of the elements on the slope valley of the abutments.

Users should specify it in 'Misc – Degenerated Hexa Layer' Menu in advance of degenerated elements, then the dialog box is pop up. Front Slice Surface No. represents of surface number of divided element part. Front Slice No. represent front element slice number of where the generate elements exists. When the generated exist among Add Element Layer List, 'Degenerated' check box should be check such as in box 'Add Element layer Configuration". If the degenerated element does not exist in the 'Applied Slices' users should not check on the 'Degenerated' button, reversely, but if the generated element exist in more than one slices among the selected 'Applied Slices', users should check on the 'Degenerated' button. A this time, the dialog box of 'Degenerated Hexa' pop up. In this dialog box, users should choose the applied position of added elements. Front position means the element which is surface contact to front slice. Rear position means the element which is in corner contact to front slice.

4.3. PENPRE

PENPRE can be used to check the input data before being analyzed by the FEA solver, Frontdbx. By using PENPRE, various input information can be displayed such as the model evolution along construction stages, the boundary conditions and the loading conditions. The graphics of PENPRE is programmed by OpenGL, the 3D graphic library; the model can be rendered with beautiful color and lights, and also can be cut, rotated, and even mirrored simply. The screen of PENPRE displays the first stage of construction. The next step for check of the sequence of construction, users can select Control – Go to the Specified Stage Menu to check the stages. Users can check the element status

or material color in this level according to the stage of construction. For check of the boundary conditions, users can select Set – Display Entity Menu to see the type of boundary and the direction.

4.4. PENPOST

PENPOST is the level in which users could analysis the solution from the solver Frontdbx. In PENPOST, as users open the input file name, the corresponding post-processing result file (*.pos) is opened automatically. The role of input file for PENPOST is to provide the information such as the geometry, the boundary condition, the loading condition and the save condition. The role of result file (*.pos) is to provide PENPOST with the analysis result only. PENPOST can display the FEA result in texts, contours and vectors. Some items are displayed in global coordinate systems and other items in local coordinate system.

A short description about the functions of the various menus following:

1. **File Menu:** In this menu the FEM data could be opened and saved. The menu contains: Open, Open Environment, Save Environment, Save Environment, Save as Environment and Exit.
2. **Set Menu:** Users could set the entity related items and the environmental variables, such as rendering light the object, select color of element, material or boundary. The menu contains: Information, Display Entities, Element Status and Font Size.
3. **Constraint Menu:** This menu is used to restrict the coordinate and the entity number for specific purpose. The menu contains: Display range and Display Entity.
4. **View Menu:** This menu is used for adjusting the screen menu for specific object such as zooming, mirror or rotates the object. The menu contains: Select View, Set View Parameter, Redraw, Previous Zoom, Zoom In, Rotate U, V, W axis and Mirror.
5. **Control Menu:** Users can specify the stages that require to be checked. The menu contains: Next Stage, Pervious Stage, Go to Specified Stage,

Next Time/Mode, Previous Times/Mode, Start Animation and Stop Animation.

6. Function Menu: In this menu users can view the Eigen values, get the results in text format and save the result in the text file. The menu contains: Eigen Value, Graph, Save the Result History, and Save Image to File.

4.5. STEPS IN MAKING THE MODEL

PENTAGON3D is the program that uses 2D entities with layer to make 3D entities. The following steps are used in making the model at the PENTMESH level:

1. Set of the Coordinate Range
2. Input Nodes with Add a Point Menu
3. Generate Nodes with Add Point Menu
4. Create 2D four node quadratic elements
5. 2D node renumbering
6. Assign the material number to the 2D elements
7. Assign the 2D boundary
8. Set of the material properties for each material numbering in FEM – Material Property Menu. In this stage the 15 material properties for each material are given in the following order:

Young modulus of elasticity, Poisson's ratio, Unit weight, Cohesion, Friction Angle, K0-X, K0-Y, K0-Z, n (Ei exponent), Kb (Bulk number), m (Kb exponent), Pa (the Atmospheric pressure), Rf (Failure ratio), K (the modulus number) and Kur (the Corresponding modulus number)
9. Set of the stage configuration for the construction system and the analysis in FEM – Stage Configuration Menu. The sequence of construction was detailed in this level.

10. Set of 3D coordinate from 2D nodes with Coordinate Layer Menu. Coordinate Layer Menu used for users in making slice of a 3D model from 2D model.
11. Degenerate elements such as described at previous paragraphs.
12. Add the 3D elements from 2D elements with Add Element Layer Menu. Add Element Layer connected with the stage configuration which is used for determines the sequence of element was built accordance to the stages.
13. Set of the 3D mechanical boundary condition from 2D nodes with Boundary Layer Menu, Boundary Layer used for establishes the boundary type in each node, users should determine for fixed, free or rotational type in x, y, z direction.
14. Add the body force with Gravity Force Layer. All element defines in the model should be identified with the gravity force.
15. Add the surface pressure with Surface Force Layer Menu. In this stage users should determine the node which is connected with the water pressure load.
16. Add the head of reservoir for each stage by Prescribed Head Layer Configuration Menu. In this stage users should determine the node which is connected with the total head in upstream and downstream.
17. Add the review bound layer by Review Bound Layer Menu. In this stage users should determine the node which is connected with the total head in downstream.
18. For seismic analysis, add ground motion stage in Stage Configuration Menu. Users should provide the additional data of ground motion history and scale the ground motion function to obtain the desirable values of peak acceleration.
19. Set of Analysis Control in FEM – Analysis Control Menu. The program solves the set of simultaneous linear equation with frontal solver method and the convergence criterion was fixed in this level.
20. Verify 3D FEM data with PENPRE level

21. Run solver process, Frontdbx.
22. Check the result at PENPOST level.

CHAPTER 5

RESULTS OF ANALYSIS

5.1. GENERAL

Concrete face rockfill dam of height 50 m and 100 m, located in a narrow valley with slope of wall at 1V:1H, have been used for the analyses purpose. The typical section is shown in Figure 5.1. For both the height, the bottom width is fixed at 20 m. The dam has a water tight impervious layer placed on the upstream slope with a "cushion" layer of finer processed rockfill between the concrete face plate and the rockfill to provide uniform support for the face plate. Poorer quality rockfill has been used as secondary rockfill with zones of free draining rock incorporated to allow discharge of leakage. Should this occurs, as the rockfill is free draining, pore pressure do not develop in the dam and the upstream and the downstream slopes are commonly at the angle of repose of the rockfill.

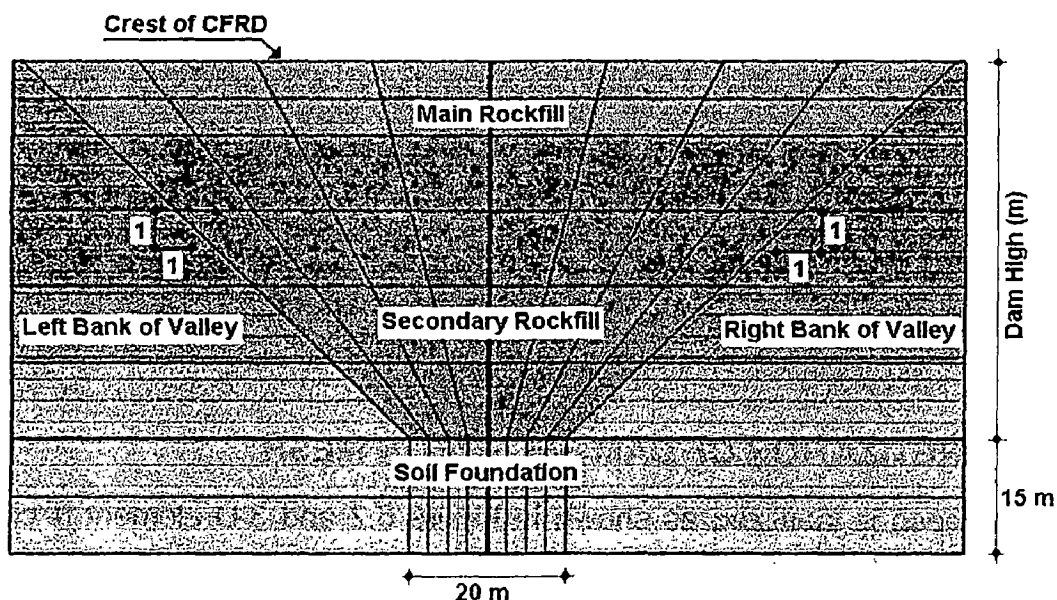


Figure 5.1 : Typical of Concrete Face Rockfill Dam from Downstream View

The slopes or the angle of repose of upstream and downstream dam faces are varied from 1V:1.30H; 1V:1.35H; 1V:1.40H; 1V:1.45H and 1V:1.50H to study the effect of slope on the behavior of dam. Free board is kept as 5 m. The soil foundation for dam is included in analysis up to depth of 15 m. The dams usually are situated in irregular shapes of valley but to reduce the size of the problem, the valley profile has been assumed symmetrical about the centre line of the valley and, therefore, only a half of the dam has been considered in the analyses.

The anticipated seismic response and performance of modern CFRDs has received only limited attention in published literature. Many engineers have argued that the CFR dam is inherently safe against potential seismic damage (Sherard and Cooke 1987) since: (1) The entire CFR embankment is dry and hence earthquake shaking cannot cause pore-water pressure build up and strength degradation; and (2) the reservoir water pressure acts externally on the upstream face and hence the entire rockfill mass acts to provide stability; whereas by contrast in earth-core rockfill (ECR) dams this may be true only for the downstream rockfill shell. Notwithstanding the merit of these arguments, it is pointed out that, to date, no modern CFR dam has been tested under strong seismic shaking to prove or disprove the adequacy of its various design features. In fact, most CFR dams have been built in areas of extremely low seismicity, such as Australia and Brazil, and it seems that some of the design concepts and features have evolved with no consideration to their seismic performance.

Hence besides the study of a CFRD under static load condition, the probable performance of CFRD due to earthquake shaking will also be observed and evaluated in this study by applying different levels of peak acceleration.

5.2. DISCRETIZATION OF DAM SECTION IN MESH

The mesh is idealized as shown in Figure 5.2 and 3-D element is created using that figure. The idealized mesh may also be called 2-D entity will be made into several numbers of slices. For this case, number of slice is 6 and started from 0, 1, 2,

3, 4 & 5. The 3-D element of dam may not be more than 500 numbers of elements because of PENTAGON-3D's discretization for standard version. The optimum number of element has been made into 420 numbers of 8 noded brick elements; each node has 3 degrees of freedom. The mesh consists of 105 nodes on a slice, thus having 1890 degrees of freedom. Since the valley is symmetrical in the z-direction, all the nodes on the central section have been assigned zero movement values in that direction. To simulate sequential construction, the dam is assumed to be raised in 5 layers with the height 10 m and 20 m respectively for 50 m and 100 m high and be filled in 4 stages. The numbers of elements in the 5 stages of construction are 34, 44, 54, 64 and 84 respectively. The element numbering has been done from left to right and from top to bottom layer.

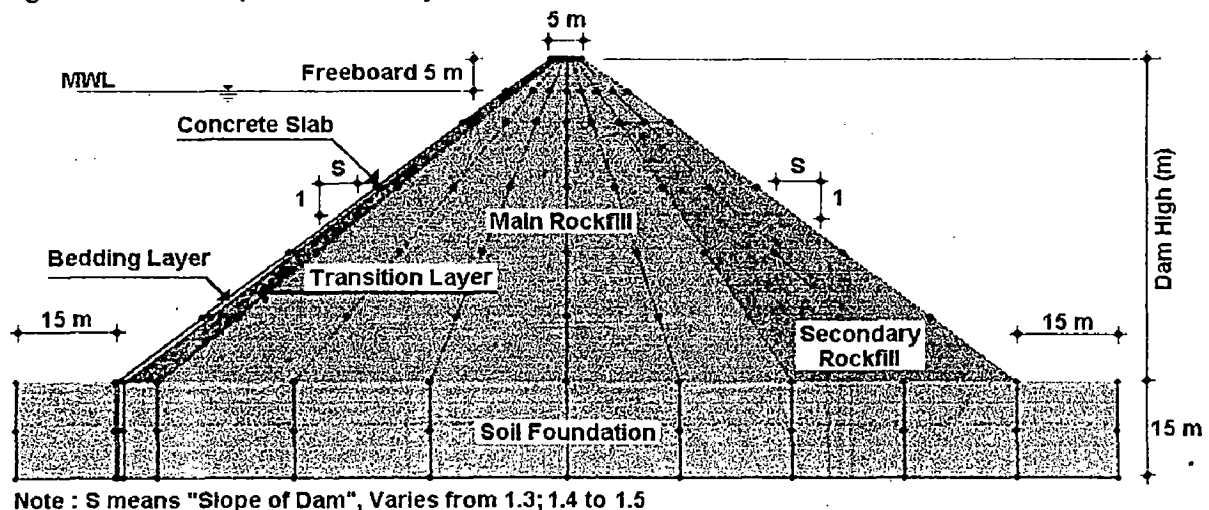


Figure 5.2 : The idealized meshing of CFRD Model

5.3. SIGN CONVENTION

The following sign convention has been followed in this study.

The positive x-direction is from centre line of dam to downstream along the river, negative y-direction is from upward to downward along the height of the dam and positive z-direction from the central section to the abutment along the dam axis as indicated in Figure 5.3.

The horizontal displacements ('u' displacements) and vertical displacement ('v' displacements) are positive in the positive x and y directions respectively.

The horizontal normal stresses (σ_{xx}) and vertical normal stresses (σ_{yy}) are pressure in the positive x and y directions and tension in the positive x and y directions.

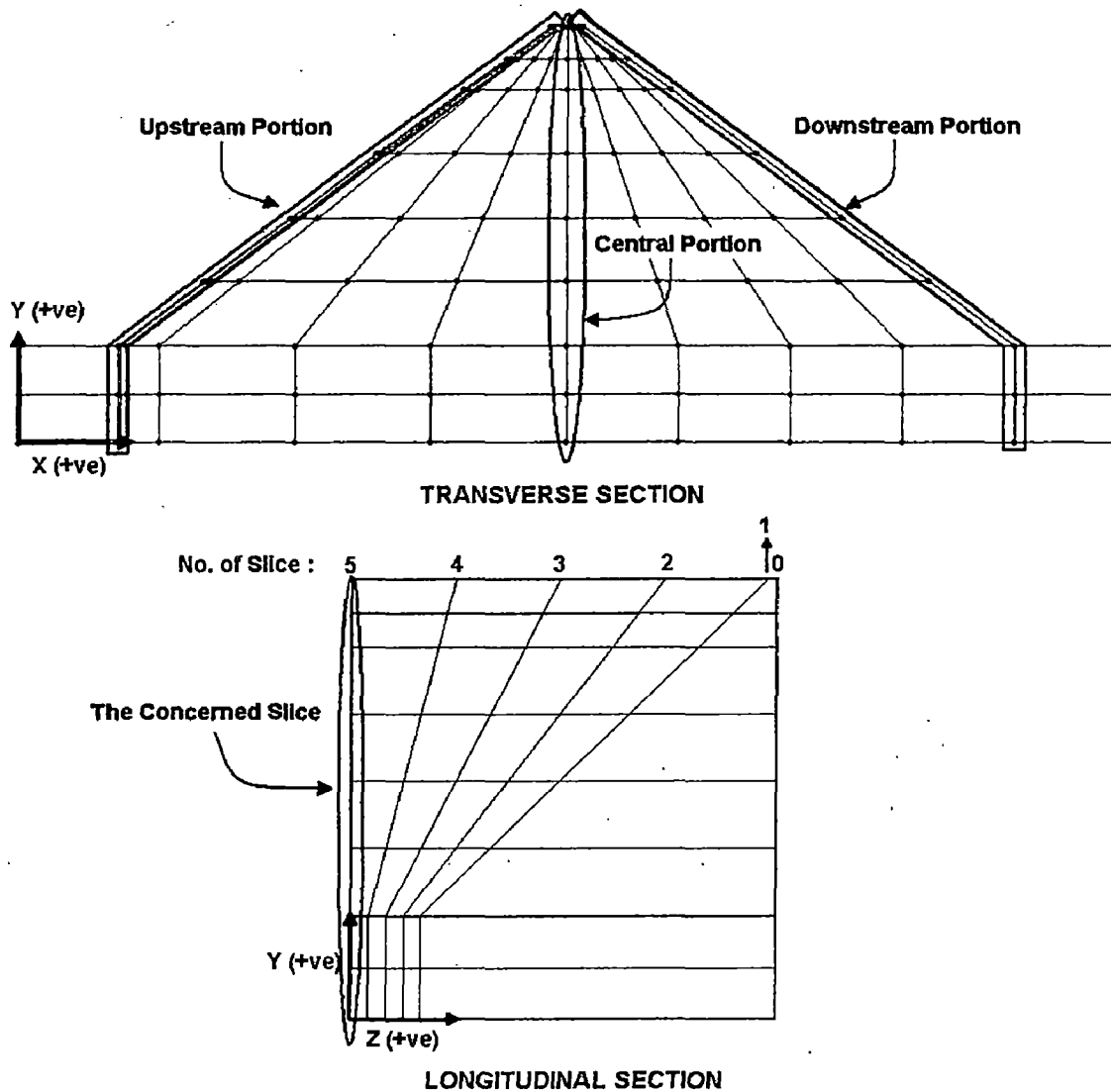


Figure 5.3 : The Concerned Portion in Analysis and Sign Convention

5.4. MATERIAL PROPERTIES

Properties of rockfill used in this study are shown in Table 5.1, These properties are modified from analysis of Yutiao Concrete Face Rockfill Dam, China, according to the report of IWHR (2000) (5). The parameter K is obtained by triaxial unloading-reloading test by Huang Yipen et al, (1993) or measured at

site by Byrne P M, Cheung H, Yan L (1987), Pai Shutian et al,(1999) and its value is three time that of corresponding loading modulus coefficient.

Table 5.1 : Model Parameters of Duncan Model

Type	Unit Weight (kN/m ³)	Friction Angle	n	Bulk-Modulus (Kb)	m	Rf	Shear-Modulus (K)
Concrete Slab	22.0	0	0	2000000	0	0	667000
Bedding	20.0	45	0.37	455	0.40	0.65	910
Transition	19.5	46	0.37	425	0.48	0.65	850
Main Rockfill	22.0	46	0.34	400	0.40	0.75	800
Secondary Rockfill	21.0	42	0.30	300	0.35	0.82	500

5.5. ANALYSES PERFORMED

Non linear 3-D analysis has been carried out to compare the effect of different slopes in Concrete Face Rockfill Dam (CFRD) under static and dynamic condition.

In analyze the behavior of slab and embankment of CFRD during period of construction and reservoir filling, the parameter result that are required to be considered to describe the behavior of CFRD is based on the deformation analysis procedures that involve the potential displacements along critical surfaces in the upstream portion, the central portion and the downstream portion of the embankment. Upstream slope is selected for study because this portion represents the concrete slab condition; while the central and the downstream portion represent the embankment condition (see at **Figure 5.3**).

Slice 5 is chosen to be the concerned slice for the study; hence Z-direction displacement is equal to zero. The displacements of 'U' and 'V' in horizontal ('x') and vertical ('y') direction and the normal stresses σ_{xx} and σ_{yy} in horizontal and vertical direction were studied for various causes at 3 different cross sections. The maximum displacements and stresses from the obtained results are highlighted for discussion of the analysis.

The study has been made for the following cases:

1. Case I : CFRD under static load condition
 - o CFRD is build regarding to the sequence as shown in Table 5.2.
 - o 5 variations of slopes and 2 kinds of dam heights are used for the analysis.

2. Case II : CFRD under dynamic load condition

- o Dynamic forces are applied after stage of construction process and reservoir filling over.
- o The study uses peak acceleration from 0.1g to 0.5g.

Table 5.2 : Number of Stages for Each Concrete Face Rockfill Dam

Height of Dam	50 m									100 m								
	1	2	3	4	5	6	7	8	9	1	2	3	4	5	6	7	8	9
Construction Process (high in m)	10	20	20	30	30	40	40	50	50	20	40	40	60	60	80	80	100	100
Reservoir Filling (head in m)	0	0	10	10	20	20	30	30	45	0	0	20	20	40	40	60	60	95

5.6. GROUND MOTION FOR DYNAMIC ANALYSIS

There are three types of dynamic analysis stages that can be used to analyze the model of CFRD: (1) The Eigen-Value Analysis, (2) The Earthquake Spectrum Analysis, (3) The Time History Analysis and The Ground Motion Analysis.

The Eigen-Value Stage computes the vibration modes susceptible. The Earthquake Spectrum Stage obtains the combined mode responses using SRSS or CQC methods. The Time History Stage allows you to define the time-load function and to apply the dynamic load which is obtained by multiplying the specified load by the load function, to the point or the elements. The ground motion analysis simulates the earthquake response in time domain.

The Eigen-Value Stage requires only the analysis control data and the mass density in the material property data. The Earthquake Spectrum Stage requires the mode combination method and its sub-data in addition to the data required by the Eigen-Value Analysis. The Time History Stage requires the following additional data:

1. To define the load function (load-time history).
2. To input the load to be multiplied by the load function.
3. To input the time step, the number of time steps, the save time interval and so on.

The Ground Motion Stage requires the following additional data:

1. To define the ground motion function (acceleration-time history).
2. To input the time step, the number of time steps, the save time interval and so on.

In this study, The Time History Analysis and The Ground Motion Analysis is used to solve the problem. Accelerograms recorded in Ofunato, Korea has been used as the input in Ground Motion Stage. Information of acceleration-time history (or ground motion function) on the records is shown in Figure 5.4. The maximum value of acceleration is 0.198506 and it happens at time 4.209 second, while the minimum value of acceleration is noted -0.180688 and it happens at time 5.734 second. Based on the peak ground acceleration (PGA) as mentioned before whereas acceleration in proportion of 'g' ('g' = 9.81 N/m²), these five values are used to scale the Ground Motion Function:

1. The maximum value of the seismic data of Ofunato.gmd is 0.198506, then to apply the 0.1g is by inputting 4.9418 ($=9.81 * 0.1 / 0.198506$) in the Scale for Ground Motion X-Dir. Scale.
2. By the same way, to apply PGA = 0.2g to 0.5g are by inputting 9.8836, 14.8254, 19.7672 and 24.709 respectively in the Scale for Ground Motion X-Dir. Scale.

Ofunato Accelerogram has the number of solution time step is 222 and output printing interval will be determined per 5 seconds. The result of analysis using PENTAGON-3D will show a maximum and a minimum values for each entity. Entity means node if the mentioned result is displacement and element if the mentioned result is stress as seen in Figure 5.5.

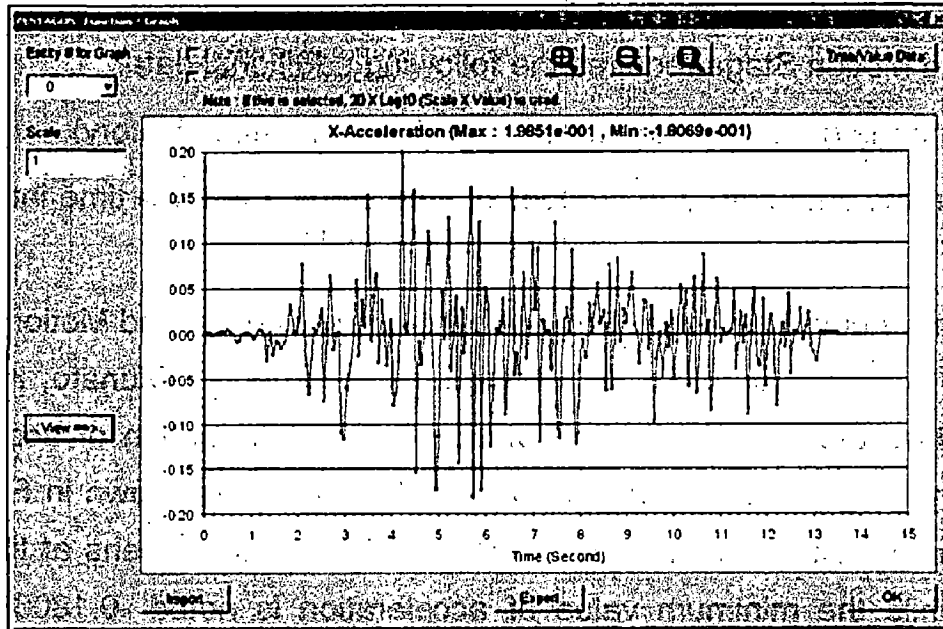


Figure 5.4 : Accelerograms recorded in Ofunato – Korea

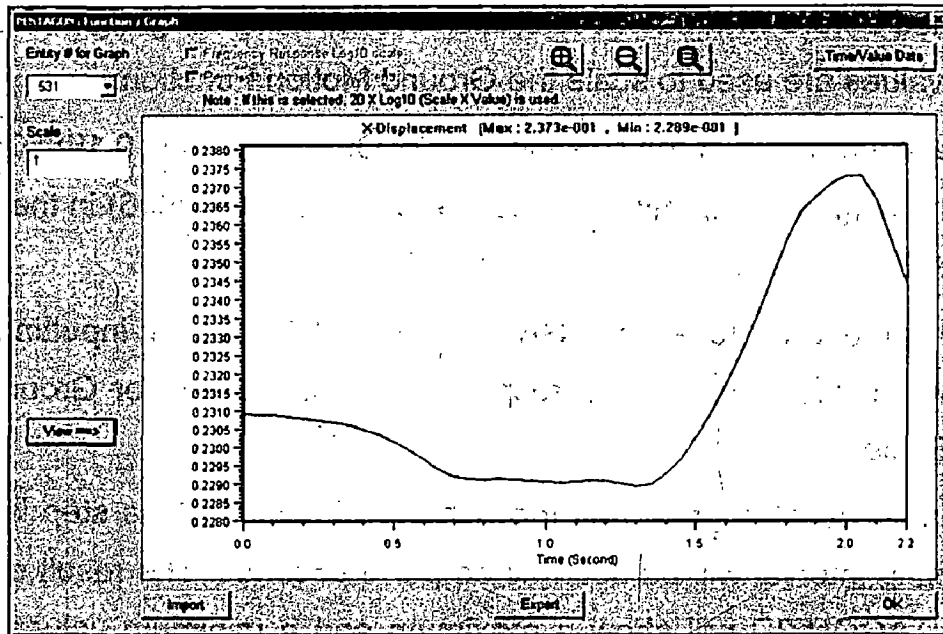


Figure 5.5 : Result of seismic analysis using PENTAGON-3D

5.7. RESULTS OF ANALYSIS

In this chapter the displacements and stresses at the end of construction and reservoir filling process for the two cases defined in chapter 5.5 are presented. The complete results are attached in the Appendix A.

5.7.1. Case I: CFRD under Static Load Condition

From the contours of u and v displacements also from horizontal (σ_{xx}) and vertical (σ_{yy}) normal stresses over the transverse section, the maximum

values are shown in Table 5.3 with special attention to the last stage of reservoir filling.

The result of analysis is performed in three different cross sections, such as upstream portion represents concrete slab, central and downstream portion represent rockfill embankment.

Table 5.3 : Result of Analysis under Static Load

o Upstream Portion										
Height of Dam : 50 m										
Max Value	1V:1.30H	Loc.	1V:1.35H	Loc.	1V:1.40H	Loc.	1V:1.45H	Loc.	1V:1.50H	Loc.
U_Displ (m)	0.298	0.8H	0.273	0.8H	0.252	0.6H	0.237	0.6H	0.223	0.6H
V_Displ (m)	-0.204	0.8H	-0.182	0.8H	-0.160	0.8H	-0.139	0.8H	-0.122	0.8H
σ_{xx} (kPa)	6.16e+3	1.0H	6.08e+3	1.0H	5.98e+3	1.0H	5.90e+3	1.0H	5.83e+3	1.0H
σ_{yy} (kPa)	-6.40e+3	0.4H	-6.62e+3	0.4H	-6.88e+3	0.4H	-7.02e+3	0.4H	-7.05e+3	0.4H
Height of Dam : 100 m										
U_Displ (m)	1.397	0.6H	1.312	0.6H	1.241	0.6H	1.184	0.6H	1.136	0.6H
V_Displ (m)	0.779	1.0H	0.924	1.0H	1.050	1.0H	1.108	1.0H	1.156	1.0H
σ_{xx} (kPa)	1.77e+4	0.9H	1.80e+4	0.9H	1.82e+4	0.9H	1.81e+4	0.9H	1.83e+4	0.9H
σ_{yy} (kPa)	-1.38e+4	0.6H	-1.47e+4	0.6H	-1.54e+4	0.6H	-1.56e+4	0.6H	-1.57e+4	0.6H
o Central Portion										
Height of Dam : 50 m										
Max Value	1V:1.30H	Loc.	1V:1.35H	Loc.	1V:1.40H	Loc.	1V:1.45H	Loc.	1V:1.50H	Loc.
U_Displ (m)	0.561	0.6H	0.532	0.6H	0.505	0.6H	0.477	0.6H	0.452	0.6H
V_Displ (m)	-0.183	0.6H	-0.170	0.6H	-0.157	0.6H	-0.142	0.4H	-0.142	0.4H
σ_{xx} (kPa)	-2.60e+2	0.2H	-2.70e+2	0.2H	-2.79e+2	0.2H	-2.85e+2	0.2H	-2.92e+2	0.2H
σ_{yy} (kPa)	-7.76e+2	0.6H	-7.87e+2	0.6H	-7.92e+2	0.6H	-8.00e+2	0.6H	-8.08e+2	0.6H
Height of Dam : 100 m										
U_Displ (m)	2.352	0.6H	2.209	0.6H	2.112	0.6H	2.016	0.6H	1.935	0.6H
V_Displ (m)	0.993	1.0H	1.079	1.0H	1.176	1.0H	1.213	1.0H	1.247	1.0H
σ_{xx} (kPa)	-3.60e+2	0.4H	-3.54e+2	0.4H	-3.55e+2	0.2H	-3.61e+2	0.2H	-3.69e+2	0.2H
σ_{yy} (kPa)	-1.40e+3	0.6H	-1.39e+3	0.6H	-1.39e+3	0.6H	-1.40e+3	0.6H	-1.40e+3	0.6H
o Downstream Portion										
Height of Dam : 50 m										
Max Value	1V:1.30H	Loc.	1V:1.35H	Loc.	1V:1.40H	Loc.	1V:1.45H	Loc.	1V:1.50H	Loc.
U_Displ (m)	0.700	0.4H	0.664	0.4H	0.628	0.4H	0.590	0.4H	0.556	0.4H
V_Displ (m)	0.588	0.2H	0.578	0.2H	0.663	0.2H	0.663	0.2H	0.658	0.2H
σ_{xx} (kPa)	-3.08e+2	0.4H	-3.06e+2	0.4H	-2.99e+2	0.4H	-2.93e+2	0.2H	-2.95e+2	0.2H
σ_{yy} (kPa)	-4.05e+2	0.4H	-4.04e+2	0.4H	-3.99e+2	0.4H	-3.85e+2	0.4H	-3.71e+2	0.4H
Height of Dam : 100 m										
U_Displ (m)	3.037	0.4H	2.850	0.4H	2.675	0.4H	2.533	0.4H	2.407	0.4H
V_Displ (m)	2.690	0.4H	2.677	0.4H	2.673	0.4H	2.654	0.4H	2.634	0.4H
σ_{xx} (kPa)	-4.43e+2	0.4H	-4.58e+2	0.2H	-4.97e+2	0.2H	-5.10e+2	0.2H	-5.18e+2	0.2H
σ_{yy} (kPa)	-8.23e+2	0.8H	-8.07e+2	0.8H	-7.85e+2	0.8H	-7.66e+2	0.8H	-7.45e+2	0.8H

5.7.2. Case II: CFRD under Dynamic Load Condition

The computed u and v displacements also horizontal (σ_{xx}) and vertical (σ_{yy}) normal stresses are shown in Table 5.4 to 5.8. The tables are categorized into peak acceleration and the maximum values of the analysis result are taken from the last stage of reservoir filling.

Table 5.4 : Result of Analysis under Peak Acceleration of 0.1g

○ **Upstream Portion**

Height of Dam : 50 m										
Max Value	1V:1.30H	Loc.	1V:1.35H	Loc.	1V:1.40H	Loc.	1V:1.45H	Loc.	1V:1.50H	Loc.
U_Displ (m)	0.303	0.8H	0.278	0.8H	0.257	0.6H	0.242	0.6H	0.228	0.6H
V_Displ (m)	-0.209	0.8H	-0.187	0.8H	-0.165	0.8H	-0.143	0.8H	-0.127	0.8H
σ_{xx} (kPa)	6.23e+3	1.0H	6.15e+3	1.0H	6.05e+3	1.0H	5.98e+3	1.0H	5.90e+3	1.0H
σ_{yy} (kPa)	-6.44e+3	0.4H	-6.63e+3	0.4H	-6.89e+3	0.4H	-7.03e+3	0.4H	-7.06e+3	0.4H
Height of Dam : 100 m										
U_Displ (m)	1.404	0.6H	1.319	0.6H	1.248	0.6H	1.192	0.6H	1.144	0.6H
V_Displ (m)	0.781	1.0H	0.926	1.0H	1.052	1.0H	1.110	1.0H	1.157	1.0H
σ_{xx} (kPa)	1.78e+4	0.9H	1.81e+4	0.9H	1.83e+4	0.9H	1.83e+4	0.9H	1.84e+4	0.9H
σ_{yy} (kPa)	-1.38e+4	0.6H	-1.47e+4	0.6H	-1.54e+4	0.6H	-1.56e+4	0.6H	-1.57e+4	0.6H

○ **Central Portion**

Height of Dam : 50 m										
Max Value	1V:1.30H	Loc.	1V:1.35H	Loc.	1V:1.40H	Loc.	1V:1.45H	Loc.	1V:1.50H	Loc.
U_Displ (m)	0.568	0.6H	0.539	0.6H	0.513	0.6H	0.485	0.6H	0.460	0.6H
V_Displ (m)	-0.183	0.6H	-0.170	0.6H	-0.157	0.6H	-0.142	0.4H	-0.142	0.4H
σ_{xx} (kPa)	-2.66e+2	0.2H	-2.78e+2	0.2H	-2.87e+2	0.2H	-2.94e+2	0.2H	-3.01e+2	0.2H
σ_{yy} (kPa)	-7.76e+2	0.6H	-7.87e+2	0.6H	-7.93e+2	0.6H	-8.01e+2	0.6H	-8.08e+2	0.6H
Height of Dam : 100 m										
U_Displ (m)	2.358	0.6H	2.215	0.6H	2.119	0.6H	2.022	0.6H	1.941	0.6H
V_Displ (m)	0.995	1.0H	1.081	1.0H	1.178	1.0H	1.214	1.0H	1.248	1.0H
σ_{xx} (kPa)	-3.64e+2	0.4H	-3.58e+2	0.4H	-3.59e+2	0.2H	-3.65e+2	0.2H	-3.73e+2	0.2H
σ_{yy} (kPa)	-1.40e+3	0.6H	-1.39e+3	0.6H	-1.39e+3	0.6H	-1.40e+3	0.6H	-1.40e+3	0.6H

○ **Downstream Portion**

Height of Dam : 50 m										
Max Value	1V:1.30H	Loc.	1V:1.35H	Loc.	1V:1.40H	Loc.	1V:1.45H	Loc.	1V:1.50H	Loc.
U_Displ (m)	0.707	0.4H	0.671	0.4H	0.635	0.4H	0.597	0.4H	0.563	0.4H
V_Displ (m)	0.588	0.2H	0.578	0.2H	0.664	0.2H	0.663	0.2H	0.658	0.2H
σ_{xx} (kPa)	-3.08e+2	0.4H	-3.06e+2	0.4H	-3.00e+2	0.4H	-2.98e+2	0.2H	-3.01e+2	0.2H
σ_{yy} (kPa)	-4.05e+2	0.4H	-4.04e+2	0.4H	-3.99e+2	0.4H	-3.85e+2	0.4H	-3.71e+2	0.4H
Height of Dam : 100 m										
U_Displ (m)	3.044	0.4H	2.856	0.4H	2.681	0.4H	2.539	0.4H	2.413	0.4H
V_Displ (m)	2.690	0.4H	2.677	0.4H	2.674	0.4H	2.654	0.4H	2.634	0.4H
σ_{xx} (kPa)	-4.44e+2	0.4H	-4.65e+2	0.2H	-5.04e+2	0.2H	-5.18e+2	0.2H	-5.26e+2	0.2H
σ_{yy} (kPa)	-8.23e+2	0.8H	-8.07e+2	0.8H	-7.85e+2	0.8H	-7.66e+2	0.8H	-7.45e+2	0.8H

Table 5.5 : Result of Analysis under Peak Acceleration of 0.2g

○ **Upstream Portion**

Height of Dam : 50 m										
Max Value	1V:1.30H	Loc.	1V:1.35H	Loc.	1V:1.40H	Loc.	1V:1.45H	Loc.	1V:1.50H	Loc.
U_Displ (m)	0.308	0.8H	0.283	0.8H	0.262	0.6H	0.246	0.6H	0.233	0.6H
V_Displ (m)	-0.214	0.8H	-0.192	0.8H	-0.170	0.8H	-0.148	0.8H	-0.131	0.8H
σ_{xx} (kPa)	6.29e+3	1.0H	6.21e+3	1.0H	6.12e+3	1.0H	6.05e+3	1.0H	5.98e+3	1.0H
σ_{yy} (kPa)	-6.48e+3	0.4H	-6.64e+3	0.4H	-6.90e+3	0.4H	-7.04e+3	0.4H	-7.07e+3	0.4H
Height of Dam : 100 m										
U_Displ (m)	1.411	0.6H	1.326	0.6H	1.255	0.6H	1.199	0.6H	1.151	0.6H
V_Displ (m)	0.783	1.0H	0.928	1.0H	1.054	1.0H	1.112	1.0H	1.159	1.0H
σ_{xx} (kPa)	1.79e+4	0.9H	1.82e+4	0.9H	1.85e+4	0.9H	1.84e+4	0.9H	1.85e+4	0.9H
σ_{yy} (kPa)	-1.38e+4	0.6H	-1.47e+4	0.6H	-1.54e+4	0.6H	-1.56e+4	0.6H	-1.57e+4	0.6H

○ **Central Portion**

Height of Dam : 50 m										
Max Value	1V:1.30H	Loc.	1V:1.35H	Loc.	1V:1.40H	Loc.	1V:1.45H	Loc.	1V:1.50H	Loc.
U_Displ (m)	0.576	0.6H	0.546	0.6H	0.520	0.6H	0.492	0.6H	0.467	0.6H
V_Displ (m)	-0.183	0.6H	-0.170	0.6H	-0.157	0.6H	-0.142	0.4H	-0.142	0.4H
σ_{xx} (kPa)	-2.72e+2	0.2H	-2.85e+2	0.2H	-2.95e+2	0.2H	-3.02e+2	0.2H	-3.11e+2	0.2H
σ_{yy} (kPa)	-7.77e+2	0.6H	-7.88e+2	0.6H	-7.94e+2	0.6H	-8.01e+2	0.6H	-8.09e+2	0.6H
Height of Dam : 100 m										
U_Displ (m)	2.364	0.6H	2.222	0.6H	2.125	0.6H	2.028	0.6H	1.947	0.6H
V_Displ (m)	0.997	1.0H	1.083	1.0H	1.179	1.0H	1.216	1.0H	1.250	1.0H
σ_{xx} (kPa)	-3.67e+2	0.4H	-3.61e+2	0.4H	-3.63e+2	0.2H	-3.69e+2	0.2H	-3.77e+2	0.2H
σ_{yy} (kPa)	-1.40e+3	0.6H	-1.39e+3	0.6H	-1.39e+3	0.6H	-1.40e+3	0.6H	-1.40e+3	0.6H

○ **Downstream Portion**

Height of Dam : 50 m										
Max Value	1V:1.30H	Loc.	1V:1.35H	Loc.	1V:1.40H	Loc.	1V:1.45H	Loc.	1V:1.50H	Loc.
U_Displ (m)	0.714	0.4H	0.678	0.4H	0.642	0.4H	0.605	0.4H	0.570	0.4H
V_Displ (m)	0.589	0.2H	0.579	0.2H	0.664	0.2H	0.663	0.2H	0.659	0.2H
σ_{xx} (kPa)	-3.08e+2	0.4H	-3.07e+2	0.4H	-3.01e+2	0.4H	-3.03e+2	0.2H	-3.06e+2	0.2H
σ_{yy} (kPa)	-4.05e+2	0.4H	-4.04e+2	0.4H	-3.99e+2	0.4H	-3.85e+2	0.4H	-3.71e+2	0.4H
Height of Dam : 100 m										
U_Displ (m)	3.050	0.4H	2.862	0.4H	2.687	0.4H	2.546	0.4H	2.419	0.4H
V_Displ (m)	2.690	0.4H	2.677	0.4H	2.674	0.4H	2.654	0.4H	2.634	0.4H
σ_{xx} (kPa)	-4.45e+2	0.4H	-4.71e+2	0.2H	-5.11e+2	0.2H	-5.25e+2	0.2H	-5.34e+2	0.2H
σ_{yy} (kPa)	-8.23e+2	0.8H	-8.07e+2	0.8H	-7.85e+2	0.8H	-7.66e+2	0.8H	-7.45e+2	0.8H

Table 5.6 : Result of Analysis under Peak Acceleration of 0.3g

○ Upstream Portion

Height of Dam : 50 m										
Max Value	1V:1.30H	Loc.	1V:1.35H	Loc.	1V:1.40H	Loc.	1V:1.45H	Loc.	1V:1.50H	Loc.
U_Displ (m)	0.313	0.8H	0.288	0.8H	0.266	0.6H	0.251	0.6H	0.237	0.6H
V_Displ (m)	-0.219	0.8H	-0.197	0.8H	-0.174	0.8H	-0.153	0.8H	-0.136	0.8H
σ_{xx} (kPa)	6.36e+3	1.0H	6.28e+3	1.0H	6.19e+3	1.0H	6.12e+3	1.0H	6.06e+3	1.0H
σ_{yy} (kPa)	-6.52e+3	0.4H	-6.68e+3	0.4H	-6.91e+3	0.4H	-7.05e+3	0.4H	-7.08e+3	0.4H
Height of Dam : 100 m										
U_Displ (m)	1.418	0.6H	1.333	0.6H	1.263	0.6H	1.206	0.6H	1.158	0.6H
V_Displ (m)	0.785	1.0H	0.930	1.0H	1.056	1.0H	1.114	1.0H	1.161	1.0H
σ_{xx} (kPa)	1.80e+4	0.9H	1.83e+4	0.9H	1.86e+4	0.9H	1.85e+4	0.9H	1.87e+4	0.9H
σ_{yy} (kPa)	-1.39e+4	0.6H	-1.47e+4	0.6H	-1.54e+4	0.6H	-1.56e+4	0.6H	-1.57e+4	0.6H

○ Central Portion

Height of Dam : 50 m										
Max Value	1V:1.30H	Loc.	1V:1.35H	Loc.	1V:1.40H	Loc.	1V:1.45H	Loc.	1V:1.50H	Loc.
U_Displ (m)	0.583	0.6H	0.554	0.6H	0.527	0.6H	0.499	0.6H	0.474	0.6H
V_Displ (m)	-0.183	0.6H	-0.170	0.6H	-0.157	0.6H	-0.142	0.4H	-0.142	0.4H
σ_{xx} (kPa)	-2.80e+2	0.2H	-2.93e+2	0.2H	-3.03e+2	0.2H	-3.11e+2	0.2H	-3.20e+2	0.2H
σ_{yy} (kPa)	-7.78e+2	0.6H	-7.88e+2	0.6H	-7.94e+2	0.6H	-8.02e+2	0.6H	-8.09e+2	0.6H
Height of Dam : 100 m										
U_Displ (m)	2.370	0.6H	2.228	0.6H	2.131	0.6H	2.035	0.6H	1.954	0.6H
V_Displ (m)	0.999	1.0H	1.084	1.0H	1.181	1.0H	1.218	1.0H	1.252	1.0H
σ_{xx} (kPa)	-3.71e+2	0.4H	-3.64e+2	0.4H	-3.67e+2	0.2H	-3.73e+2	0.2H	-3.81e+2	0.2H
σ_{yy} (kPa)	-1.40e+3	0.6H	-1.39e+3	0.6H	-1.39e+3	0.6H	-1.40e+3	0.6H	-1.40e+3	0.6H

○ Downstream Portion

Height of Dam : 50 m										
Max Value	1V:1.30H	Loc.	1V:1.35H	Loc.	1V:1.40H	Loc.	1V:1.45H	Loc.	1V:1.50H	Loc.
U_Displ (m)	0.721	0.4H	0.685	0.4H	0.649	0.4H	0.612	0.4H	0.577	0.4H
V_Displ (m)	0.589	0.2H	0.579	0.2H	0.665	0.2H	0.664	0.2H	0.659	0.2H
σ_{xx} (kPa)	-3.08e+2	0.4H	-3.07e+2	0.4H	-3.05e+2	0.4H	-3.09e+2	0.2H	-3.12e+2	0.2H
σ_{yy} (kPa)	-4.06e+2	0.4H	-4.04e+2	0.4H	-3.99e+2	0.4H	-3.85e+2	0.4H	-3.72e+2	0.4H
Height of Dam : 100 m										
U_Displ (m)	3.056	0.4H	2.868	0.4H	2.694	0.4H	2.552	0.4H	2.426	0.4H
V_Displ (m)	2.690	0.4H	2.677	0.4H	2.674	0.4H	2.654	0.4H	2.634	0.4H
σ_{xx} (kPa)	-4.47e+2	0.4H	-4.78e+2	0.2H	-5.18e+2	0.2H	-5.33e+2	0.2H	-5.42e+2	0.2H
σ_{yy} (kPa)	-8.23e+2	0.8H	-8.07e+2	0.8H	-7.85e+2	0.8H	-7.66e+2	0.8H	-7.45e+2	0.8H

Table 5.7 : Result of Analysis under Peak Acceleration of 0.4g

○ **Upstream Portion**

Height of Dam : 50 m										
Max Value	1V:1.30H	Loc.	1V:1.35H	Loc.	1V:1.40H	Loc.	1V:1.45H	Loc.	1V:1.50H	Loc.
U_Displ (m)	0.318	0.8H	0.292	0.8H	0.271	0.6H	0.256	0.6H	0.242	0.6H
V_Displ (m)	-0.224	0.8H	-0.201	0.8H	-0.179	0.8H	-0.157	0.8H	-0.141	0.8H
σ_{xx} (kPa)	6.42e+3	1.0H	6.35e+3	1.0H	6.27e+3	1.0H	6.20e+3	1.0H	6.14e+3	1.0H
σ_{yy} (kPa)	-6.56e+3	0.4H	-6.71e+3	0.4H	-6.92e+3	0.4H	-7.06e+3	0.4H	-7.09e+3	0.4H
Height of Dam : 100 m										
U_Displ (m)	1.426	0.6H	1.341	0.6H	1.270	0.6H	1.214	0.6H	1.166	0.6H
V_Displ (m)	0.787	1.0H	0.932	1.0H	1.057	1.0H	1.115	1.0H	1.163	1.0H
σ_{xx} (kPa)	1.81e+4	0.9H	1.84e+4	0.9H	1.87e+4	0.9H	1.86e+4	0.9H	1.88e+4	0.9H
σ_{yy} (kPa)	-1.39e+4	0.6H	-1.47e+4	0.6H	-1.54e+4	0.6H	-1.56e+4	0.6H	-1.57e+4	0.6H

○ **Central Portion**

Height of Dam : 50 m										
Max Value	1V:1.30H	Loc.	1V:1.35H	Loc.	1V:1.40H	Loc.	1V:1.45H	Loc.	1V:1.50H	Loc.
U_Displ (m)	0.591	0.6H	0.561	0.6H	0.535	0.6H	0.506	0.6H	0.481	0.6H
V_Displ (m)	-0.183	0.6H	-0.170	0.6H	-0.157	0.6H	-0.142	0.4H	-0.142	0.4H
σ_{xx} (kPa)	-2.87e+2	0.2H	-3.02e+2	0.2H	-3.12e+2	0.2H	-3.20e+2	0.2H	-3.29e+2	0.2H
σ_{yy} (kPa)	-7.78e+2	0.6H	-7.89e+2	0.6H	-7.95e+2	0.6H	-8.03e+2	0.6H	-8.10e+2	0.6H
Height of Dam : 100 m										
U_Displ (m)	2.377	0.6H	2.234	0.6H	2.138	0.6H	2.041	0.6H	1.960	0.6H
V_Displ (m)	1.000	1.0H	1.086	1.0H	1.183	1.0H	1.220	1.0H	1.254	1.0H
σ_{xx} (kPa)	-3.75e+2	0.4H	-3.67e+2	0.4H	-3.72e+2	0.2H	-3.77e+2	0.2H	-3.86e+2	0.2H
σ_{yy} (kPa)	-1.40e+3	0.6H	-1.39e+3	0.6H	-1.39e+3	0.6H	-1.40e+3	0.6H	-1.40e+3	0.6H

○ **Downstream Portion**

Height of Dam : 50 m										
Max Value	1V:1.30H	Loc.	1V:1.35H	Loc.	1V:1.40H	Loc.	1V:1.45H	Loc.	1V:1.50H	Loc.
U_Displ (m)	0.728	0.4H	0.692	0.4H	0.656	0.4H	0.619	0.4H	0.584	0.4H
V_Displ (m)	0.590	0.2H	0.579	0.2H	0.665	0.2H	0.664	0.2H	0.660	0.2H
σ_{xx} (kPa)	-3.08e+2	0.4H	-3.07e+2	0.4H	-3.10e+2	0.4H	-3.14e+2	0.2H	-3.17e+2	0.2H
σ_{yy} (kPa)	-4.06e+2	0.4H	-4.04e+2	0.4H	-3.99e+2	0.4H	-3.86e+2	0.4H	-3.72e+2	0.4H
Height of Dam : 100 m										
U_Displ (m)	3.062	0.4H	2.875	0.4H	2.700	0.4H	2.558	0.4H	2.432	0.4H
V_Displ (m)	2.690	0.4H	2.677	0.4H	2.674	0.4H	2.654	0.4H	2.634	0.4H
σ_{xx} (kPa)	-4.53e+2	0.4H	-4.84e+2	0.2H	-5.25e+2	0.2H	-5.40e+2	0.2H	-5.51e+2	0.2H
σ_{yy} (kPa)	-8.23e+2	0.8H	-8.07e+2	0.8H	-7.85e+2	0.8H	-7.66e+2	0.8H	-7.45e+2	0.8H

Table 5.8 : Result of Analysis under Peak Acceleration of 0.5g

○ **Upstream Portion**

Height of Dam : 50 m										
Max Value	1V:1.30H	Loc.	1V:1.35H	Loc.	1V:1.40H	Loc.	1V:1.45H	Loc.	1V:1.50H	Loc.
U_Displ (m)	0.323	0.8H	0.297	0.8H	0.276	0.6H	0.260	0.6H	0.247	0.6H
V_Displ (m)	-0.229	0.8H	-0.206	0.8H	-0.184	0.8H	-0.162	0.8H	-0.145	0.8H
σ_{xx} (kPa)	6.49e+3	1.0H	6.42e+3	1.0H	6.34e+3	1.0H	6.27e+3	1.0H	6.21e+3	1.0H
σ_{yy} (kPa)	-6.60e+3	0.4H	-6.75e+3	0.4H	-6.93e+3	0.4H	-7.07e+3	0.4H	-7.10e+3	0.4H
Height of Dam : 100 m										
U_Displ (m)	1.433	0.6H	1.348	0.6H	1.277	0.6H	1.221	0.6H	1.173	0.6H
V_Displ (m)	0.789	1.0H	0.933	1.0H	1.059	1.0H	1.117	1.0H	1.164	1.0H
σ_{xx} (kPa)	1.82e+4	0.9H	1.85e+4	0.9H	1.88e+4	0.9H	1.87e+4	0.9H	1.89e+4	0.9H
σ_{yy} (kPa)	-1.39e+4	0.6H	-1.47e+4	0.6H	-1.54e+4	0.6H	-1.56e+4	0.6H	-1.57e+4	0.6H

○ **Central Portion**

Height of Dam : 50 m										
Max Value	1V:1.30H	Loc.	1V:1.35H	Loc.	1V:1.40H	Loc.	1V:1.45H	Loc.	1V:1.50H	Loc.
U_Displ (m)	0.598	0.6H	0.568	0.6H	0.542	0.6H	0.514	0.6H	0.489	0.6H
V_Displ (m)	-0.183	0.6H	-0.170	0.6H	-0.157	0.6H	-0.142	0.4H	-0.142	0.4H
σ_{xx} (kPa)	-2.94e+2	0.2H	-3.10e+2	0.2H	-3.20e+2	0.2H	-3.28e+2	0.2H	-3.38e+2	0.2H
σ_{yy} (kPa)	-7.79e+2	0.6H	-7.90e+2	0.6H	-7.95e+2	0.6H	-8.03e+2	0.6H	-8.11e+2	0.6H
Height of Dam : 100 m										
U_Displ (m)	2.383	0.6H	2.240	0.6H	2.144	0.6H	2.047	0.6H	1.966	0.6H
V_Displ (m)	1.002	1.0H	1.088	1.0H	1.185	1.0H	1.221	1.0H	1.255	1.0H
σ_{xx} (kPa)	-3.78e+2	0.4H	-3.71e+2	0.4H	-3.76e+2	0.2H	-3.81e+2	0.2H	-3.90e+2	0.2H
σ_{yy} (kPa)	-1.40e+3	0.6H	-1.39e+3	0.6H	-1.39e+3	0.6H	-1.40e+3	0.6H	-1.40e+3	0.6H

○ **Downstream Portion**

Height of Dam : 50 m										
Max Value	1V:1.30H	Loc.	1V:1.35H	Loc.	1V:1.40H	Loc.	1V:1.45H	Loc.	1V:1.50H	Loc.
U_Displ (m)	0.735	0.4H	0.699	0.4H	0.663	0.4H	0.626	0.4H	0.591	0.4H
V_Displ (m)	0.590	0.2H	0.580	0.2H	0.666	0.2H	0.665	0.2H	0.660	0.2H
σ_{xx} (kPa)	-3.08e+2	0.4H	-3.07e+2	0.4H	-3.14e+2	0.4H	-3.19e+2	0.2H	-3.23e+2	0.2H
σ_{yy} (kPa)	-4.06e+2	0.4H	-4.05e+2	0.4H	-3.99e+2	0.4H	-3.86e+2	0.4H	-3.72e+2	0.4H
Height of Dam : 100 m										
U_Displ (m)	3.069	0.4H	2.881	0.4H	2.706	0.4H	2.565	0.4H	2.438	0.4H
V_Displ (m)	2.690	0.4H	2.678	0.4H	2.674	0.4H	2.654	0.4H	2.634	0.4H
σ_{xx} (kPa)	-4.59e+2	0.4H	-4.91e+2	0.2H	-5.32e+2	0.2H	-5.48e+2	0.2H	-5.59e+2	0.2H
σ_{yy} (kPa)	-8.23e+2	0.8H	-8.07e+2	0.8H	-7.85e+2	0.8H	-7.66e+2	0.8H	-7.45e+2	0.8H

CHAPTER 6

DISCUSSION OF RESULTS

The contours for displacements and stresses for each type of CFRD as obtained by FEM analysis for the two cases are given in Chapter 5. The results at various heights, slopes and sections for static and dynamic conditions are discussed below.

6.1. DISCUSSION OF RESULTS OF CASE I STUDY

The displacements and stresses in respect of Case I are discussed for upstream portion, central portion and downstream portion in following paragraph.

6.1.1. Upstream Portion

6.1.1.1. Horizontal Displacements - U

1. The contours of horizontal displacements from stage 1 to stage 9 are shown in Appendix A. From Table 5.3, the maximum U value of CFRD 50 m for slope 1V:1.30H to 1V:1.50H gradually decreases from 0.298 m to 0.223 m. It shows that the horizontal displacement reduces with flattening of slope. The comparisons of the last stage values for all slopes are shown in Figure 6.1.
2. Location of maximum horizontal displacement for CFRD 50 m for slope 1V:1.30H to 1V:1.50H moves from 0.8H to 0.6H.
3. From Table 5.3, the maximum U value of CFRD 100 m for slope 1V:1.30H to 1V:1.50H gradually decreases from 1.397 m to 1.136 m. It also shows that the flatter slope gives less horizontal displacement. The

comparisons of the last stage values for all slopes are shown in Figure 6.2.

4. No movement in location of maximum horizontal displacement is found in CFRD 100 m for slope 1V:1.30H to 1V:1.50H. It is at 0.6H.

6.1.1.2. Vertical Displacements - V

1. The contours of vertical displacements from stage 1 to stage 9 are shown in Appendix A. From Table 5.3, the maximum V value of CFRD 50 m for slope 1V:1.30H to 1V:1.50H gradually decreases from -0.204 m to -0.122 m. It shows that the flatter slope gives lesser of vertical displacement. The comparisons of the last stage values for all slopes are shown in Figure 6.1.
2. No movement in location of maximum vertical displacement is found in CFRD 50 m for slopes 1V:1.30H to 1V:1.50H, it occurs at 0.8H.
3. From Table 5.3, the maximum V value of CFRD 100 m for slopes 1V:1.30H to 1V:1.50H gradually increases from 0.779 m to 1.156 m. This trend is opposite of that observed with CFRD 50 m. The flatter slope of CFRD 100 m gave the larger values of vertical displacement. The comparisons of the last stage values for all slopes are shown in Figure 6.2.
4. The location of maximum vertical displacement for all slopes was found at the top of dam.

6.1.1.3. Horizontal Normal Stresses - σ_{xx}

1. From Table 5.3, the maximum σ_{xx} value of CFRD 50 m for slope 1V:1.30H to 1V:1.50H gradually decreases from 6.16e+3 kPa to 5.83e+3 kPa. It shows that the flatter slope in CFRD 50 m gives lesser horizontal normal stress.
2. Location of maximum σ_{xx} of CFRD 50 m for slope 1V:1.30H to 1V:1.50H also shifts from 0.8H to 0.6H as location of maximum u displacement for CFRD 50 m.

3. From Table 5.3, the maximum σ_{xx} value of CFRD 100 m for slope 1V:1.30H to 1V:1.50H gradually increases from $1.77e+4$ kPa to $1.83e+4$ kPa. It shows that the flatter slope of CFRD 100 m gives the larger value of horizontal normal stress.
4. The location of maximum σ_{xx} for all slopes is 0.6H for CFRD 100 m.

6.1.1.4. Vertical Normal Stresses - σ_{yy}

1. From Table 5.3, the maximum σ_{yy} value of CFRD 50 m for slope 1V:1.30H to 1V:1.50H gradually increases from $-6.40e+3$ kPa to $-7.05e+3$ kPa. It shows that the flatter slope in CFRD 50 m gives larger vertical normal stress.
2. Location of maximum σ_{yy} is same as location of maximum σ_{xx}
3. From Table 5.3, the maximum σ_{xx} value of CFRD 100 m for slope 1V:1.30H to 1V:1.50H gradually increases from $-1.38e+4$ kPa to $-1.57e+4$ kPa. It shows that the flatter slope of CFRD 100 m gives the larger value of vertical normal stress.
4. Location of maximum σ_{yy} is same as location of maximum σ_{xx}

6.1.2. Central Portion

6.1.2.1. Horizontal Displacements - U

1. The contours of horizontal displacements from stage 1 to stage 9 are shown in Appendix A. From Table 5.3, the maximum U value of CFRD 50 m for slopes 1V:1.30H to 1V:1.50H gradually decreases from 0.561 m to 0.452 m. It shows that the flatter slope gives the smaller value of horizontal displacement. The comparisons of the last stage values for all slopes are shown in Figure 6.1.
2. For all slopes 1V:1.30H to 1V:1.50H, the location of maximum horizontal displacement at CFRD 50 m is found at 0.6H.
3. From Table 5.3, the maximum U value of CFRD 100 m for slope 1V:1.30H to 1V:1.50H gradually decreases from 2.352 m to 1.935 m. It

also shows that the flatter slope gives the smaller value of horizontal displacement. The comparison of the last stage for all slopes is shown in Figure 6.2.

4. For all slopes 1V:1.30H to 1V:1.50H, the location of maximum horizontal displacement at CFRD 100 m is found at 0.6H.

6.1.2.2. Vertical Displacements - V

1. The contours of horizontal displacements from stage 1 to stage 9 are shown in Appendix A. From Table 5.3, the maximum V value of CFRD 50 m for slope 1V:1.30H to 1V:1.50H gradually decreases from -0.183 m to -0.142 m. It shows that the flatter slope gives the lower values of vertical displacement. The comparisons of the last stage values for all slopes are shown in Figure 6.1.
2. Location of maximum vertical displacement for CFRD 50 m for slopes 1V:1.30H to 1V:1.50H moves from 0.6H to 0.4H.
3. From Table 5.3, the maximum V value of CFRD 100 m for slope 1V:1.30H to 1V:1.50H gradually increases from 0.993 m to 1.247 m. This trend is opposite to that observed with CFRD 50 m. The flatter slope of CFRD 100 m gives the larger value of vertical displacement. The comparisons of the last stage values for all slopes are shown in Figure 6.2.
4. No movement is found in CFRD 100 m for slope 1V:1.30H to 1V:1.50H. The location of maximum vertical displacement at all the slopes is at the top of dam.

6.1.2.3. Horizontal Normal Stresses - σ_{xx}

1. From Table 5.3, the maximum σ_{xx} value of CFRD 50 m for slope 1V:1.30H to 1V:1.50H gradually increases from -2.60e+2 kPa to -2.92e+2 kPa. It shows that the flatter slope in CFRD 50 m gives the higher values of horizontal normal stress. It is opposite to upstream portion.

2. Location of maximum σ_{xx} is same as the location of maximum u displacement for CFRD 50 m, it at 0.6H.
3. From Table 5.3, the maximum σ_{xx} value of CFRD 100 m for slope 1V:1.30H to 1V:1.50H gradually increases from $-3.60e+2$ kPa to $-3.69e+2$ kPa. It shows that the flatter slope of CFRD 100 m gives the higher value of horizontal normal stress.
4. For CFRD 100 m, location of maximum σ_{xx} is at 0.6H.

6.1.2.4. Vertical Normal Stresses - σ_{yy}

1. From Table 5.3, the maximum σ_{yy} value of CFRD 50 m for slope 1V:1.30H to 1V:1.50H gradually increases from $-7.76e+2$ kPa to $-8.08e+2$ kPa. It shows that the flatter slope in CFRD 50 m gives the larger values of vertical normal stress.
2. Location of maximum σ_{yy} is same as location of maximum vertical displacement, it moves from 0.6H to 0.4H.
3. From Table 5.3, the maximum σ_{xx} value of CFRD 100 m for slope 1V:1.30H to 1V:1.50H is same. The value is $-1.40e+3$ kPa. It shows that the flatter slope of CFRD 100 m does not affect the vertical normal stress.
4. Location of maximum σ_{yy} is at the dam crest

6.1.3. Downstream Portion

6.1.3.1. Horizontal Displacements - U

1. The contours of horizontal displacements from stage 1 to stage 9 are shown in Appendix A. From Table 5.3, the maximum U value of CFRD 50 m for slope 1V:1.30H to 1V:1.50H gradually decreases from 0.700 m to 0.556 m. It shows that the flatter slope gives the smaller values of horizontal displacement. The comparisons of the last stage values for all slopes are shown in Figure 6.1.

2. No movement in location of maximum horizontal displacement is found in CFRD 50 m for slope 1V:1.30H to 1V:1.50H, it occurs at 0.4H.
3. From Table 5.3, the maximum U value of CFRD 100 m for slope 1V:1.30H to 1V:1.50H gradually decreases from 3.037 m to 2.407 m. It also shows that the flatter slope gives less horizontal displacement. The comparisons of the last stage values for all slopes are shown in Figure 6.2.
4. No movement in location of maximum horizontal displacement is found in CFRD 100 m for slope 1V:1.30H to 1V:1.50H, it occurs at 0.4H.

6.1.3.2. Vertical Displacements - V

1. The contours of vertical displacements from stage 1 to stage 9 are shown in Appendix A. From Table 5.3, the maximum V value of CFRD 50 m for slope 1V:1.30H to 1V:1.50H gradually increases from 0.588 m to 0.658 m. It shows that the flatter slope gives the higher values of vertical displacement. The comparisons of the last stage values for all slopes are shown in Figure 6.1.
2. No movement in maximum vertical displacement is found in CFRD 50 m for slopes 1V:1.30H to 1V:1.50H, it occurs at 0.2H.
3. From Table 5.3, the maximum V value of CFRD 100 m for slopes 1V:1.30H to 1V:1.50H gradually decreases from 2.690 m to 2.634 m. This trend is opposite of that observed with CFRD 50 m. The flatter slope of CFRD 100 m gives the smaller values of vertical displacement. The comparisons of the last stage values for all slopes are shown in Figure 6.2.
4. No movement in location of maximum vertical displacement is found in CFRD 100 m for slope 1V:1.30H to 1V:1.50H, it occurs at 0.2H.

6.1.3.3. Horizontal Normal Stresses - σ_{xx}

1. From Table 5.3, the maximum σ_{xx} value of CFRD 50 m for slopes 1V:1.30H to 1V:1.50H gradually decreases from $-3.08e+2$ kPa to

-2.95e+2 kPa. It shows that the flatter slope in CFRD 50 m gives the smaller values of horizontal normal stress.

2. Location of maximum σ_{xx} is same as location of maximum u displacement for CFRD 50 m, at 0.4H.
3. From Table 5.3, the maximum σ_{xx} value of CFRD 100 m for slope 1V:1.30H to 1V:1.50H gradually increases from -4.43e+2 kPa to -5.18e+2 kPa. It shows that the flatter slope of CFRD 100 m gave the higher result of horizontal normal stress.
4. For CFRD 100 m, location of maximum σ_{xx} is at 0.4H.

6.1.3.4. Vertical Normal Stresses - σ_{yy}

1. From Table 5.3, the maximum σ_{yy} value of CFRD 50 m for slope 1V:1.30H to 1V:1.50H gradually decreases from -4.05e+2 kPa to -3.71e+2 kPa. It shows that the flatter slope in CFRD 50 m gives the smaller values of vertical normal stress.
2. Same as maximum v displacement for CFRD 50 m, location of maximum σ_{yy} is at 0.2H.
3. From Table 5.3, the maximum σ_{xx} value of CFRD 100 m for slope 1V:1.30H to 1V:1.50H gradually decreases from -8.23e+2 kPa to -7.45e+2 kPa. It shows that the flatter slope in CFRD 100 m gives the smaller values of vertical normal stress.
4. Location of maximum σ_{yy} is at 0.2H.

6.2. DISCUSSION OF RESULTS OF CASE II STUDY

The displacements and stresses in respect of Case II : CFRD under dynamic load condition are given in following paragraph. Slopes of 1V:1.30H and 1V:1.5H are discussed to represent the behavior of dam under earthquake shaking. Results are shown in Table 5.4 to 5.8 and Figure at Appendices B.

6.2.1. CFRD 50 m High

6.2.1.1. Slope 1V:1.30H at 0.1g to 0.5g Peak Acceleration

1. The computed response in horizontal displacement at upstream portion increases from 29.81 cm to 32.29 cm in elevation +40m with peak acceleration 0.5g. 32.29 cm is the maximum displacement that happens in concrete slab. The minimum value of horizontal displacement at the same elevation is 29.15 cm. For result of other peak acceleration (0.1g, 0.2g, 0.3g and 0.4g) is between 29.15 cm and 32.29 cm.
2. Vertical displacement at upstream portion also increases from -20.43 cm to -22.87 cm, at elevation +40m with peak acceleration 0.5g. The minimum value is -19.81 cm. At elevation +40m, concrete slab part shows a critical point where a maximum horizontal displacement and a maximum vertical displacement occur at that place. Some engineering measures should be taken in order to prevent the displacement of the slab from exceeding allowable value.
3. Maximum horizontal displacement of central portion is 59.80 cm and minimum displacement is 54.47 cm. It happens at elevation +30m with peak acceleration of 0.5g. Seismic load has increased deformation from 56.10 cm to 59.80 cm.
4. Vertical displacement at the central portion does not show the significant result. At elevation +30m, the maximum value of vertical displacement is -18.27 cm and minimum value is -18.07 cm while displacement without seismic effect is -18.265 cm. It indicated that 0.5g peak acceleration does not influence the vertical displacement at central portion of CFRD.
5. Horizontal displacement at downstream portion increases from 69.98 cm to 73.52 cm, at elevation +20m with peak acceleration 0.5g. The

minimum value of horizontal displacement is 68.36 cm. It explained that at elevation +20m, the secondary rockfill part shows a larger value than concrete slab portion and central portion of CFRD. It is caused of the difference of material parameters.

6. Vertical displacement at the downstream section also does not show the significant results. At elevation +10m, the maximum value is 59.01 cm and minimum value is 58.55 cm while displacement without seismic effect is 58.77 cm hence it indicate 0.5g peak acceleration does not affect the vertical displacement at the downstream portion.

6.2.1.2. Slope 1V:1.50H at 0.1g to 0.5g Peak Acceleration

1. The computed response in horizontal displacement at upstream portion increases from 22.33 cm to 24.67 cm in elevation +30 m and with peak acceleration 0.5g. 24.67 cm is the maximum displacement that happens in concrete slab, while the minimum value of horizontal displacement at the same elevation is 21.74 cm. For result of other peak acceleration (0.1g, 0.2g, 0.3g and 0.4g) is between 21.74 cm and 24.67 cm.
2. Vertical displacement at upstream portion also increases from -12.19 cm to -14.52 cm, at elevation +40 m with peak acceleration 0.5g. The minimum value is -11.58 cm. Location of displacement still at elevation +40m although horizontal displacement has shifted from elevation +40 m to elevation +30m and some engineering measures still need to be taken in order to prevent the displacement of the slab from exceeding allowable value.
3. The maximum horizontal displacement of central portion is 48.86 cm and minimum displacement is 43.59 cm. It happens at elevation +30 m with peak acceleration of 0.5g. It can be seen that seismic loading has increased deformation from 45.23 cm to 48.86 cm.
4. Vertical displacement at the central portion does not show the significant results. At elevation +20 m, the maximum value is -14.16 cm. Maximum vertical displacement usually occurs at elevation +30 m and shifted. The

minimum value of vertical displacement is -14.14 cm while displacement without seismic effect is -14.16 cm. It indicated that 0.5g peak acceleration also does not affect the vertical displacement at central portion.

5. Horizontal displacement at downstream portion increases from 55.56 cm to 59.11 cm, at elevation +20 m with peak acceleration 0.5g. The minimum value of horizontal displacement is 53.95 cm. It explained that at elevation +20m, secondary rockfill part shows a larger value than concrete slab portion and the central portion. It is caused of the difference of material parameters.
6. Vertical displacement at the downstream portion also does not show the significant results. At elevation +10m, the maximum value is 66.01 cm and minimum value is 65.60 cm while displacement without seismic effect is 65.80 cm hence it indicate that 0.5g peak acceleration does not affect the vertical displacement at the downstream portion.

6.2.2. CFRD 100 m High

6.2.2.1. Slope 1V:1.30H at 0.1g to 0.5g Peak Acceleration

1. The computed response in horizontal displacement at upstream portion increases from 1.40 m to 1.43 m in elevation +60m and with peak acceleration 0.5g. 1.43 m is the maximum displacement that happens in concrete slab, while the minimum value of horizontal displacement at the same elevation is 1.39 m. For result of other peak acceleration (0.1g, 0.2g, 0.3g and 0.4g) is between 1.39 m and 1.43 m.
2. Vertical displacement at upstream portion also increases from -30.5 cm to -32.0 cm, at elevation +60m with peak acceleration 0.5g. The minimum value is -29.72 cm. At elevation +60m, concrete slab part shows a critical point where a maximum horizontal displacement and a maximum vertical displacement occur at that place. Some engineering measures should be taken in order to prevent the displacement of the slab from exceeding allowable value.

3. Maximum horizontal displacement of central portion is 2.38 m and minimum displacement is 2.36 m, at elevation +60m with peak acceleration of 0.5g. Seismic loading has increased deformation from 2.35 m to 2.38 m.
4. Vertical displacement at the central portion does not show the significant results. At elevation +20m, the maximum value is -31.75 cm and minimum value is -31.75 cm while displacement without seismic effect is -31.75 cm. It indicated that 0.5g peak acceleration does not affect the vertical displacement at central portion of CFRD.
5. Horizontal displacement at downstream portion increases from 3.04 m to 3.07 m, at elevation +40 m with peak acceleration 0.5g. The minimum value of horizontal displacement is 3.02 m. It explained that at elevation +40m, secondary rockfill part shows a larger value than concrete slab part and the middle of dam part. It is caused of the difference of material parameters.
6. Vertical displacement at the downstream section also does not show the significant results. At elevation +40m, the maximum value is 2.69 m and minimum value is 2.69 m while displacement without seismic effect is 2.69 cm hence it indicate that 0.5g peak acceleration do not affect the vertical displacement at the downstream portion.

6.2.2.2 Slope 1V:1.50H at 0.1g to 0.5g Peak Acceleration

1. The computed response in horizontal displacement at upstream portion increases from 1.14 m to 1.17 m in elevation +60 m and with peak acceleration 0.5g and 1.17 m is the maximum displacement that happens in concrete slab, while the minimum value of horizontal displacement at the same elevation is 1.13 m. For result of other peak acceleration (0.1g, 0.2g, 0.3g and 0.4g) is between 1.13 m and 1.17 m.
2. Vertical displacement at upstream portion also increases from -10.40 cm to -11.21 cm, at elevation +20 m with peak acceleration 0.5g. The minimum value is -10.14 cm. As CFRD 100m with slope 1V:1.45H, the

location of maximum vertical displacement on this dam also moved from elevation +60m to elevation +20m but location of horizontal displacement still at elevation +60m. Therefore some engineering measures need to be taken in order to prevent the displacement of the slab from exceeding allowable value.

3. The maximum horizontal displacement of the central portion is 1.97 m and minimum displacement is 1.92 m. It happens at elevation +60m with peak acceleration of 0.5g. Seismic loading has increased deformation from 193 m to 1.97 m.
4. Vertical displacement at the central portion does not show the significant results. At elevation +20 m, the maximum value is -30.17 cm and minimum value is also -30.17 cm while displacement without seismic effect is -30.17 cm. It indicated that 0.5g peak acceleration also does not affect the vertical displacement at the central portion.
5. Horizontal displacement at downstream portion increases from 2.41 m to 2.44 m, at elevation +40 m with peak acceleration 0.5g. The minimum value of horizontal displacement is 2.39 m. It explained that at elevation +40m of secondary rockfill part shows a larger value than concrete slab portion and the central portion of CFRD. It is caused of the difference of the material parameters.
6. Vertical displacement at the downstream portion also does not show the significant results. At elevation +40m, the maximum and minimum values are 2.63 m and displacement without seismic effect is also 2.63 m hence it indicate that 0.5g peak acceleration does not affect the vertical displacement at the downstream portion.

6.3. RATIO OF DISPLACEMENT UNDER STATIC LOAD

From the result of analysis at Chapter 5, there shows the maximum values of $u_{\text{displacement}}$, $v_{\text{displacement}}$, σ_{xx} and σ_{yy} for all type of dam. It can be noted that by comparing $u_{\text{displacement}}$ and $v_{\text{displacement}}$ values in CFRD 50 m and 100 m, it has the average ratio of 4. That mean, ratio of

displacement is found as square of the height of dam and the ratio of stresses is found in the ratio of height of dams.

The formulation of displacement ratio can be made as :

$$\text{Ratio}_{(\text{displacement})} = (h_1/h_2)^2 \quad (1)$$

With $h_1 =$ high of first dam (= 100 m)

$h_2 =$ high of second dam (=50 m)

With the formulation above, u and v displacement of CFRD with desired height can be found using one of the mentioned data (u_displacement data of CFRD 50 m or 100 m).

Location of maximum u_displacement on each type of slope is almost similar. In Stage 8, location does not change, still at 0.8H. Meanwhile for Stage 9, location of maximum u_displacement shifted from 0.8H or 0.6H to 0.4H. That means location of maximum u_displacement from upstream portion to downstream portion gradually decrease up to 0.4H.

Location of maximum v_displacement on each type of slope is almost similar. In Stage 8, location does not change, $\pm 0.8H$. Meanwhile for Stage 9, location of maximum u_displacement shifted from 0.8H to 1.0H.

6.4. RATIO OF DISPLACEMENT UNDER DYNAMIC LOAD

The displacements in respect of dam with slope of 1V:1.30H are discussed over Upstream Portion (Location 1), Centre Portion (Location 2) and Downstream Portion (Location 3) in this paragraph. The last stage of CFRD under static load and last stage of CFRD under dynamic load are used to analyze the ratio of displacement.

6.4.1. CFRD with Slope 1V:1.30H

6.4.1.1. U_Displacements under Acceleration of 0.1g

Maximum u_displacement value of CFRD 50 m in each location is presented in Table 6.1. Ratio in Location 1 is 1.017. That means CFRD under peak acceleration of 0.1g has increased u_displacement at 1.7%. At Location 2

and 3 increase up to 1.2% and 1% respectively. Location of maximum value is same as CFRD under static load.

Table 6.1 : U_Displacement of CFRD 50 m in Static and Dynamic Condition

Location	Max U_Displacement in Stage				Ratio (b/a)
	Last Stage (a)		Seismic 0.1g (b)		
	Value (m)	Location	Value (m)	Location	
1	0.293	0.6H	0.303	0.6H	1.017
2	0.561	0.6H	0.568	0.6H	1.012
3	0.700	0.4H	0.707	0.4H	1.010

In CFRD 100 m, maximum value of u_displacement in each location is presented in Table 6.2. Ratio in Location 1 is 1.005. That means CFRD under peak acceleration of 0.1g has increased u_displacement at 0.5%. At Location 2 and 3 increase up to 0.3% and 0.2% respectively. Location of maximum value is also same as CFRD under static load.

Table 6.2 : U_Displacement of CFRD 100 m in Static and Dynamic Condition

Location	Max U_Displacement in Stage				Ratio (b/a)
	Last Stage (a)		Seismic 0.1g (b)		
	Value (m)	Location	Value (m)	Location	
1	1.987	0.6H	1.994	0.6H	1.005
2	2.352	0.6H	2.358	0.6H	1.003
3	3.037	0.4H	3.044	0.4H	1.002

The correlation of u_displacement between CFRD 50 m and CFRD 100 m is presented in Table 6.3. There shows the ratio for three locations vary from 0.213 to 0.241. Average ratio for these values is 0.228.

Table 6.3 : U_Displacement Ratio of CFRD 50 m to 100 m

Location	U_Displacement Ratio in Stage			
	Last Stage (a)		Seismic 0.1g (b)	
	Ratio	Location	Ratio	Location
1	0.213	0.6H-0.6H	0.216	0.6H-0.6H
2	0.239	0.6H	0.241	0.6H
3	0.230	0.4H	0.232	0.4H

6.4.1.2. V_Displacements under Acceleration of 0.1g

Maximum v_displacement value of CFRD 50 m in each location is presented in Table 6.4. Ratio in Location 1 is 1.025. That means CFRD under peak acceleration of 0.1g has increased v_displacement at 2.5%, while at Location 2 and 3 are not affected by seismic load.

Table 6.4 : V_Displacement of CFRD 50 m in Static and Dynamic Condition

Location	Max V_Displacement in Stage				Ratio (b/a)
	Last Stage (a)		Seismic 0.1g (b)		
	Value (m)	Location	Value (m)	Location	
1	-0.204	0.8H	-0.209	0.8H	1.025
2	-0.183	0.6H	-0.183	0.6H	1.000
3	0.588	0.2H	0.588	0.2H	1.000

In CFRD 100 m, maximum value of v_displacement in each location is presented in Table 6.5. Ratio in Location 1 is 1.003. That means CFRD under peak acceleration of 0.1g has increased u_displacement at 0.3%. At Location 2 increases up to 0.2% and Location 3 is not affected by seismic load.

Table 6.5 : V_Displacement of CFRD 100 m in Static and Dynamic Condition

Location	Max V_Displacement in Stage				Ratio (b/a)
	Last Stage (a)		Seismic 0.1g (b)		
	Value (m)	Location	Value (m)	Location	
1	0.779	1.0H	0.781	1.0H	1.003
2	0.993	1.0H	0.995	1.0H	1.002
3	2.690	0.3H	2.690	0.3H	1.000

The correlation of u_displacement between CFRD 50 m and CFRD 100 m is presented in Table 6.6. There shows the ratio for three locations vary from 0.184 to 0.268. Average ratio for these values is 0.228.

Table 6.6 : V_Displacement Ratio of CFRD 50 m to 100 m

Location	V_Displacement Ratio in Stage			
	Last Stage (a)		Seismic 0.1g (b)	
	Ratio	Location	Ratio	Location
1	0.262	0.8H-1.0H	0.268	0.8H-1.0H
2	0.184	0.6H-1.0H	0.184	0.6H-1.0H
3	0.219	0.2H-0.3H	0.219	0.2H-0.3H

6.4.2. CFRD with Flatter Slope

The make sure whether the analysis results in CFRD with flatter slope has the same indication with CFRD slope of 1V:1.30H or slightly different, hence CFRD with slope of 1V:1.40H and 1V:1.50H has been chosen to the next analysis. By the same way as the above paragraph, the conclusion of result for different high of CFRD may be shown at Table 6.7 and 6.8.

Table 6.7 : Ratio of U & V Displacements of CFRD 50 m

Location	Average Ratio			
	U Displacement		V Displacement	
	1V:1.40H	1V:1.50H	1V:1.40H	1V:1.50H
1	1.020	1.022	1.031	1.189
2	1.018	1.019	1.000	1.000
3	1.011	1.013	1.002	1.003

Table 6.8 : Ratio of U & V Displacements of CFRD 100 m

Location	Average Ratio			
	U Displacement		V Displacement	
	0.1g	0.3g	0.3g	0.5g
1	1.005	1.007	1.002	1.007
2	1.003	1.003	1.002	1.006
3	1.002	1.002	1.000	1.000

By generalize slope variation; percent of increment for CFRD 50 m and 100 m may be made as the following table.

Table 6.9 : The Generalized Increment of U & V Displacements for CFRD 50 m under Variation of Seismic Load

Location	Average Ratio (%)					
	U Displacement			V Displacement		
	0.1g	0.3g	0.5g	0.1g	0.3g	0.5g
1	1.071	6.62	9.56	18.14	20.19	15.37
2	1.153	4.38	7.37	0.00	0.00	0.00
3	1.121	3.57	5.62	0.15	0.21	0.37

Table 6.10 : The Generalized Increment of U & V Displacements for CFRD 100 m under Variation of Seismic Load

Location	Average Ratio (%)					
	U Displacement			V Displacement		
	0.1g	0.3g	0.5g	0.1g	0.3g	0.5g
1	0.590	1.738	2.912	0.380	0.591	0.944
2	0.299	0.882	1.478	0.338	0.477	0.771
3	0.235	0.708	1.167	0.000	0.000	0.000

6.5. ANALYSIS FOR CFRD WITH SINGLE STAGE OF RESERVOIR FILLING

CFRD with 5 stages of construction process and 4 stages of reservoir filling has been used for this study. To know whether the behavior of CFRD in multi stages and in single stage of reservoir filling has a similarity or definitely different, hence a model has been made for that purpose.

Regarding to the result of analysis, CFRD with slope 1V:1.50H has smaller effect in displacements and stresses; hence this paragraph will discuss briefly the behavior of CFRD slope 1V:1.50H with single stage of reservoir filling compared to the result of CFRD multi stages. The results of analysis are discussed in following paragraph.

6.5.1. CFRD 50 m

From Figure 6.3 conclusion on the behavior of the CFRD under single stage of reservoir filling can be drawn as below:

1. Upstream Portion: The value of displacements and stresses is shown below. For Multi Stages have smaller values of horizontal & vertical displacement and horizontal normal stress than Single Stage. Single Stages has a smaller value only for vertical normal stress.

Max Value	Multi Stages	Single Stages
U_Displ (m)	0.223	0.271
V_Displ (m)	-0.122	-0.127
σ_{xx} (kPa)	5.83e+3	6.40e+3
σ_{yy} (kPa)	-7.05e+3	5.60e+3

2. **Central Portion:** The value of displacements and stresses is shown below. For Multi Stages have smaller values of vertical displacement and vertical normal stress than Single Stage. Single Stages has smaller values for horizontal displacement and horizontal normal stress.

Max Value	Multi Stages	Single Stages
U_Displ (m)	0.452	0.358
V_Displ (m)	-0.142	-0.190
σ_{xx} (kPa)	-2.92e+2	-1.98e+2
σ_{yy} (kPa)	-8.08e+2	-8.82e+3

3. **Downstream Portion:** The value of displacements and stresses is shown below. Single Stages has smaller values for all of displacements and stresses.

Max Value	Multi Stages	Single Stages
U_Displ (m)	0.556	0.421
V_Displ (m)	-0.658	-0.293
σ_{xx} (kPa)	-2.95e+2	-2.45e+2
σ_{yy} (kPa)	-3.71e+2	-3.61e+3

Comparison between CFRD 50 m Multi Stages and Single Stage of reservoir filling showed that single stage filling has higher value of deformation and stresses, mainly in the upstream portion.

6.5.2. CFRD 100 m

From Figure 6.4 conclusion on the behavior of the CFRD under single stage of reservoir filling can be drawn as below:

1. **Upstream Portion:** The value of displacements and stresses is shown below. For Multi Stages have smaller values of horizontal & vertical displacement and horizontal normal stress than Single Stage. Single Stages has a smaller value for vertical normal stress.

Max Value	Multi Stages	Single Stages
U_Displ (m)	1.136	1.167
V_Displ (m)	1.156	1.180
σ_{xx} (kPa)	1.83e+4	1.94e+4
σ_{yy} (kPa)	-1.57e+4	1.48e+4

2. **Central Portion:** The value of displacements and stresses is shown below. For Multi Stages has a smaller value of vertical normal stress than

Single Stage. Single Stages has smaller values for horizontal & vertical displacements and horizontal normal stress.

Max Value	Multi Stages	Single Stages
U_Displ (m)	1.935	1.460
V_Displ (m)	1.247	1.242
σ_{xx} (kPa)	-3.69e+2	-2.15e+2
σ_{yy} (kPa)	-1.40e+3	-1.62e+2

3. Downstream Portion: The value of displacements and stresses is shown below. For Multi Stages has a smaller value of horizontal normal stress than Single Stage. Single Stages has smaller values for horizontal & vertical displacements and vertical normal stress.

Max Value	Multi Stages	Single Stages
U_Displ (m)	2.407	1.934
V_Displ (m)	2.634	1.665
σ_{xx} (kPa)	-5.18e+2	-5.68e+2
σ_{yy} (kPa)	-7.45e+2	-5.03e+2

Comparison between CFRD 100 m Multi Stages and Single Stage of reservoir filling showed that single stage filling has also higher value of deformation and stresses, mainly in the upstream portion.

Figure 6.1 : Horizontal and Vertical Displacements of CFRD 50 m at Different Slopes

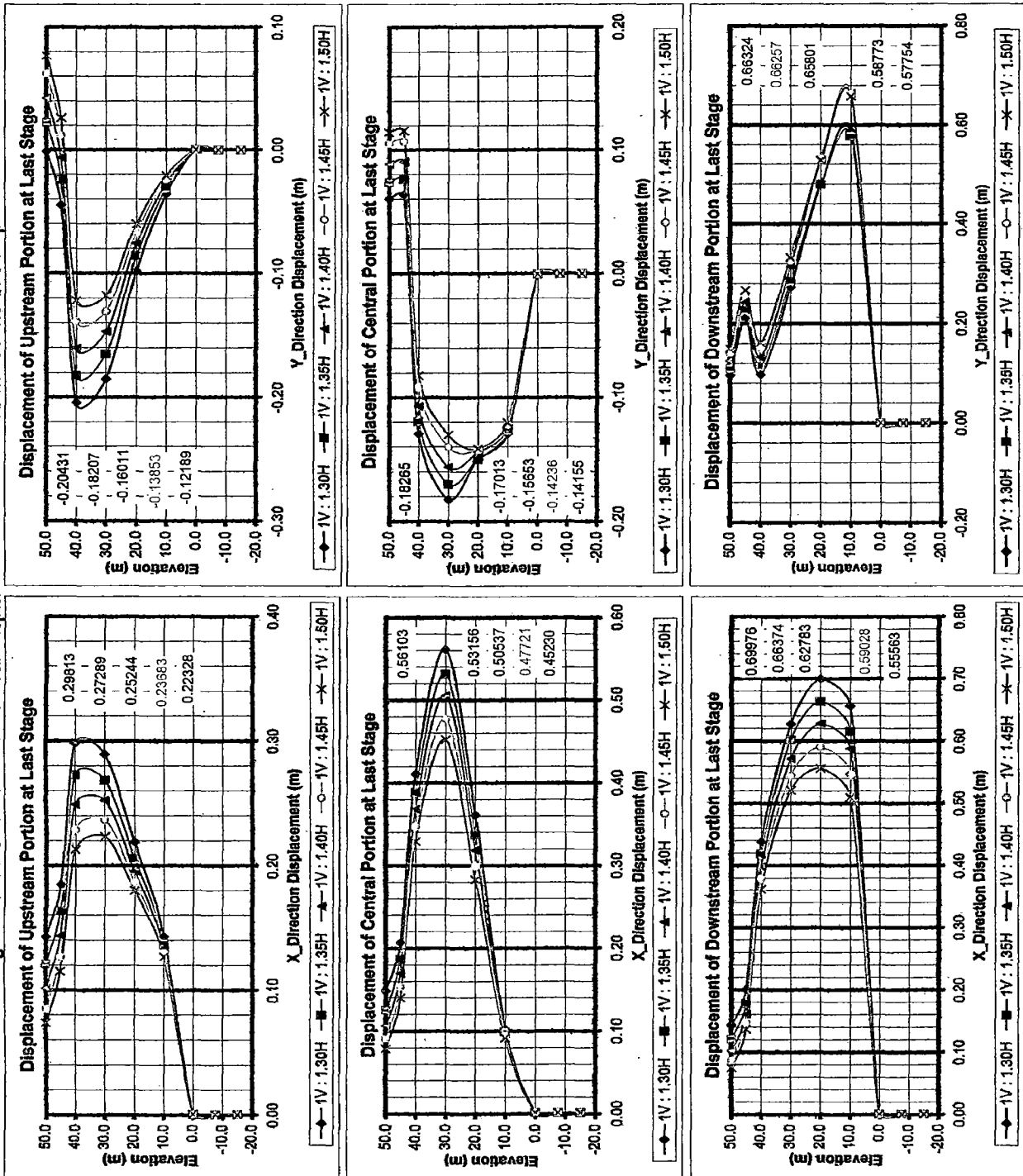


Figure 6.2 : Horizontal and Vertical Displacements of CFRD 100 m at Different Slopes

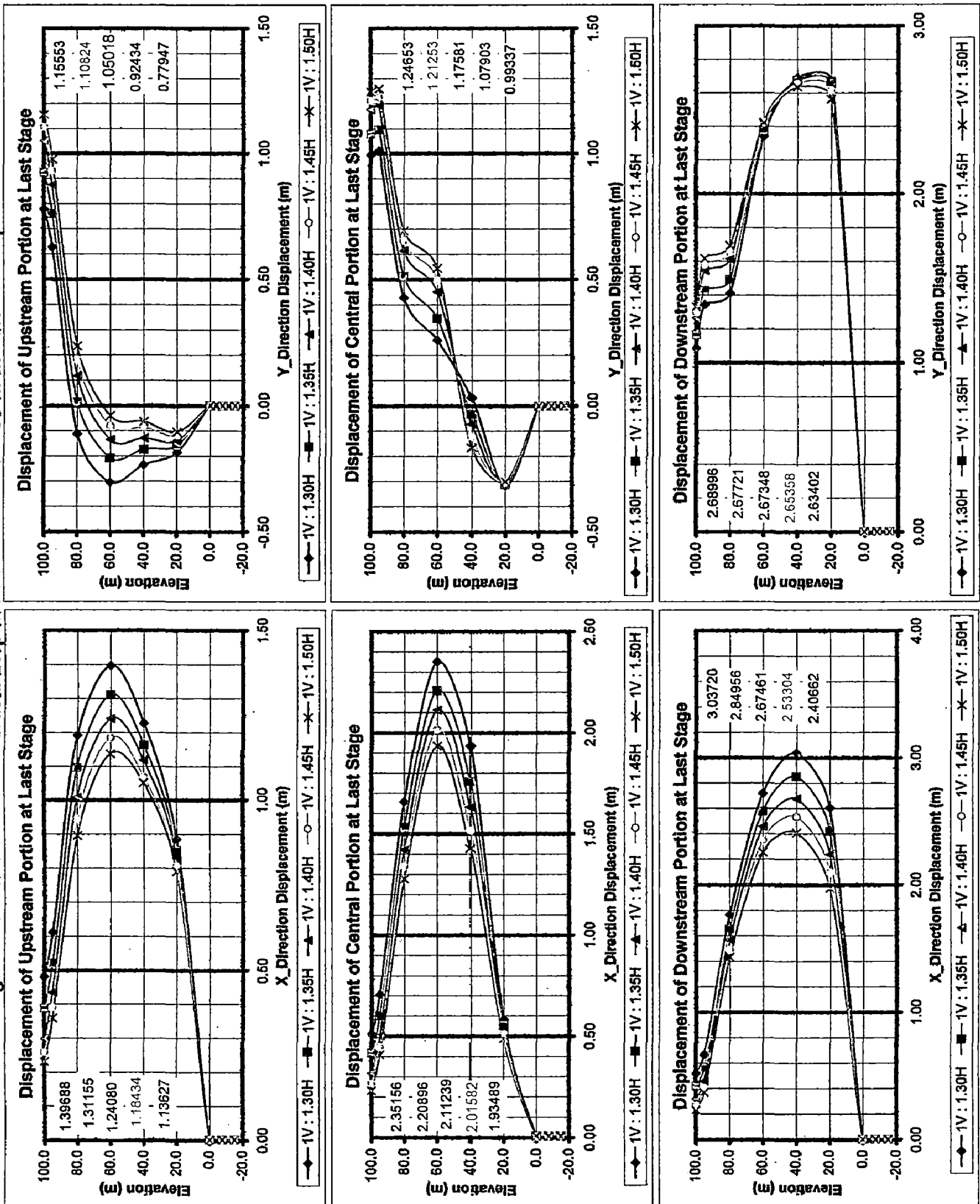


Figure 6.3 : Comparison between Multi Stages and Single Reservoir Filling Stage of CFRD 50 M Slope 1V:1.50H

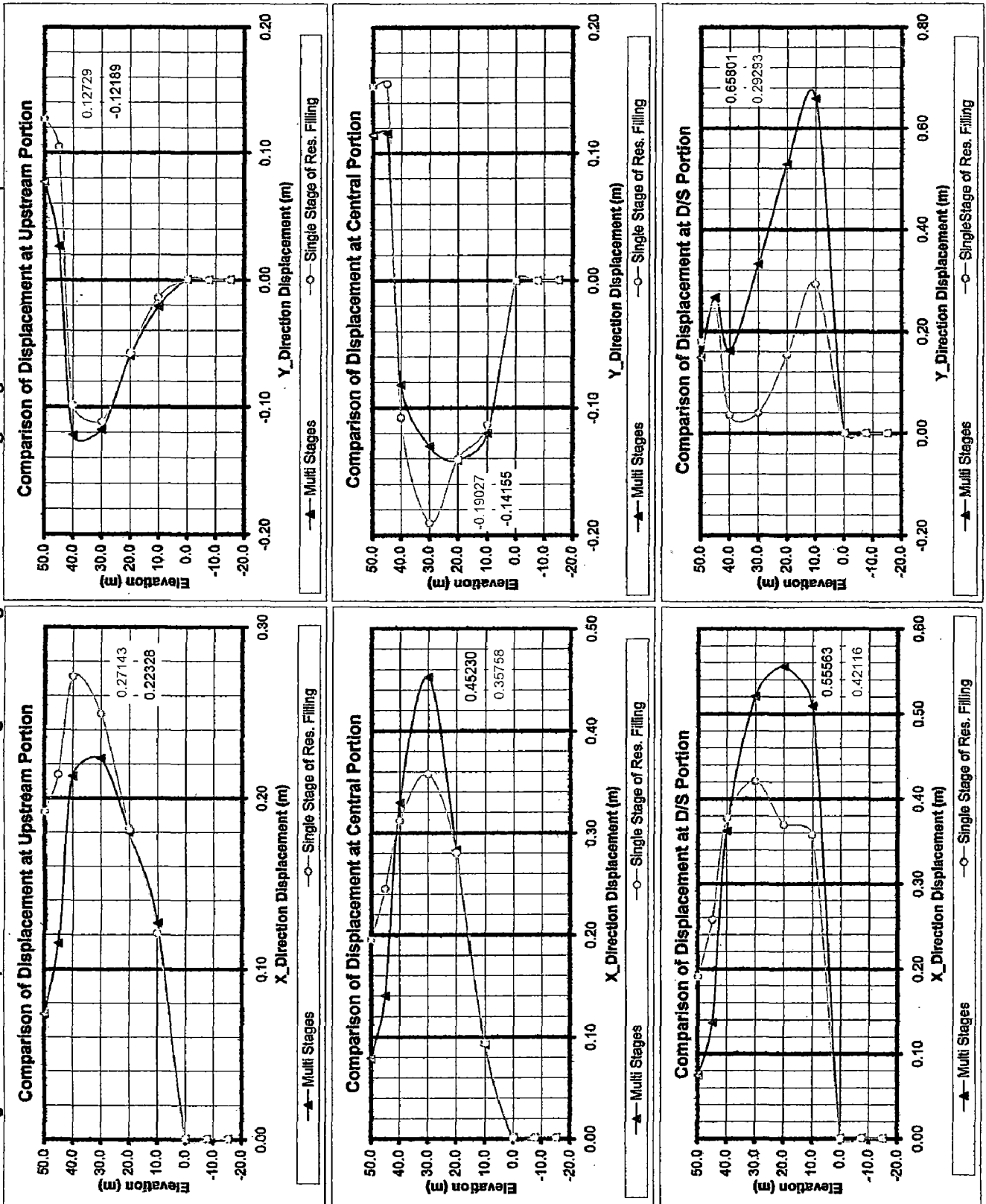
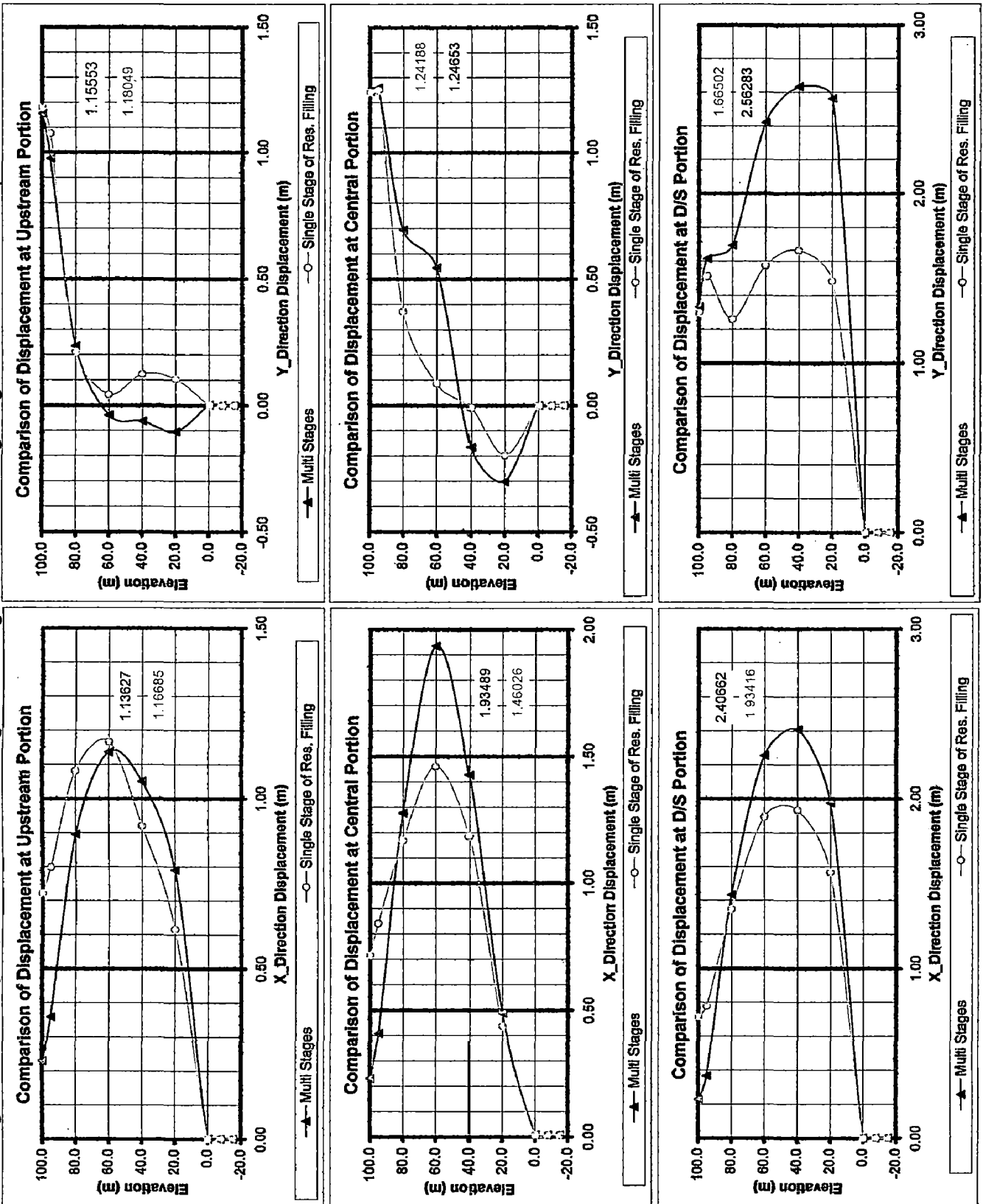


Figure 6.4 : Comparison between Multi Stages and Single Reservoir Filling Stage of CFRD 100 M Slope 1V:1.50H



CHAPTER 7

CONCLUSIONS

There is presently little analytical and observational evidence on the behavior of concrete-face slabs during seismic shaking. The choice of slab thickness with steel reinforcement is based solely on precedent, with performance under static loads being the only design consideration. To fill this gap, finite element study of the response of a typical 50 m and 100 m CFRD to static and seismic shaking has been presented using a realistic modeling for concrete slab, bedding, transition layer and the embankment materials. The model of CFRD uses the material parameters as simple incremental elastic and isotropic hyperbolic model developed by Duncan and Chang (1970) to capture the non linear behavior and pressure dependency. The main conclusions may be drawn as follow:

7.1. CONCLUSION OF CASE I STUDY

CFRD has been built with multi stages process and effect of static load as below:

1. The horizontal displacement of upstream, central and downstream portion toward the downstream direction from the beginning of construction to the last stage of reservoir filling, dam with slope 1V:1.50H is found minimum in both heights of 50 m and 100 m.
2. The vertical displacement at dam 50 m and 100 m high do not depict similar behavior of upstream, central and downstream portion. Maximum value has been found at different locations. For CFRD 50 m, slope 1V:1.50H has

resulted in minimum displacement and for CFRD 100 m, slope 1V:1.30H has resulted in minimum displacement. In case of 100 m high dam, the results show settlement in upstream portion and heaving of crest and downstream portion. This indicates the necessity of flattening downstream slope.

3. The horizontal normal stress of upstream portion towards the downstream direction while stresses in central and downstream portion counter act it. Generally the slope is found to have insignificant effect on these stresses.
4. The vertical normal stress of upstream, central and downstream portion in downward direction from the beginning of construction to the last stage of reservoir filling. The upstream portion has the maximum stress with all these slopes. This stress in central and downstream portion is found insignificant as compared to upstream portion. These stresses are found to increase in the ratio of the height of dam. Slope is found to have insignificant effect on the value of the stresses.

7.2. CONCLUSION OF CASE II STUDY

CFRD under dynamic load has results as below:

The results have shown that in both heights of dam, the application of peak ground acceleration up to 0.5g has resulted into a maximum of 15% in the displacements and stresses over the static load values. This confirms the findings of other researchers that concrete face rockfill dam can safely stand by earthquakes.

7.3. GENERAL OBSERVATIONS

1. Multi stage process has smaller values of deformation and stresses as compared to single stage of reservoir filling, at upstream portion.
2. Ratio of displacement is found as square of the height of dam and the ratio of stresses is found in the ratio of height of dams.

3. Reservoir filling largely affects the deformations and stresses in upstream portion as compared to central portion and downstream portion.

7.4. SUGGESTIONS FOR FURTHER STUDY

1. The study has been done with slope from 1V:1.30H to 1V:1.50H under seismic load (peak acceleration) of 0.1g to 0.5g. Analysis should be carried out for other heights and slopes as well as for stronger seismic loads, in order to have better understanding of the behavior of CFRD.
2. The study was conducted assuming a strong foundation and may be extended with a flexible foundation to take care of other situations.

REFERENCES

- (1) Central Board of Irrigation and Power India (1992), "Rockfill Dams-Finite Element Analysis to Determine Stresses and Deformations in Membrane Type Rockfill Dam", Ministry of Water Resources India, Oxford & IBH Publishing, New Delhi, India.
- (2) Sherard, J.L, Woodward, R.J, Gizienski, S.F and Clevenger, W.A (1966), "Earth and Earth-Rock Dams", John Wiley and Sons, Inc, New York, USA
- (3) Australian National Committee on Large Dams (1991), "Guidelines on Concrete-Faced Rockfill Dams", Australia.
- (4) J. Barry Cooke and James L. Sherard (1985), "Concrete Face Rockfill Dams-Design, Construction, and Performance", ASCE Geotechnical Symposium, Detroit, USA.
- (5) Liu Xia, Wu Xingzheng, Xin Junxia, and Tian Hangong, "Three-Dimensional Stress and Displacement Analysis of Yutiao Concrete Faced Rockfill Dam".
- (6) Mike D Fitzpatrick, Bruce A Cole, Frank L Kinstler, and Bram P Knoop. (1985), "Design of Concrete-Faced Rockfill Dams", ASCE Geotechnical Symposium, Detroit, USA.
- (7) Robin Fell, Patrick Mc. Gregor, and David Stapledon (1992), "Geotechnical Engineering of Embankment Dams", CAA Balkema, Rotterdam, pp. 519 – 551.
- (8) Singh, R.P. (1991), "Three Dimensional Analysis of Rockfill Dams under Gravity Loading", Ph. D. Thesis, Water Resources Development Training Centre, University of Roorkee, India
- (9) Justo, J.L. and Saura, J. (1983), "Three Dimensional Analysis of Infiernillo Dam during Construction and Filling of the Reservoir". Int. Journal of Numerical Methods in Geomechanics, Vol. 7, pp. 225 – 243
- (10) Penman, A.D.M. and Charles, J.A. (1976), "The Quality and Suitability of Rockfill Used in Dam Construction", Proc. ICOLD 12th Congress, Mexico, Q.44, R.26, pp. 533 – 556
- (11) Potts, D.M. and Zdravkovic, L (2001), "Finite Element Analysis in Geotechnical Engineering : Application", First Edition, Thomas Telford, London, U.K
- (12) Duncan, J.M. and Chang, C.Y. (1970), "Nonlinear Analysis of Stresses and Strain in Soils", Journal of the Soil Mechanics and Foundations Division, ASCE, Vol. 96, No. SM5, pp. 1629 – 1653

- (13) Eisenstein, Z., Krishnayya, A.V.G. and Morgenstern, N.R. (1972), "An Analysis of the Cracking at Duncan Dam", Proc. Of ASCE Specialty Conference on Performance of Earth and Earth Supported Structures, Purdue University, Lafayette, Indiana, Vol. 1, pp. 765-778
- (14) Botta, L.P.I., Varde, O.A., Paitovi, O. and Andersson, C.A. (1985), "Comparison between Predicted and Observed Behavior of Alicura Dam, Argentina", Proc. ICOLD 15th Congress, Lausanne, Q.56, R.43, pp. 813 – 838
- (15) Kulhawy, F.H. and Duncan, J.M. (1972), "Stresses and Movements in Oroville Dam", Journal of the Soil Mechanics and Foundations Division, ASCE, No. SM7, pp. 653 – 665
- (16) Priscu, R., Stenatiu, D. and Dobrescu, D. (1985), "Capabilities of Mathematical Models to Predict Dam Behaviour during Erection of Riusor Rockfill Dam", Proc. ICOLD 15th Congress, Lausanne, Q.56, R.34, pp. 667 – 677
- (17) Yasunaka, M., Tanaka, T. and Nakano, R. (1985), "The Behaviour of Fukuda Rockfill Dam during Construction and Impounding of the Reservoir", Proc. ICOLD 15th Congress, Lausanne, Q.56, R.24, pp. 499 – 519
- (18) Domaschuk, L. and Valliappan, P. (1975), "Nonlinear Settlement Analysis by Finite Element", Journal of the Geotechnical Engineering Division, ASCE, Vol. 101, No. GT7, pp.601-614
- (19) Hansen, J.B. (1963), "Discussion Hyperbolic Stress-Strain Response: Cohesive Soils", Journal of the Soil Mechanics and Foundations Division, ASCE, Vol. 89, No. SM4, pp. 241-242
- (20) Izumi, H., Kamemura, K. and Sato, S. (1976), "Finite Element Analysis of Stresses and Movements in Excavation", Int. Conference of Numerical Methods in Geomechanics, ASCE, pp. 701 – 712
- (21) Kondner, R.L. (1963), "Hyperbolic Stress-Strain Response: Cohesive Soils", Journal of the Soil Mechanics and Foundations Division, ASCE, Vol. 89, No. SM1, pp. 115-143
- (22) Kovacevic, N., Vaughan, P.R. and Potts, D.M. (2002), "A Comparison between X Observed and Predicted Deformations of Winscar Dam", Proc. of the Eight International Symposium on Numerical Models in Geomechanics, Rome, Italia, pp. 565-571

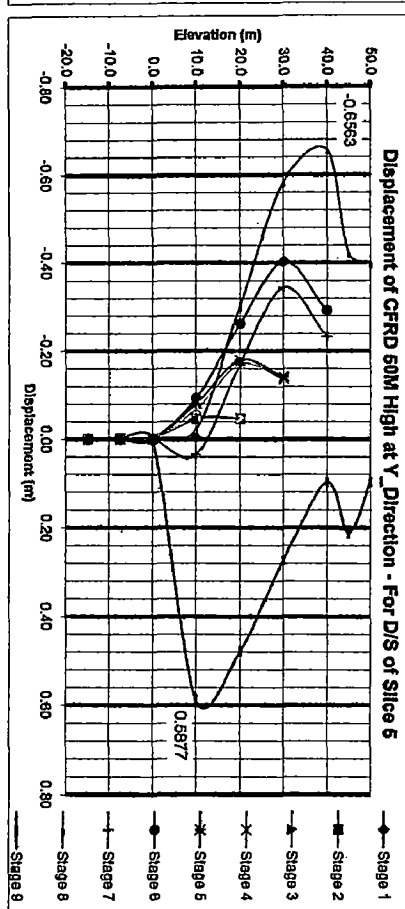
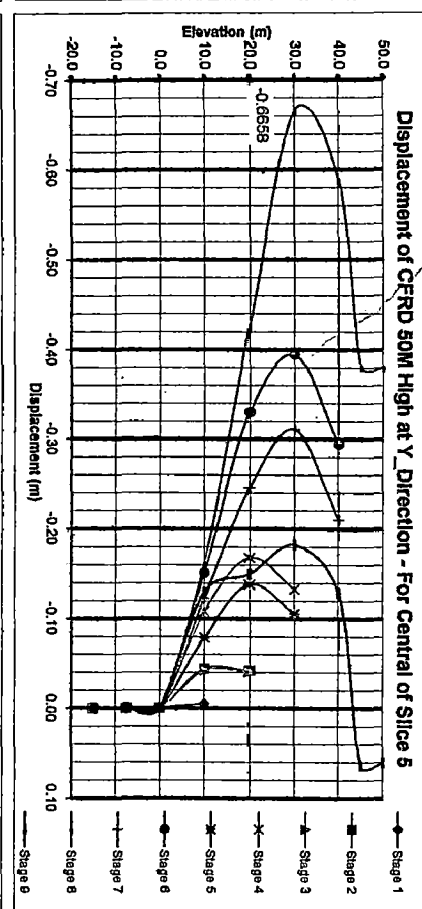
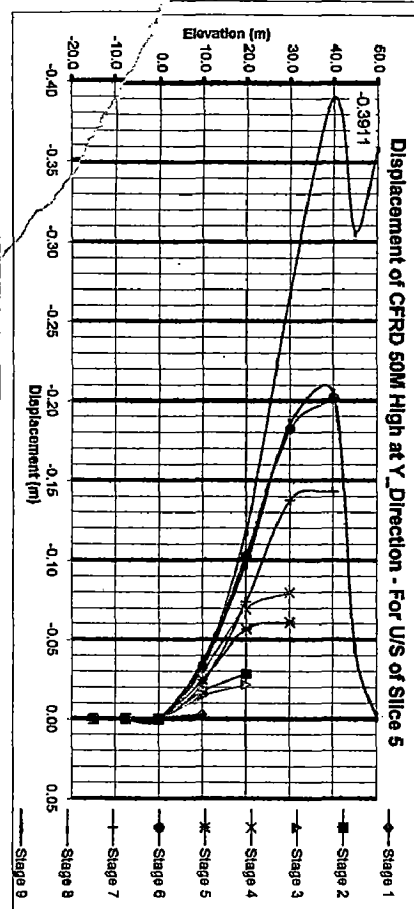
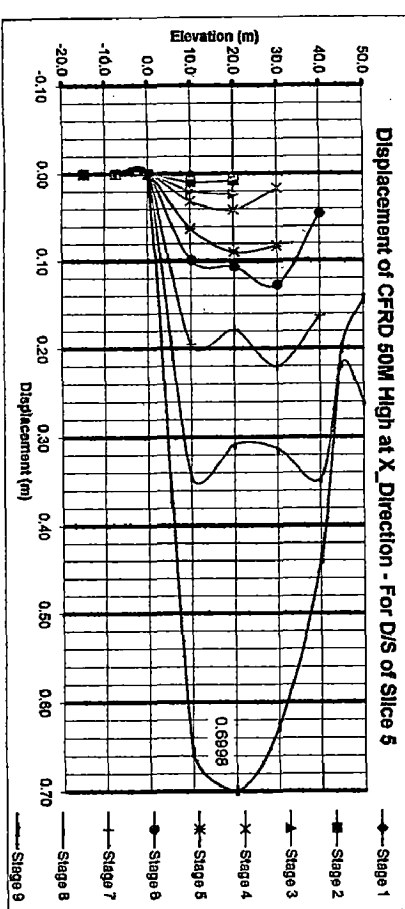
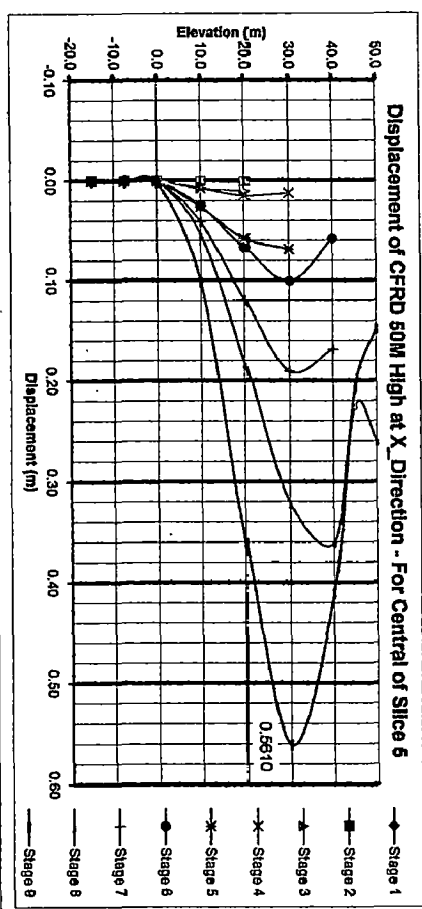
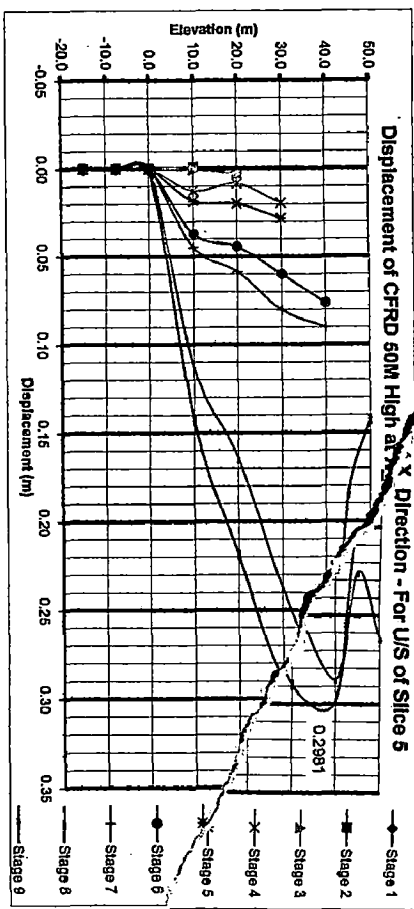
BIBLIOGRAPHY

- (1) James L. Sherard and J. Barry Cooke (1987), "Concrete Face Rockfill Dam: I. Assessment", *Journal of Geotechnical Engineering*, Vol. 113, No. 10, pp. 1096 – 1112.
- (2) J. Barry Cooke and James L. Sherard (1987), "Concrete Face Rockfill Dam: II. Design", *Journal of Geotechnical Engineering*, Vol. 113, No. 10, pp. 1113 – 1131.
- (3) Syed Khalid, Bharat Singh, G.C. Nayak and O.P. Jain (1990), "Nonlinear Analysis of Concrete Face Rockfill Dam", *Journal of Geotechnical Engineering*, Vol. 116, No. 5, pp. 822 – 837.
- (4) Bureau, G., Volpe, R.L., Roth, W.H. and Udaka, T., (1985), "Seismic Analysis of Concrete Face Rockfill Dams", *ASCE Geotechnical Symposium*, Detroit, USA.
- (5) Seed, H.B., Seed, R.B., Lai, S.S., and Khamenehpour, B., (1985), "Seismic Design of Concrete Faced Rockfill Dams" *ASCE Geotechnical Symposium*, Detroit, USA.
- (6) Gavan Hunter and Robin Fell (2003), "Rockfill Modulus and Settlement of Concrete Face Rockfill Dams", *Journal of Geotechnical and Geoenvironmental Engineering*, Vol. 129, No. 10.

APPENDICES

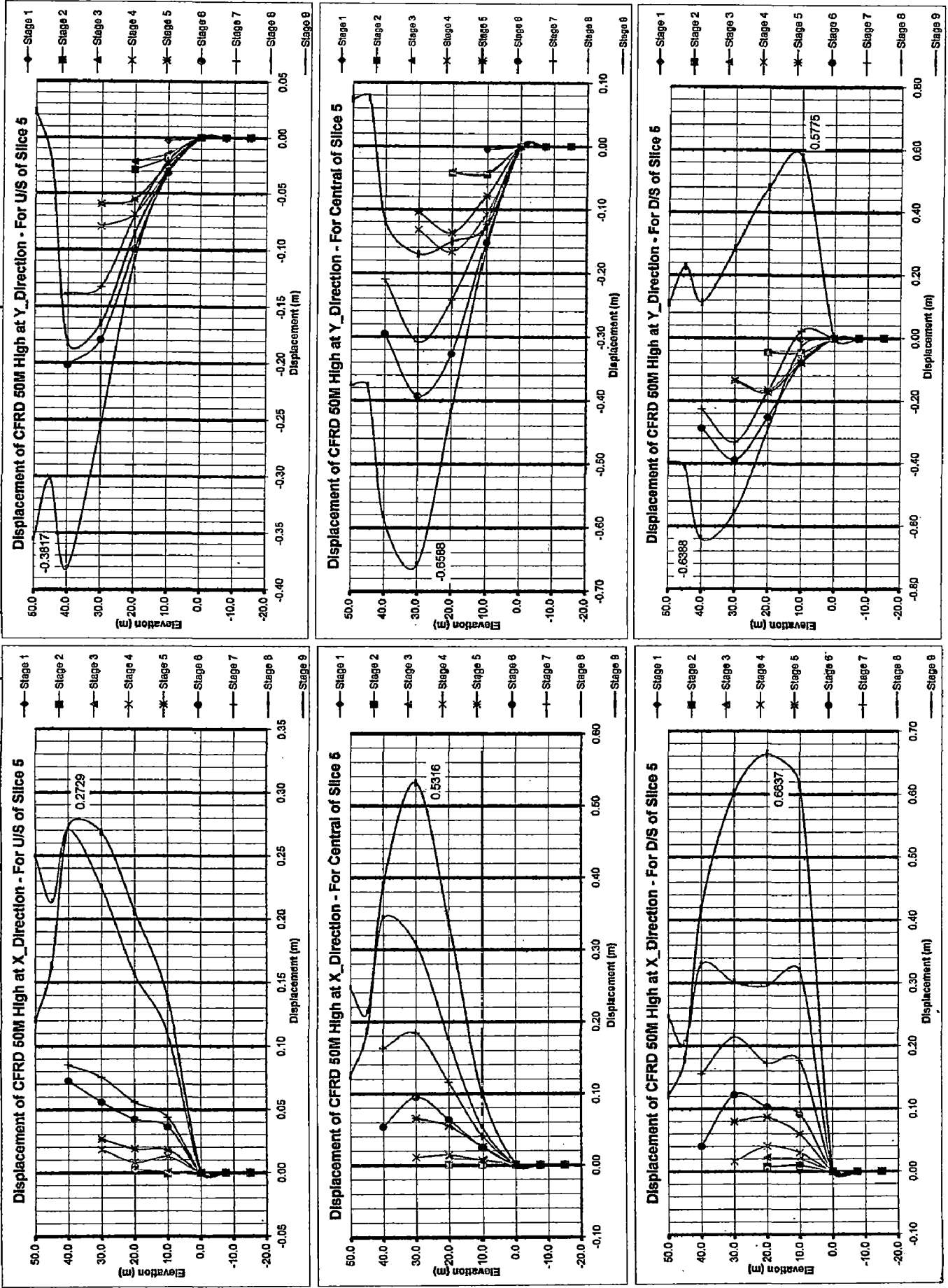
APPENDIX A :

Figure A.1 : Graphs Depict Displacement of CFRD 50 m High at X_Direction - For U/S of Slope 1V:1.30H



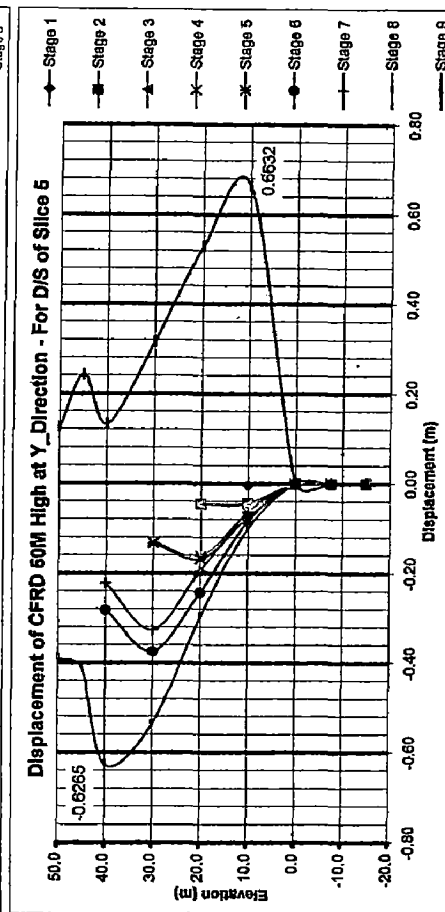
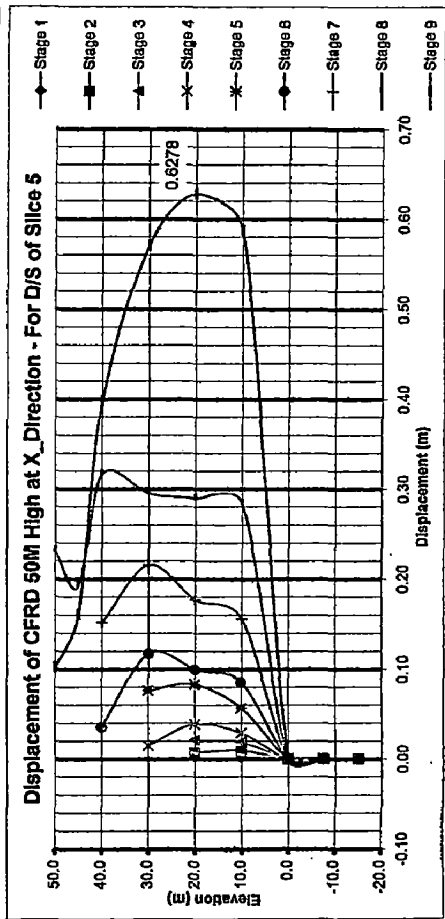
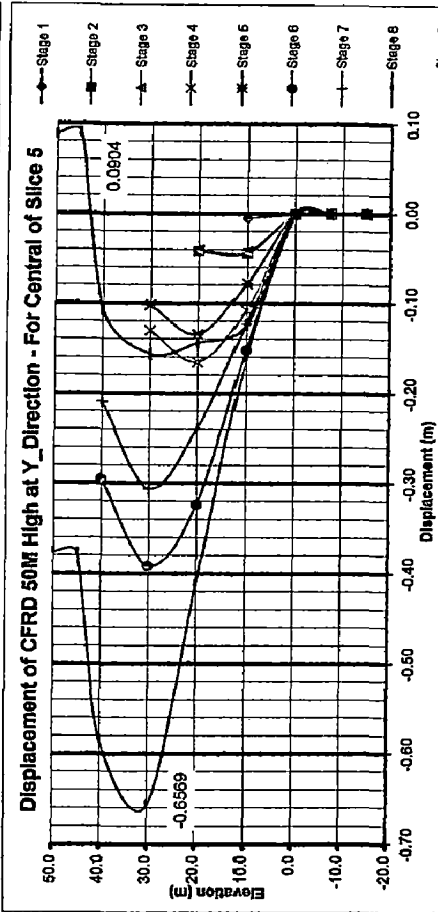
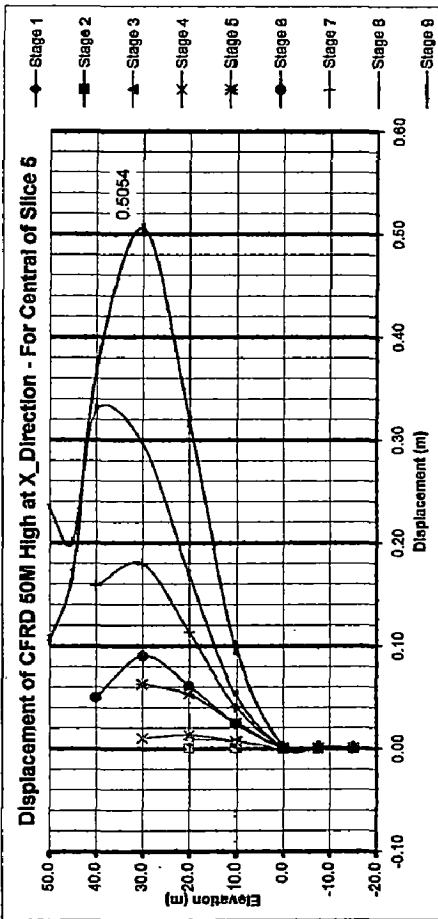
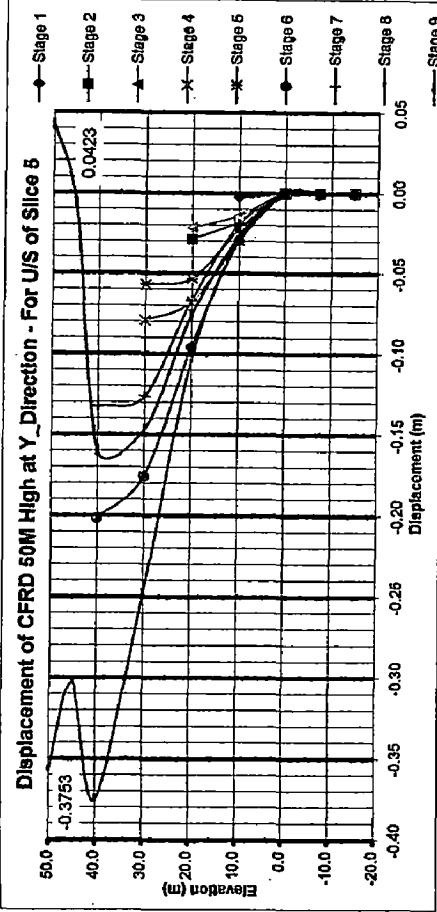
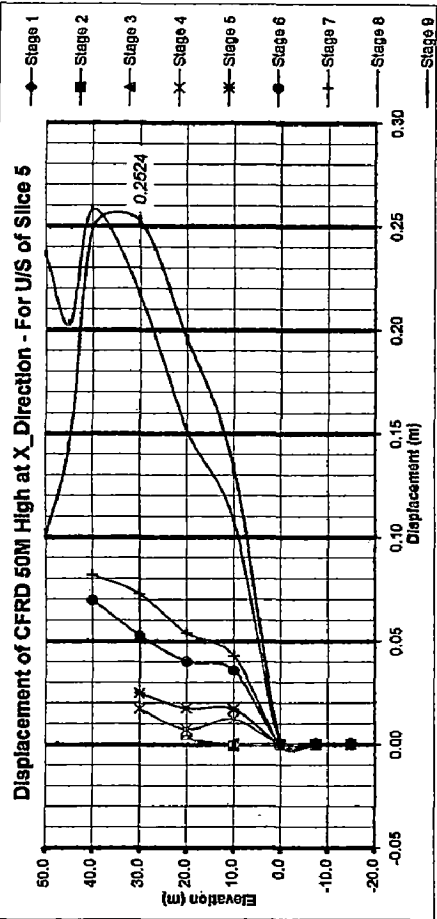
APPENDIX A :

Figure A.2 : Graphs Depict Displacement of CFRD 50 m with Slope 1V:1.35H



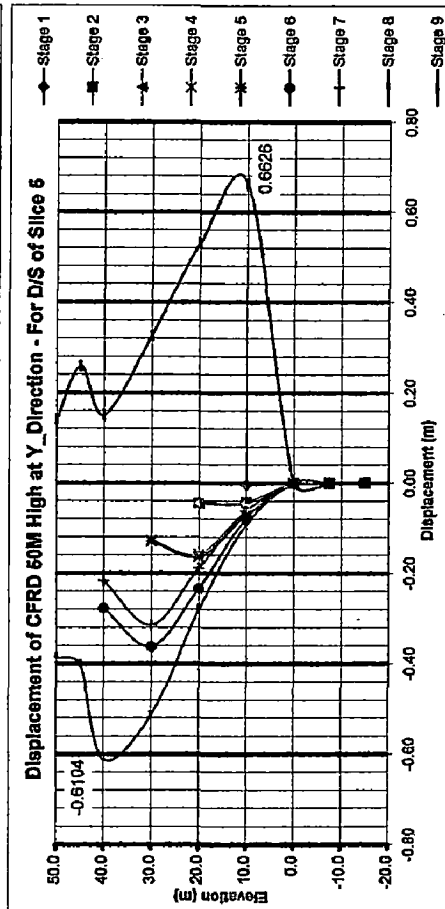
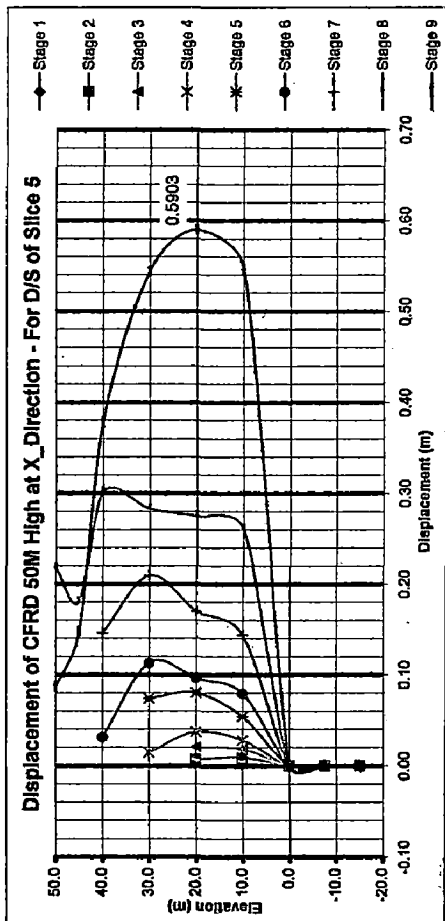
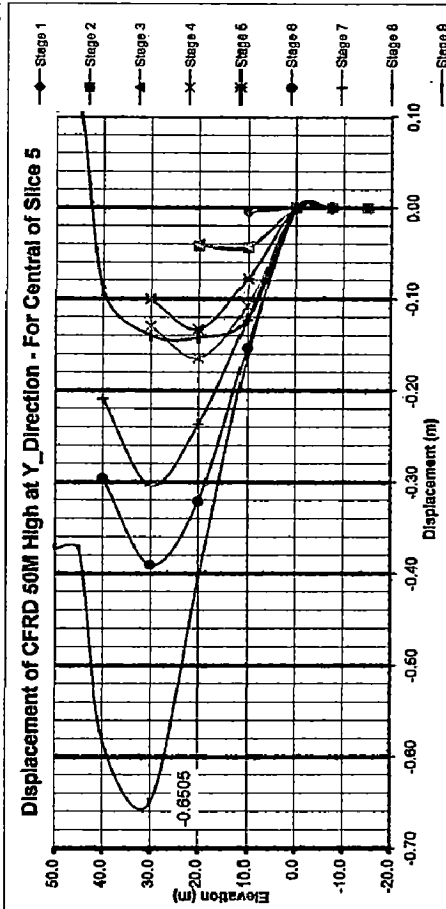
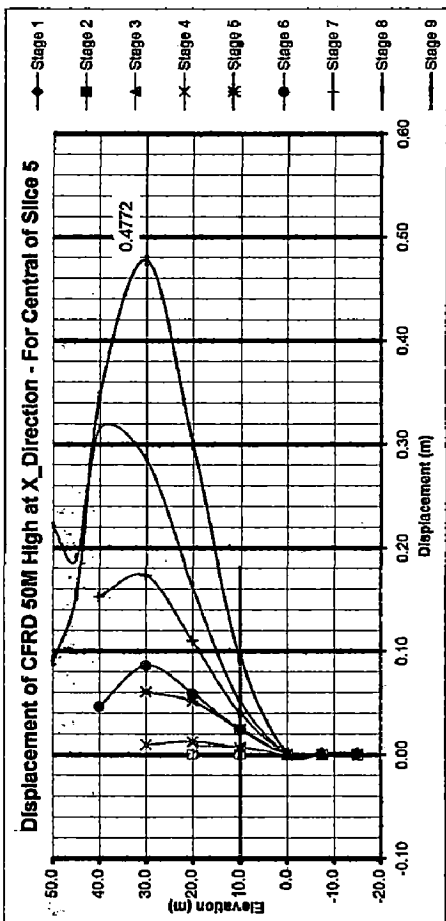
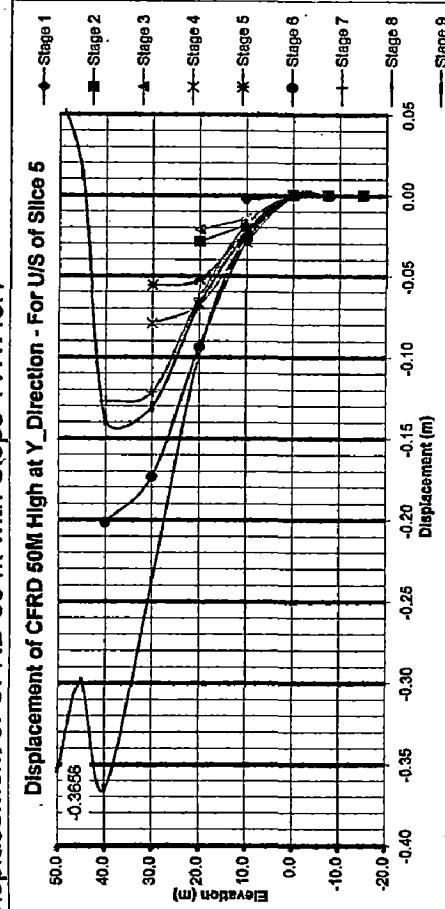
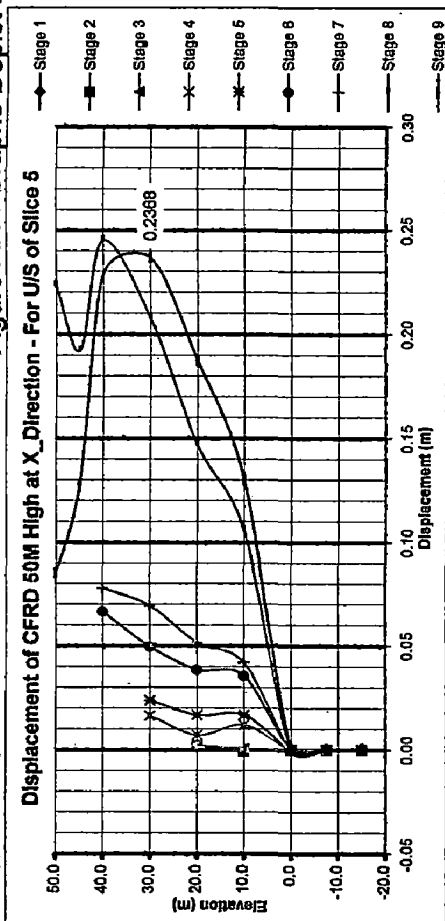
APPENDIX A :

Figure A.3 : Graphs Depict Displacement of CFRD 50 m with Slope 1V:1.40H



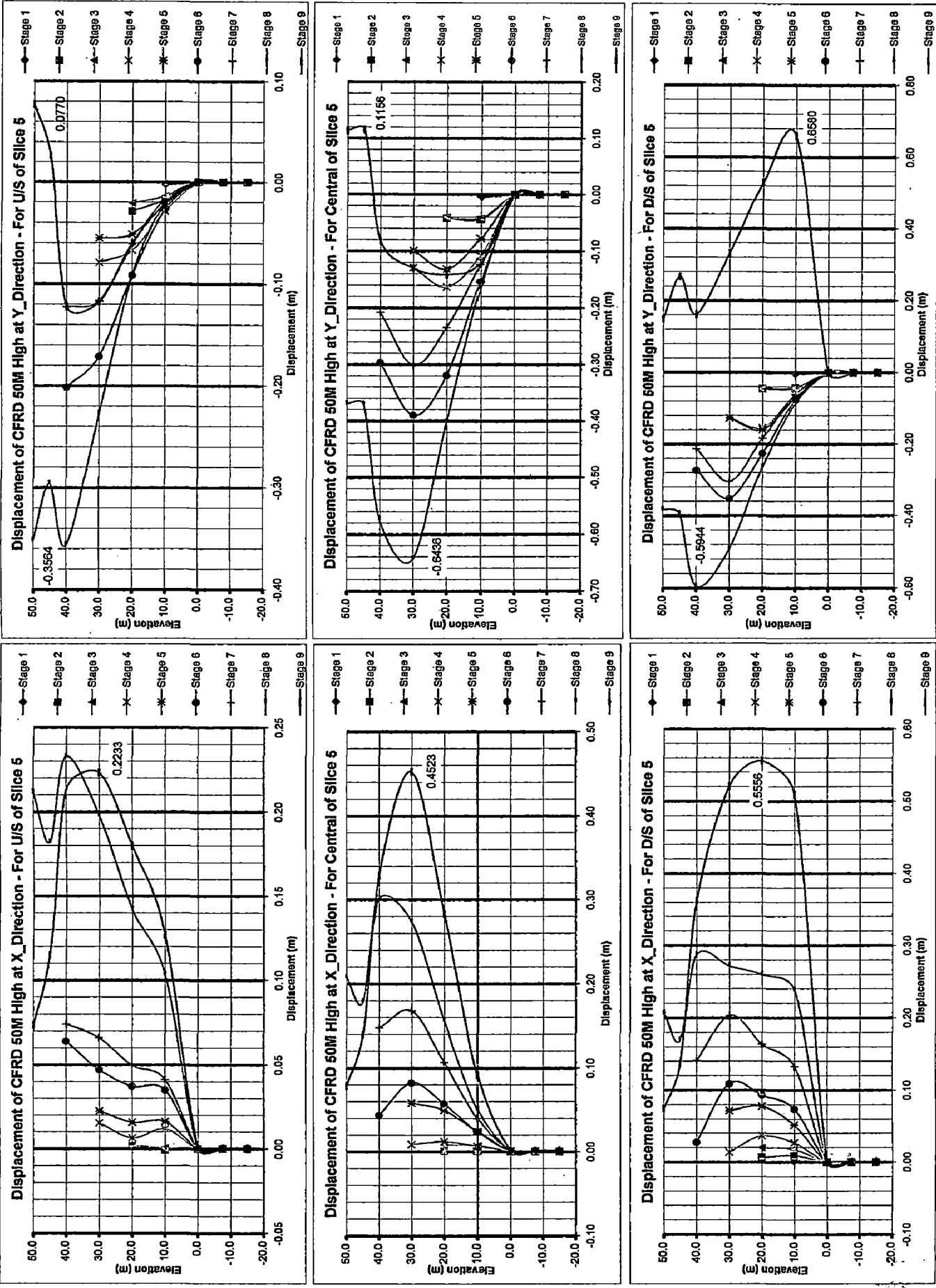
APPENDIX A :

Figure A.4 : Graphs Depict Displacement of CFRD 50 m with Slope 1V:1.45H



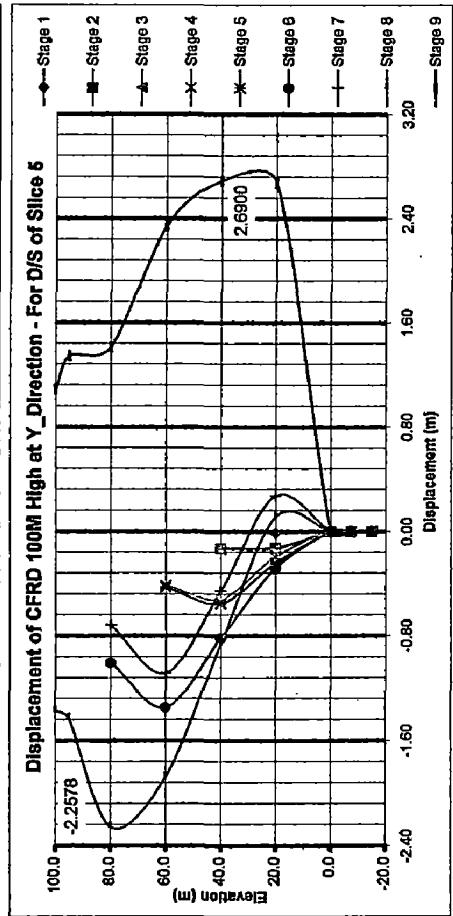
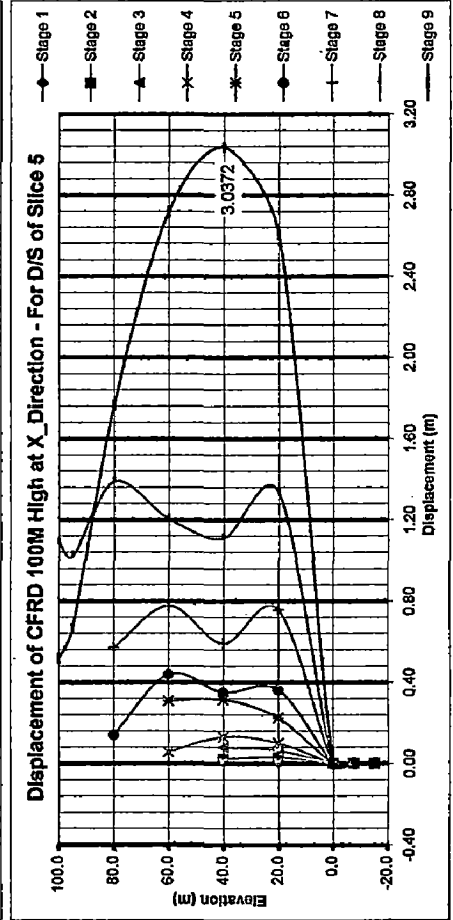
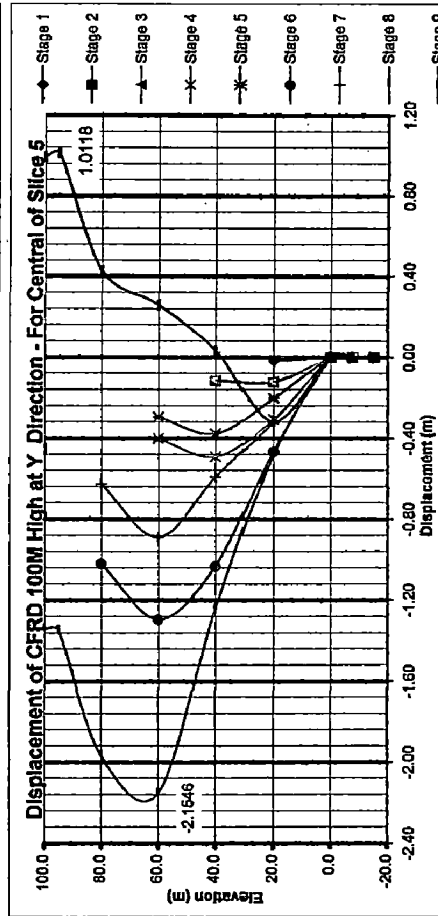
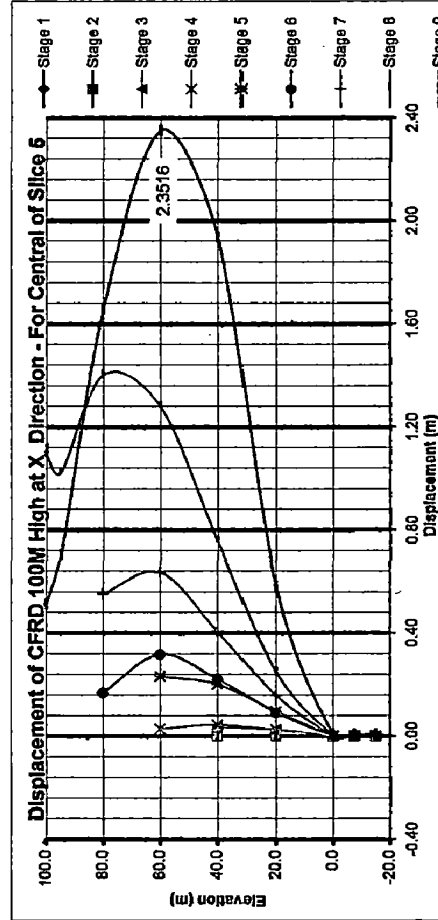
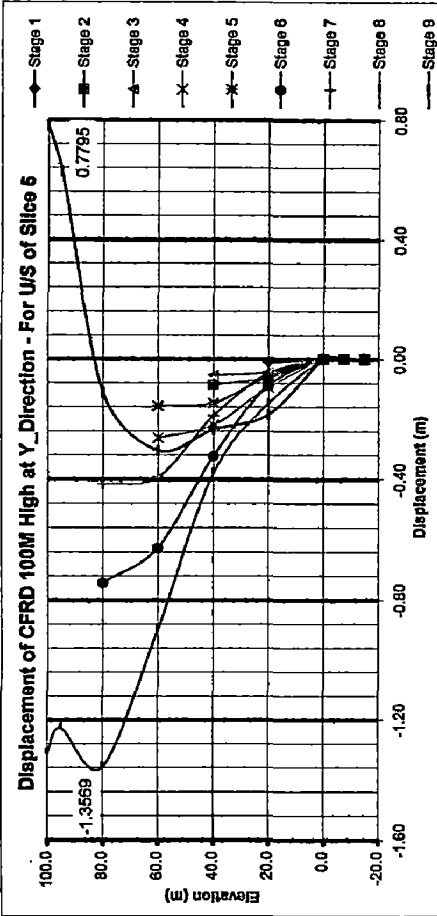
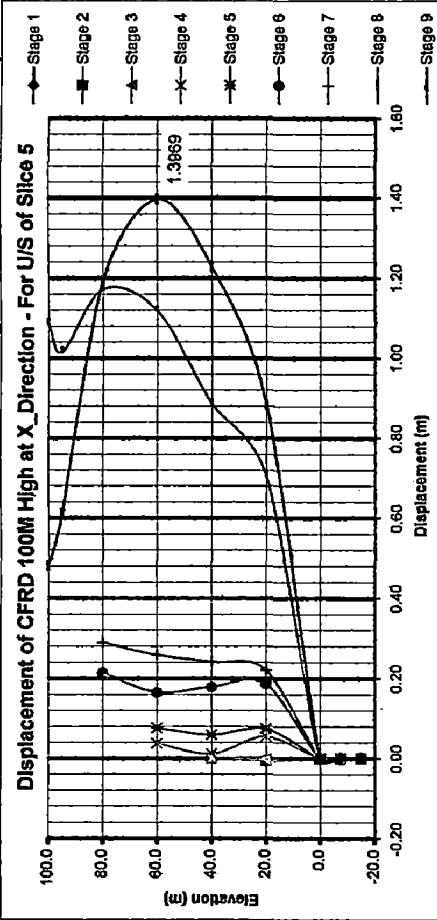
APPENDIX A :

Figure A.5 : Graphs Depict Displacement of CFRD 50 m with Slope 1V:1.50H



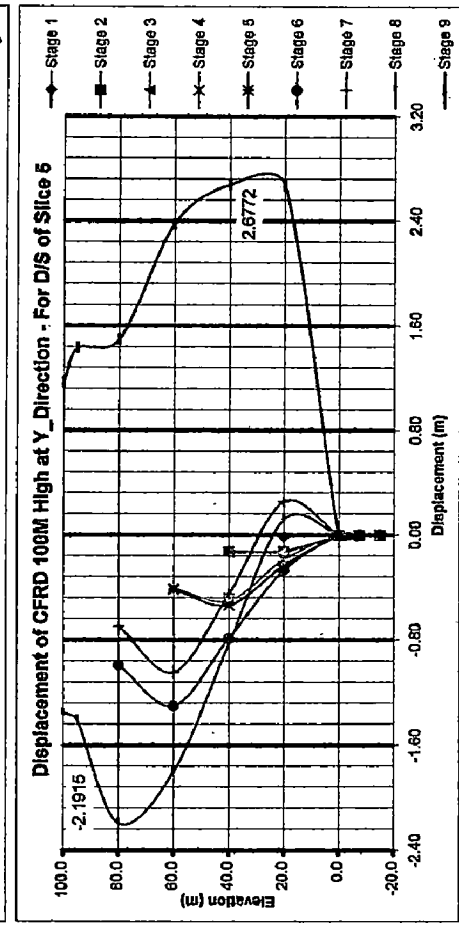
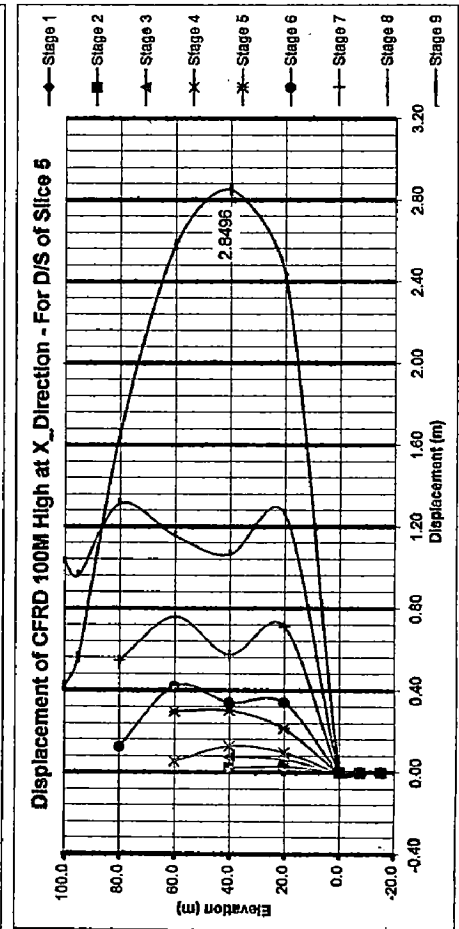
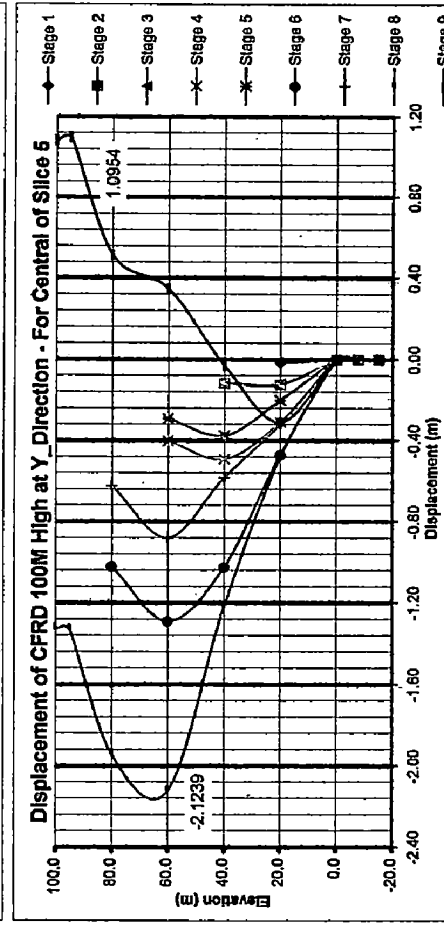
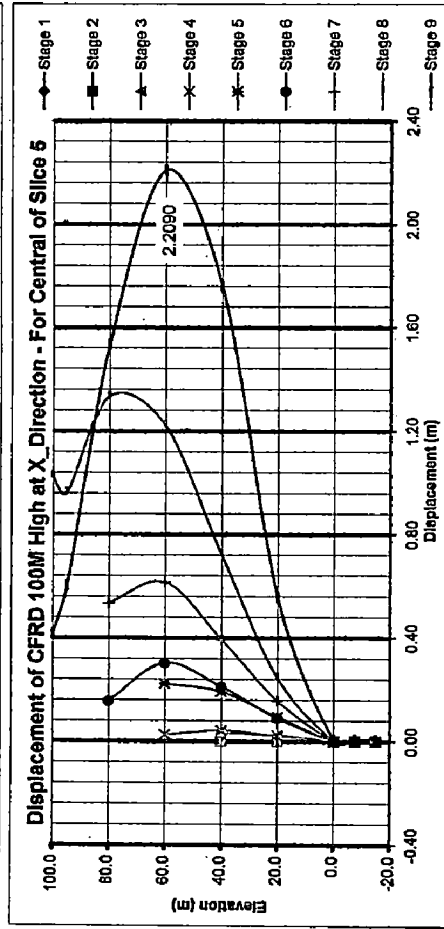
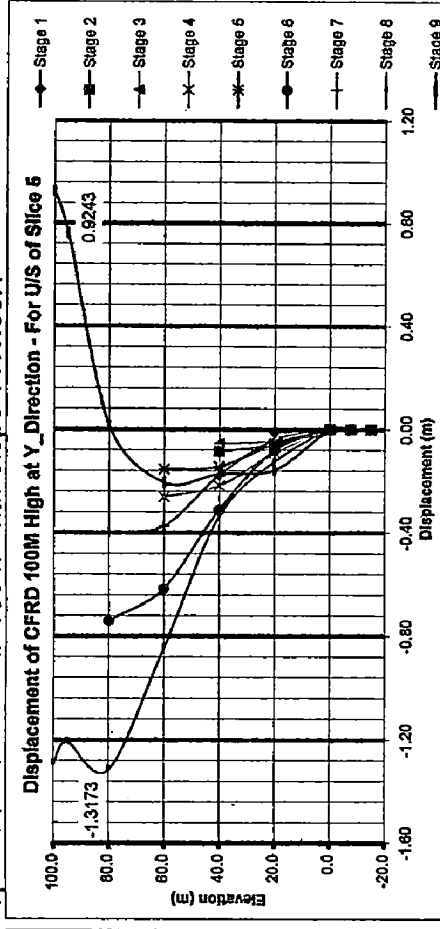
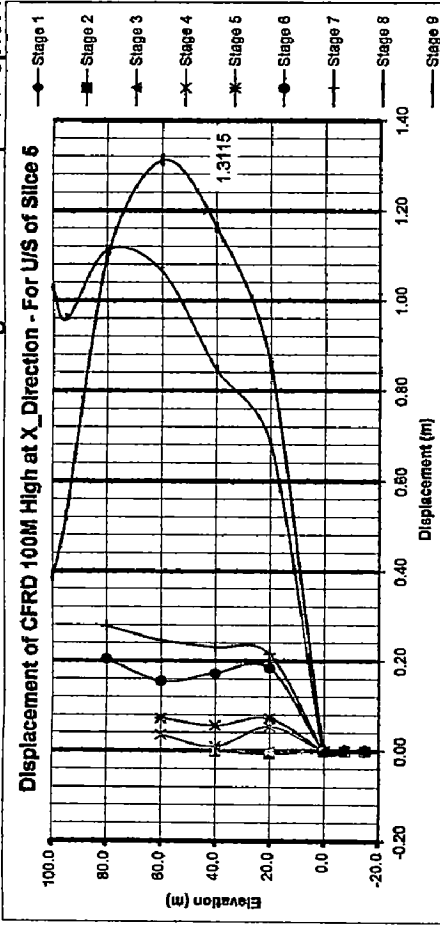
APPENDIX A :

Figure A.6 : Graphs Depict Displacement of CFRD 100 m with Slope 1V:1.30H



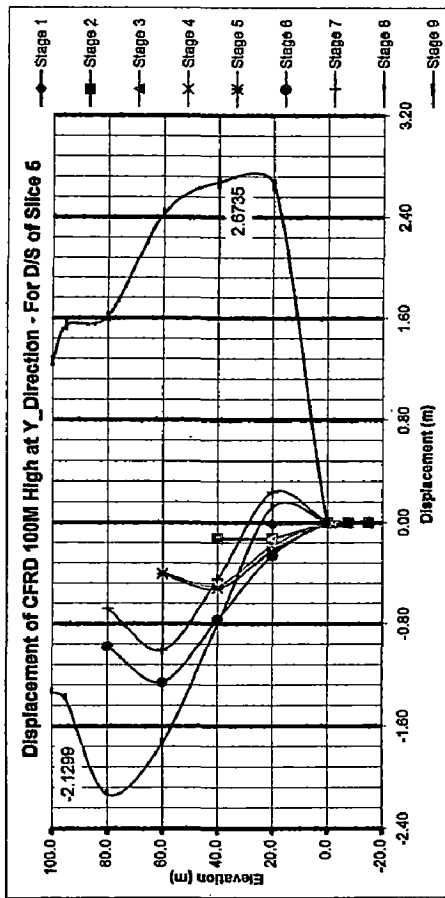
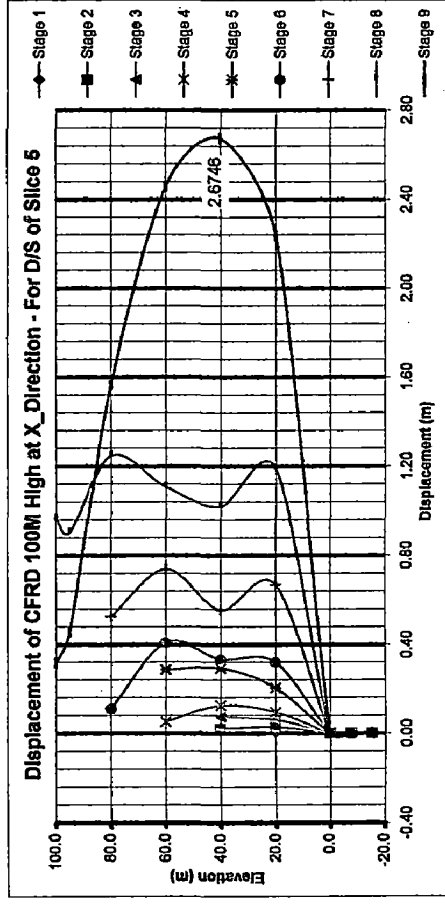
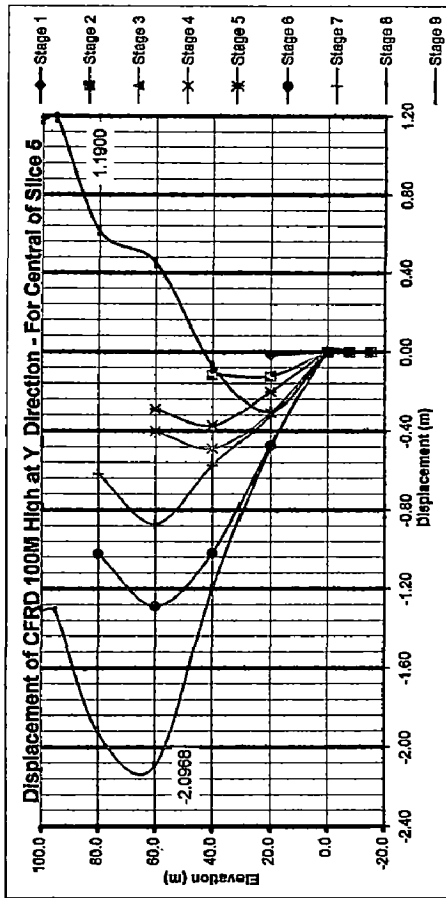
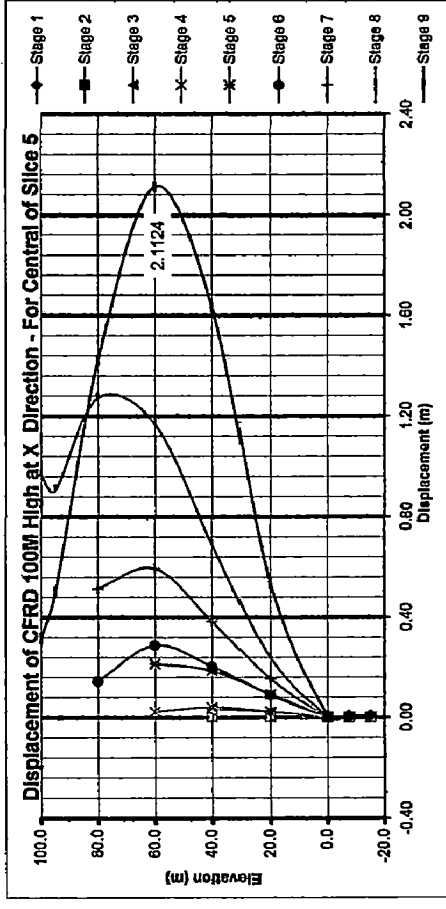
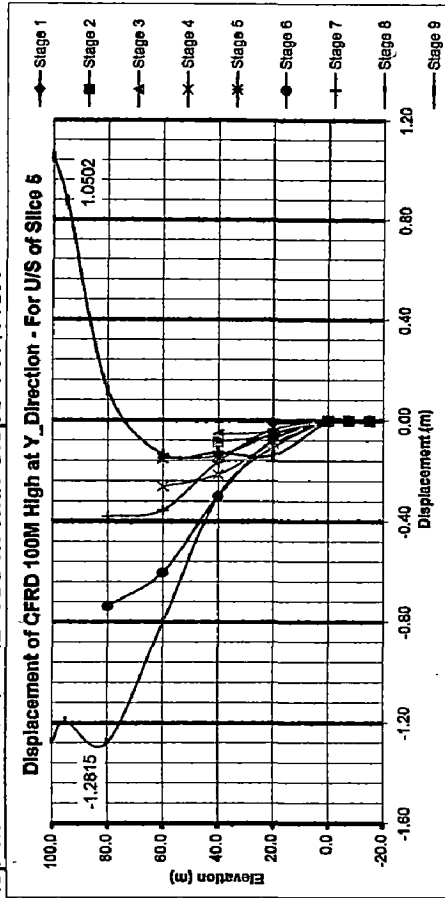
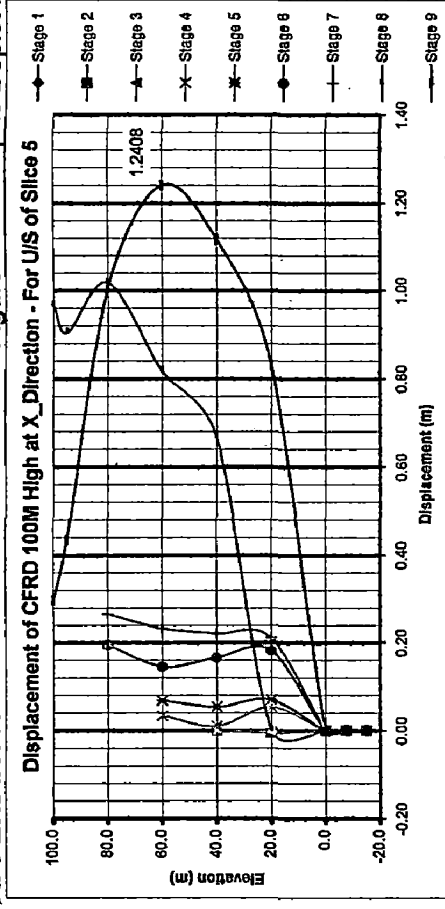
APPENDIX A :

Figure A.7 : Graphs Depict Displacement of CFRD 100 m with Slope 1V:1.35H



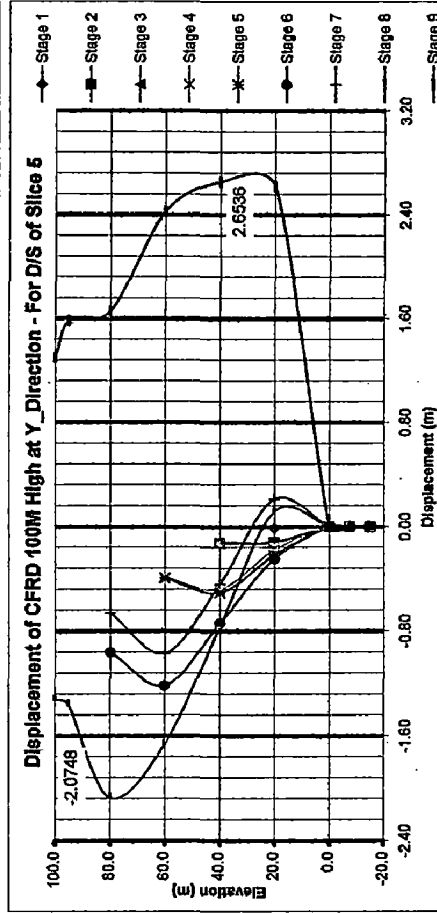
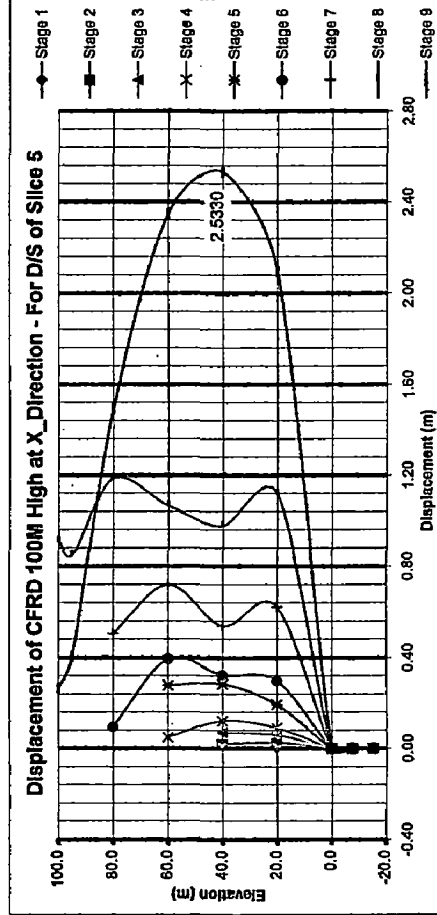
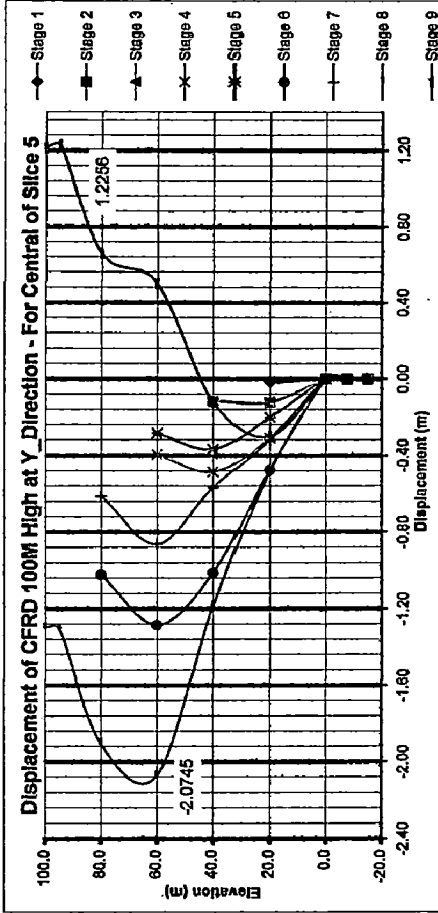
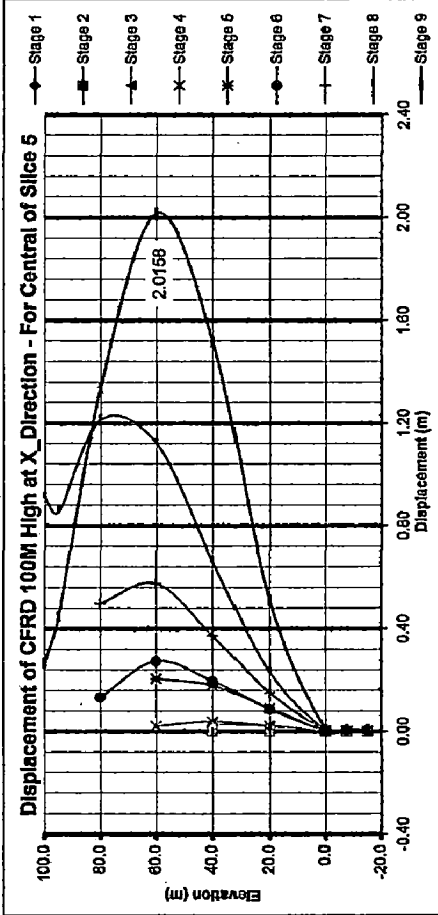
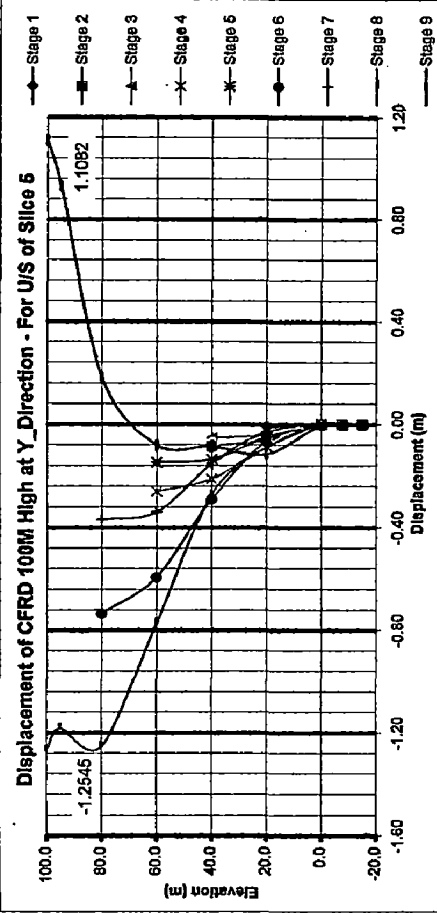
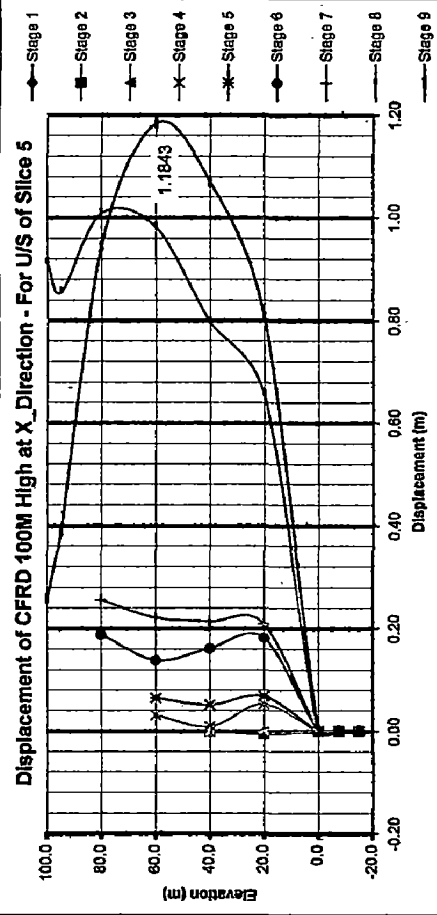
APPENDIX A :

Figure A.8 : Graphs Depict Displacement of CFRD 100 m with Slope 1V:1.40H



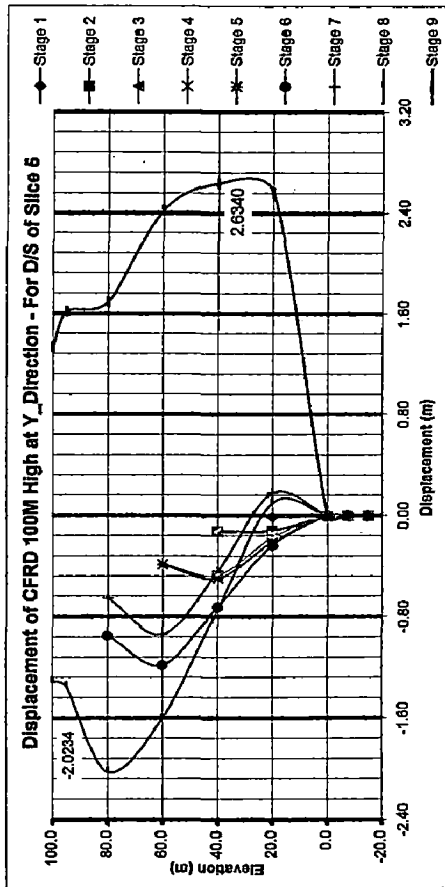
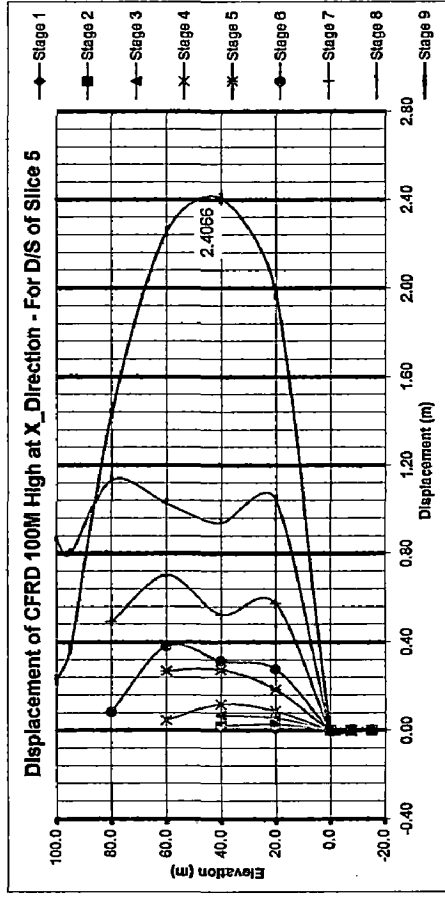
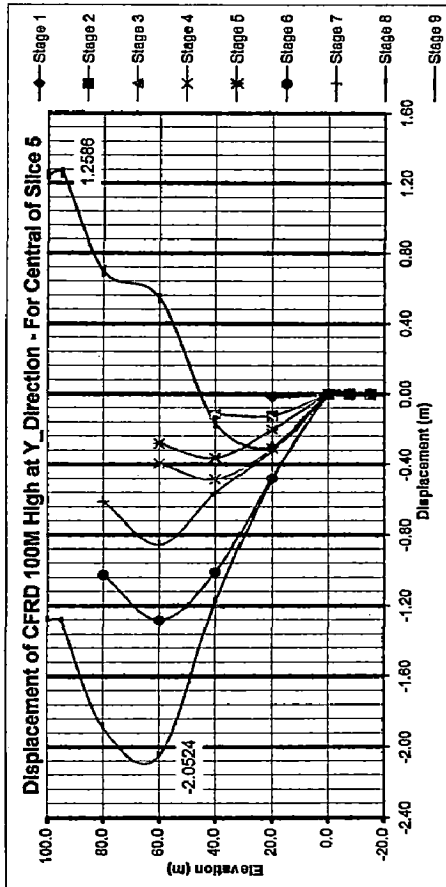
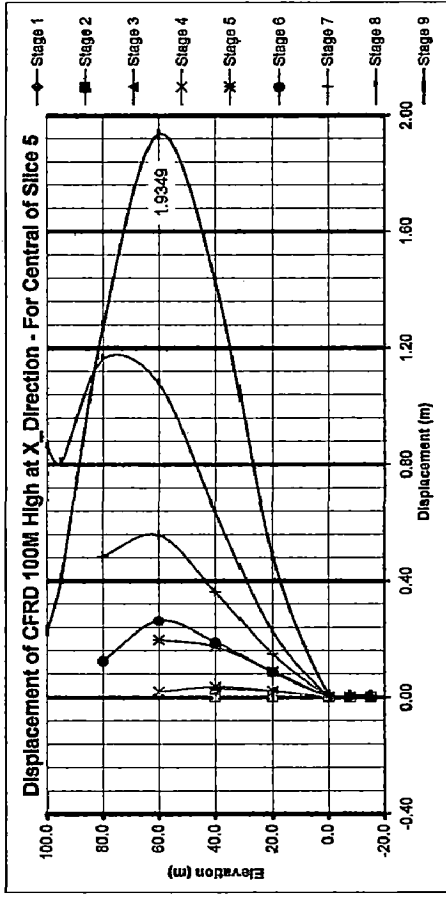
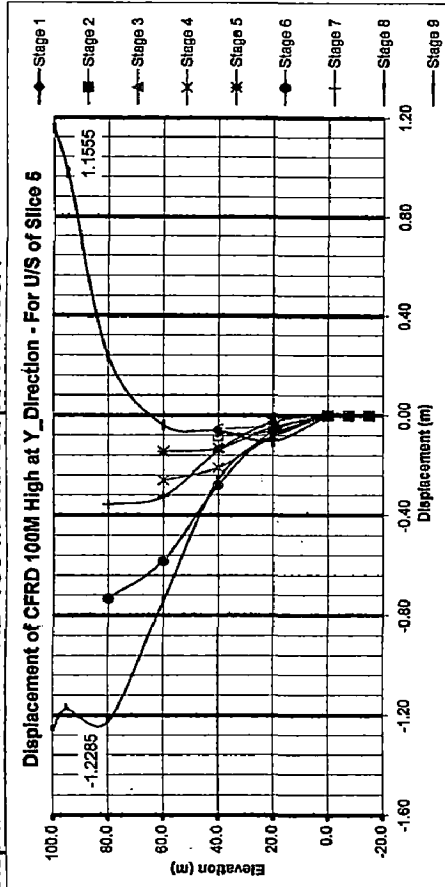
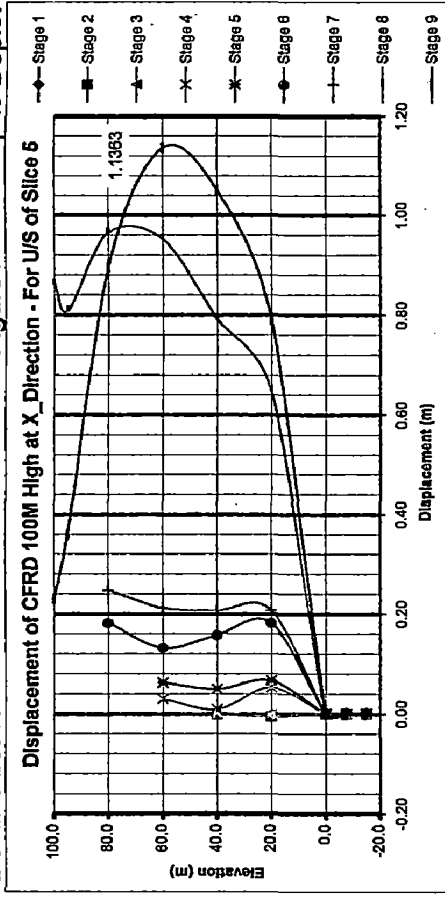
APPENDIX A :

Figure A.9 : Graphs Depict Displacement of CFRD 100 m with Slope 1V:1.45H

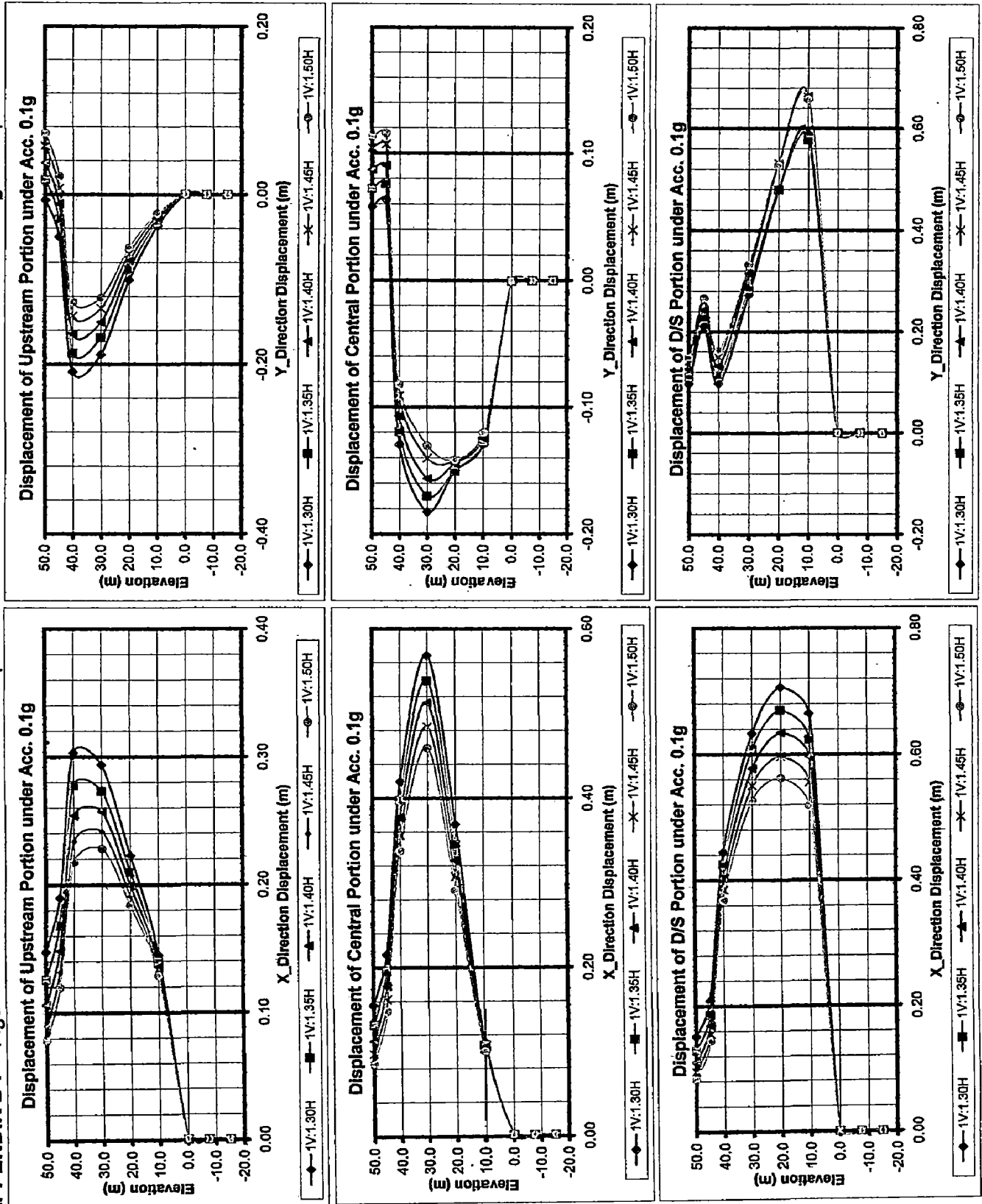


APPENDIX A :

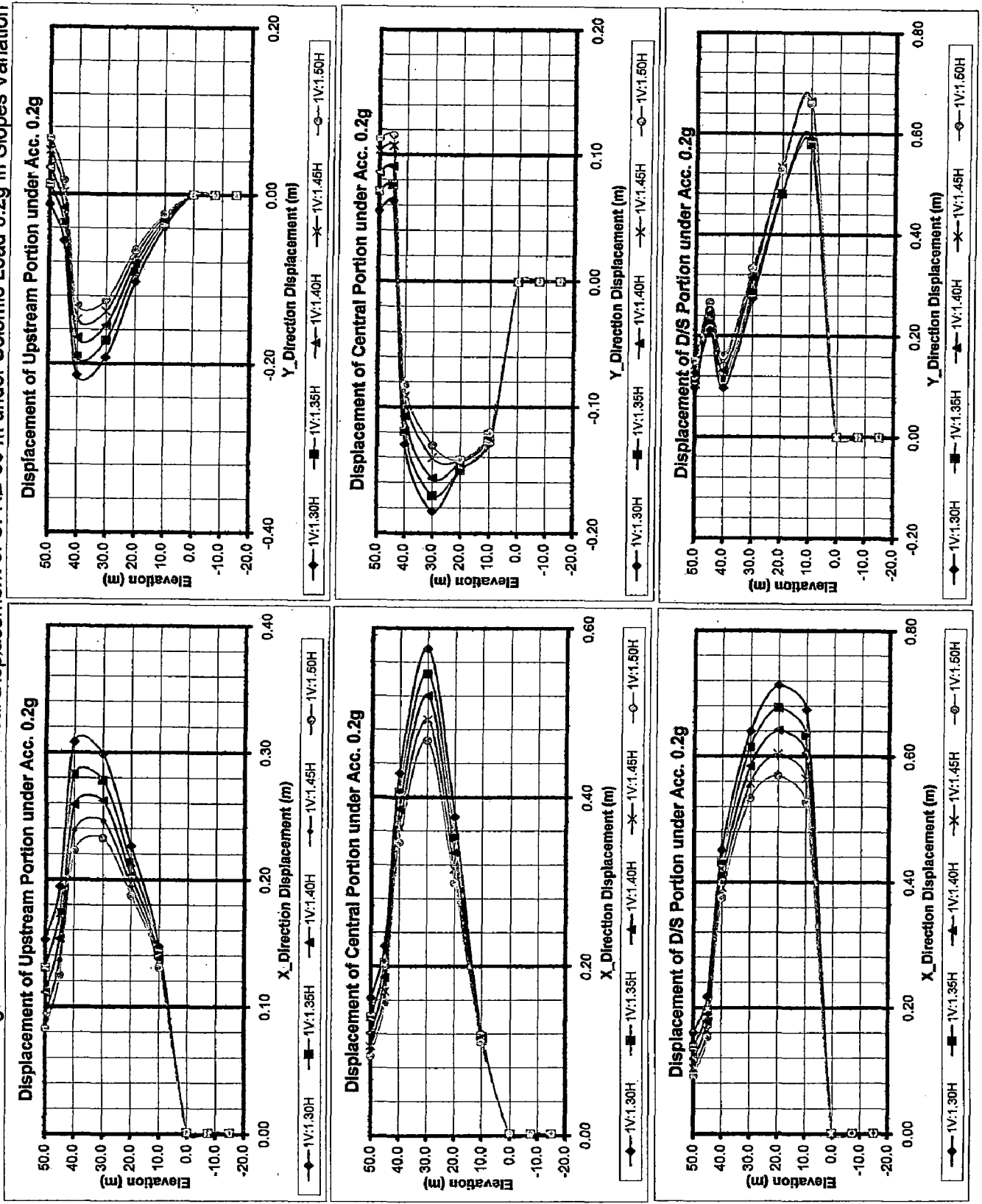
Figure A.10 : Graphs Depict Displacement of CFRD 100 m with Slope 1V:1.50H



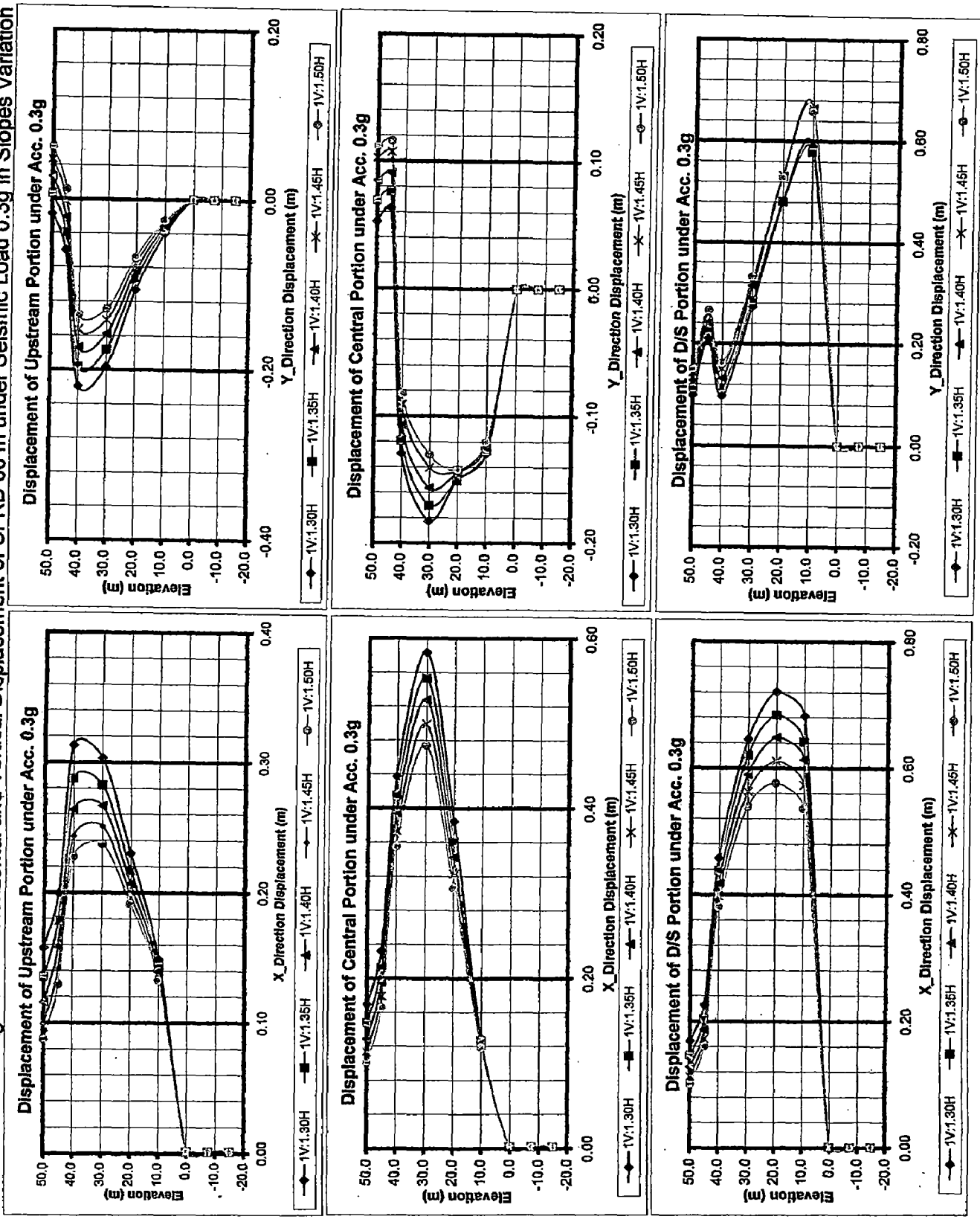
APPENDIX B : Figure B. 1 : Horizontal and Vertical Displacement of CFRD 50 m under Seismic Load 0.1g in Slopes Variation



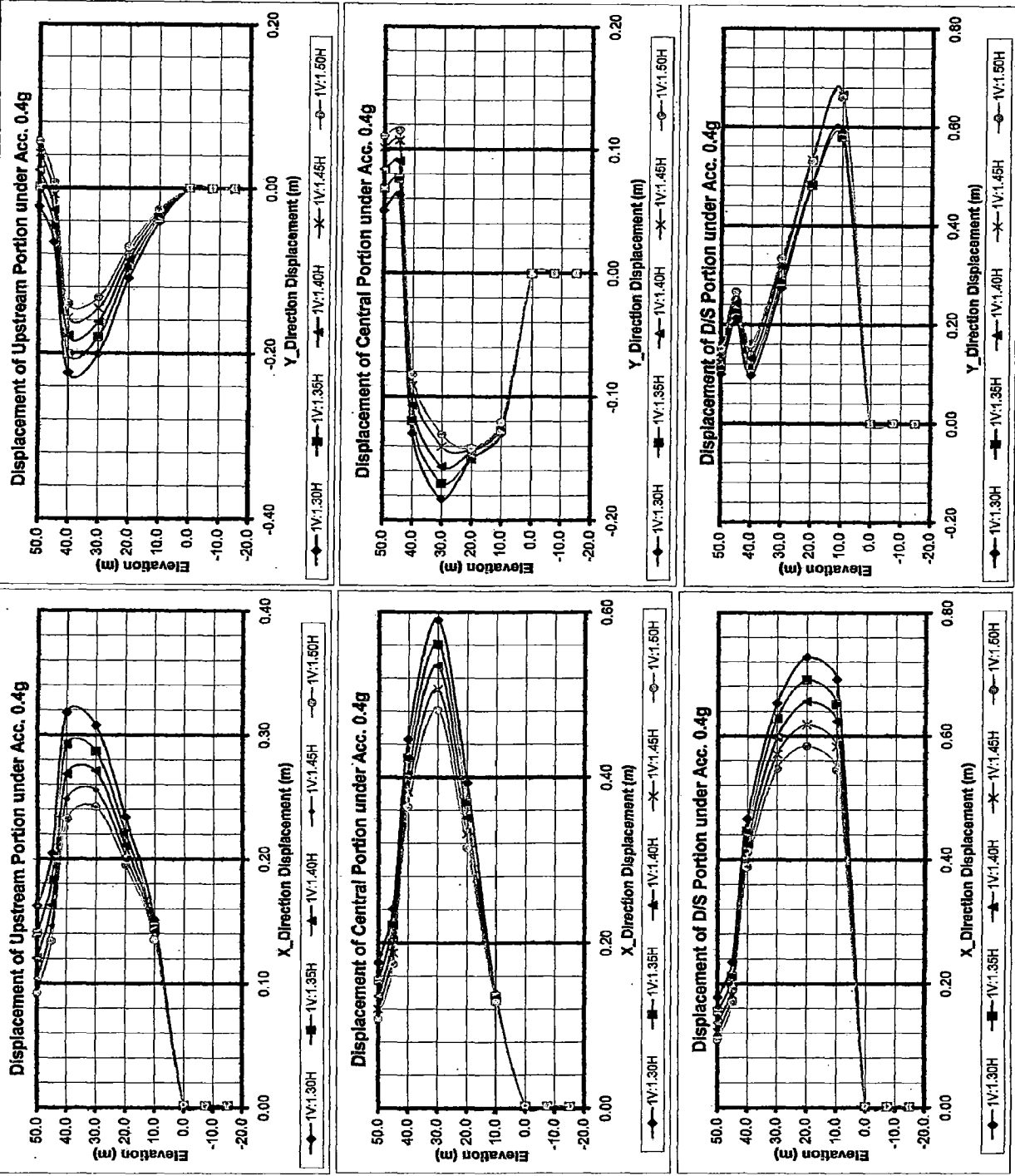
APPENDIX B : Figure B. 2 : Horizontal and Vertical Displacement of CFRD 50 m under Seismic Load 0.2g in Slopes Variation



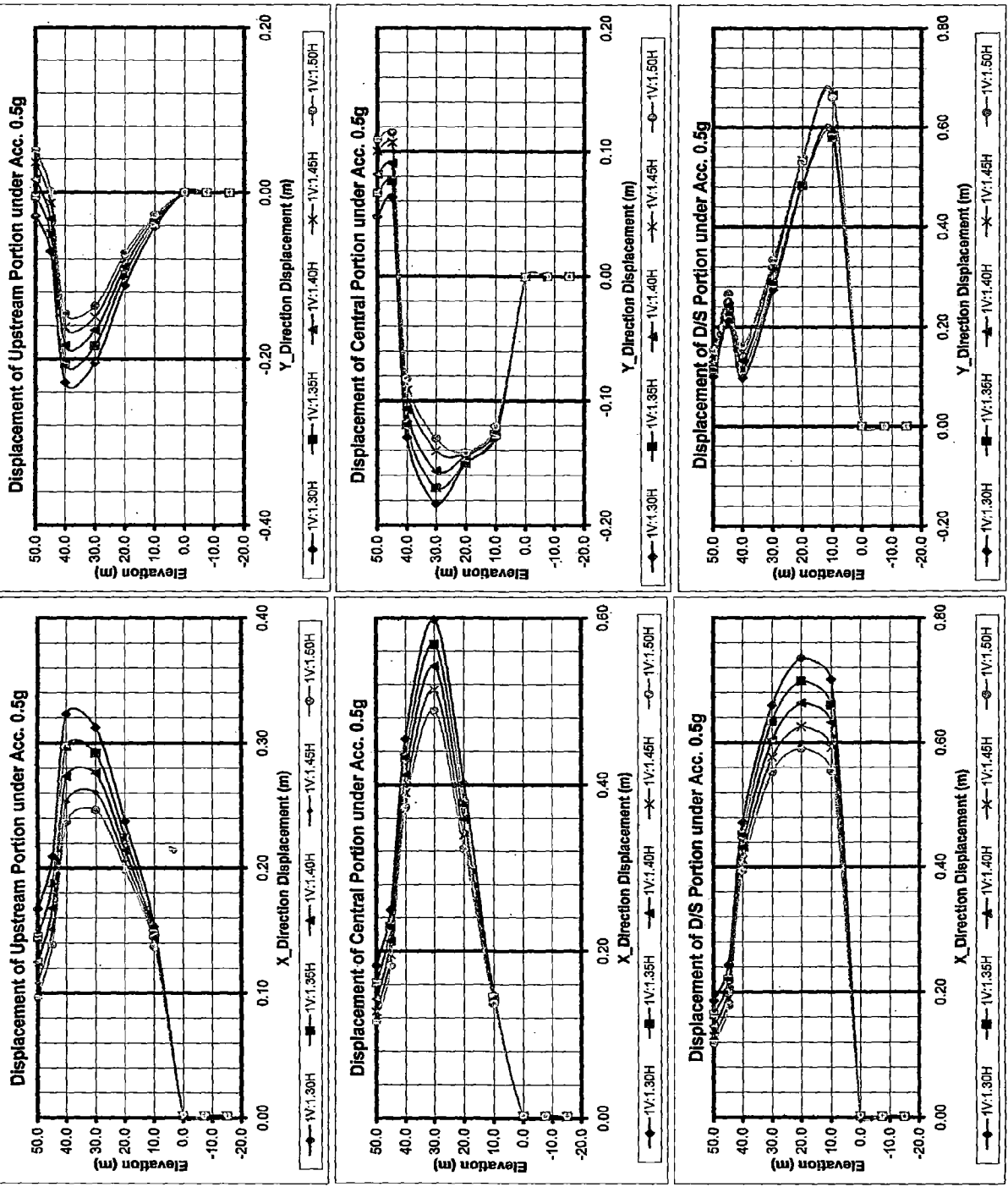
APPENDIX B : Figure B. 3 : Horizontal and Vertical Displacement of CFRD 50 m under Seismic Load 0.3g in Slopes Variation



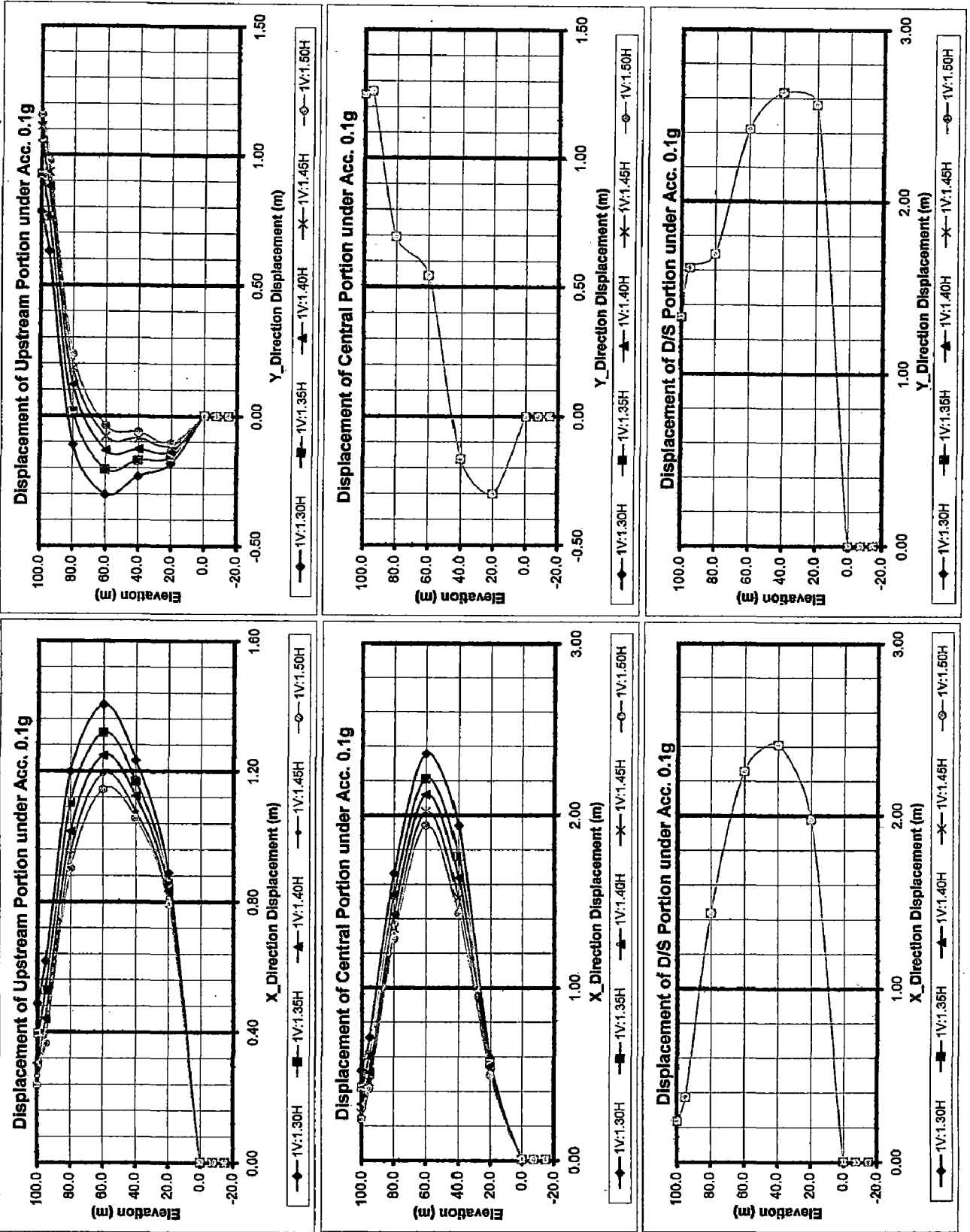
APPENDIX B: Figure B. 4: Horizontal and Vertical Displacement of CFRD 50 m under Seismic Load 0.4g in Slopes Variation



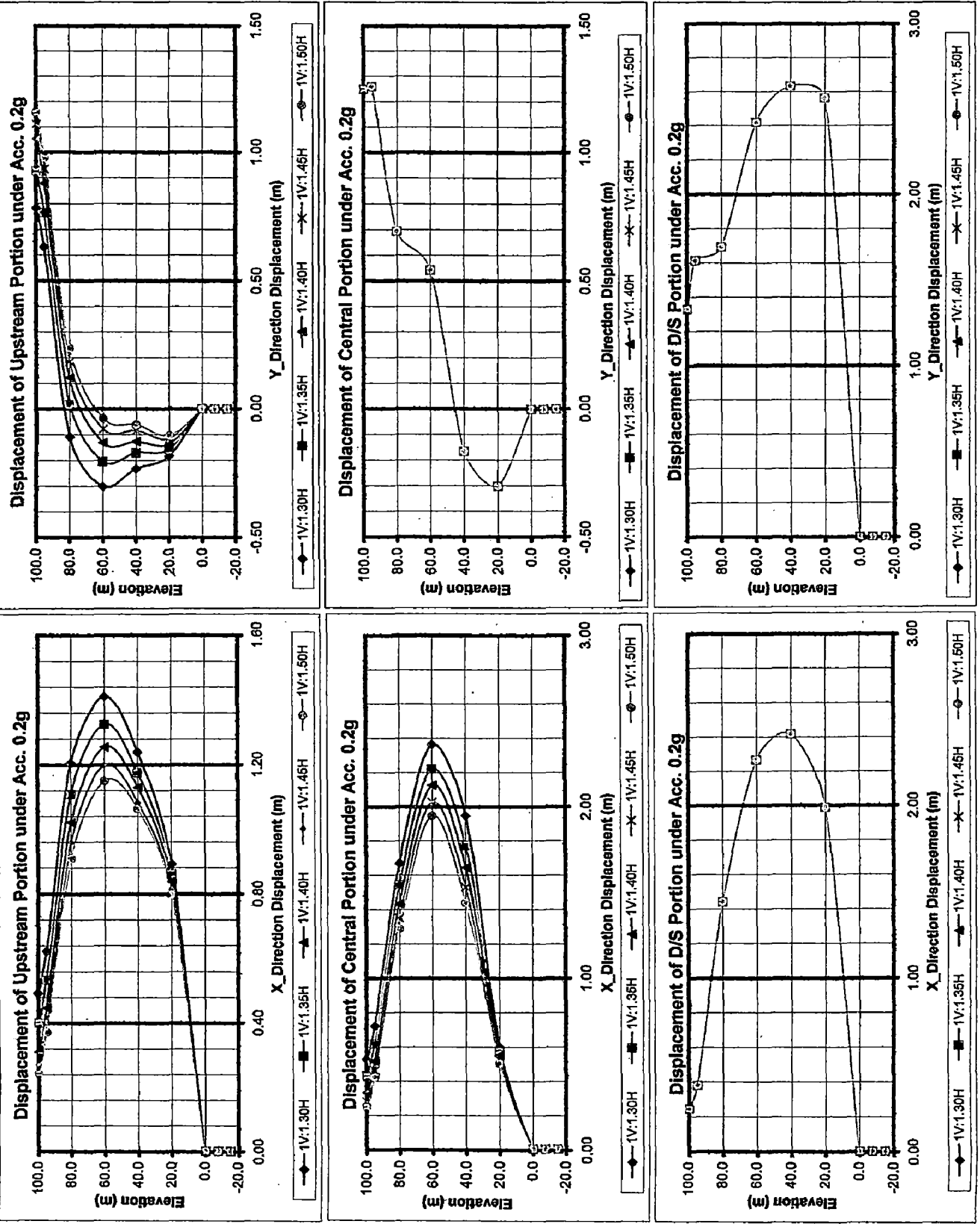
APPENDIX B : Figure B. 5 : Horizontal and Vertical Displacement of CFRD 50 m under Seismic Load 0.5g in Slopes Variation



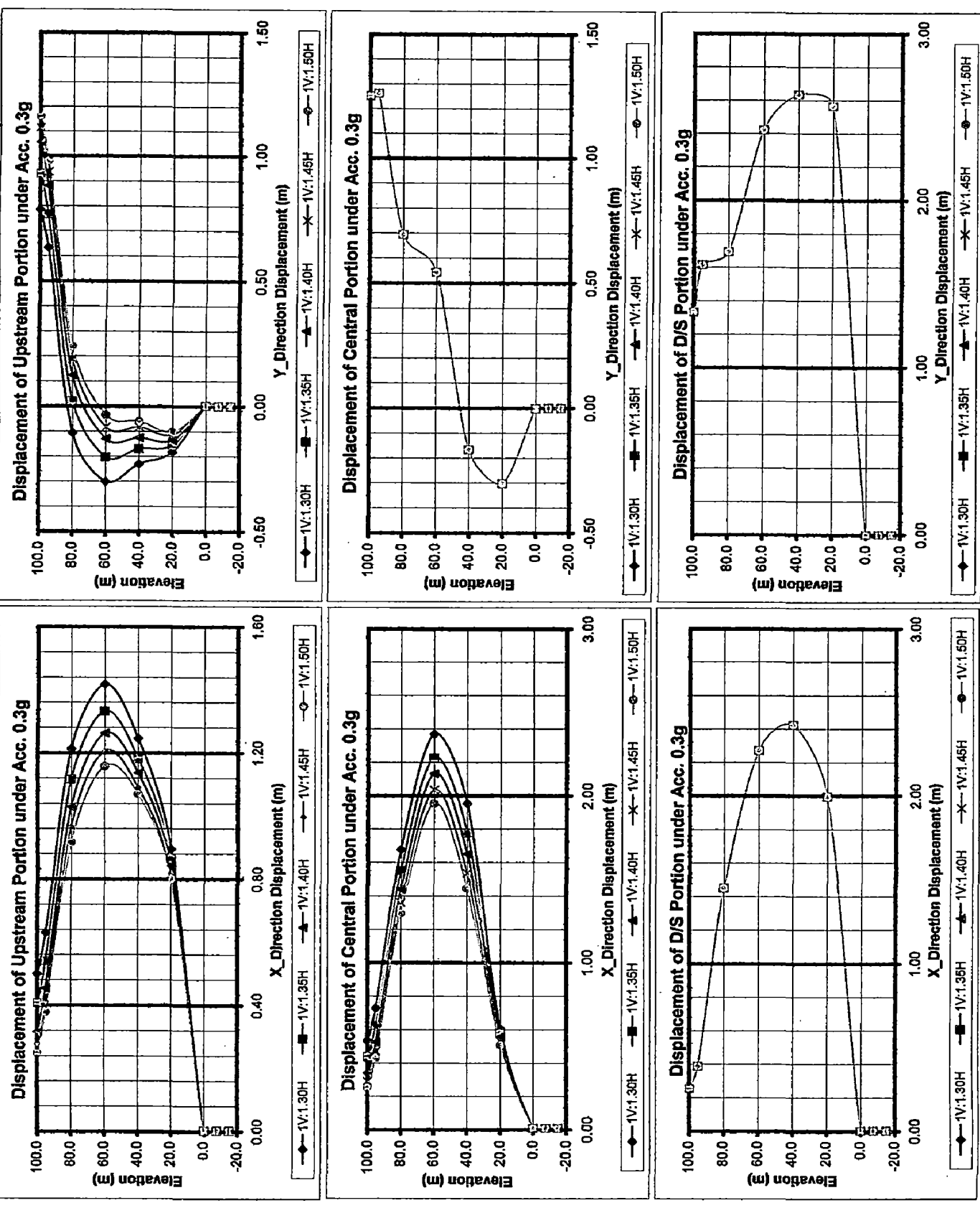
APPENDIX B : Figure B. 6 : Horizontal and Vertical Displacement of CFRD 100 m under Seismic Load 0.1g in Slopes Variation



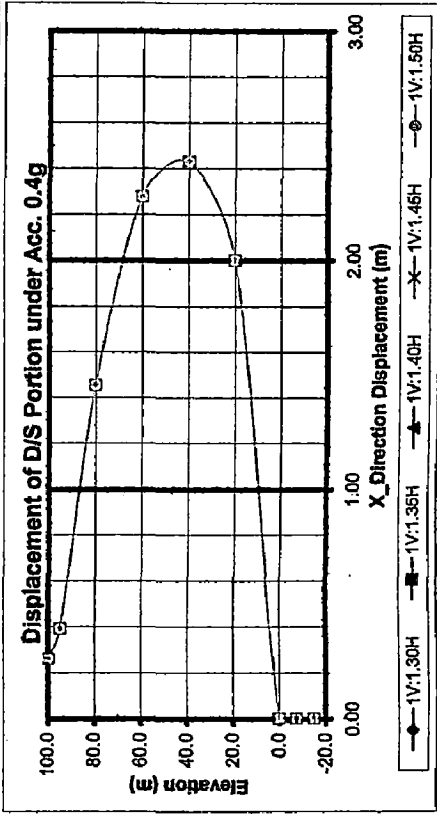
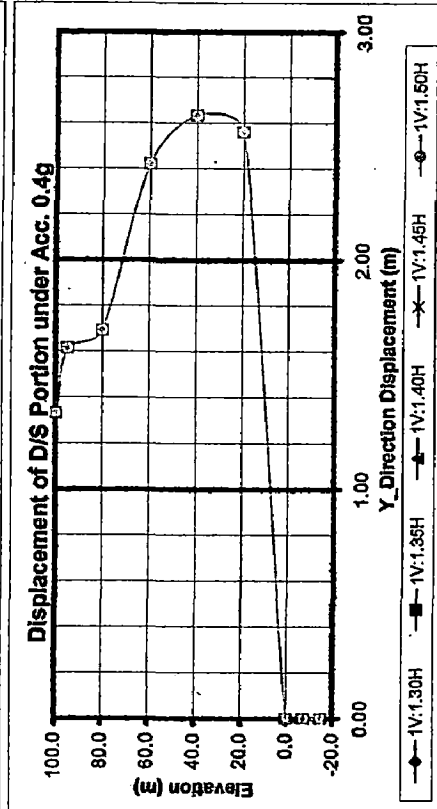
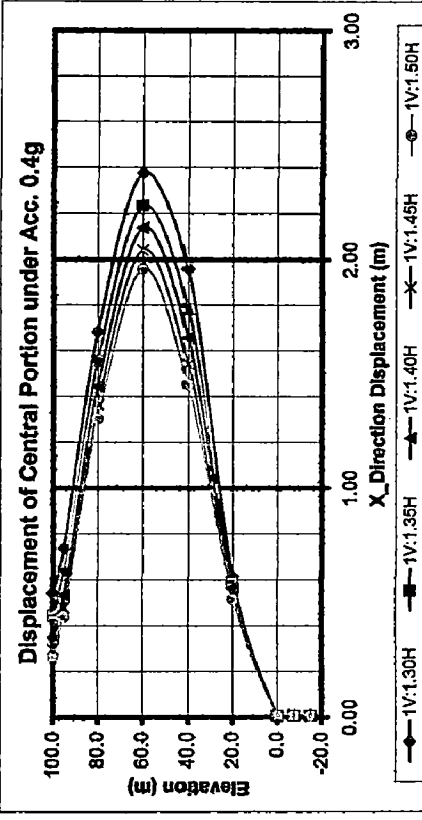
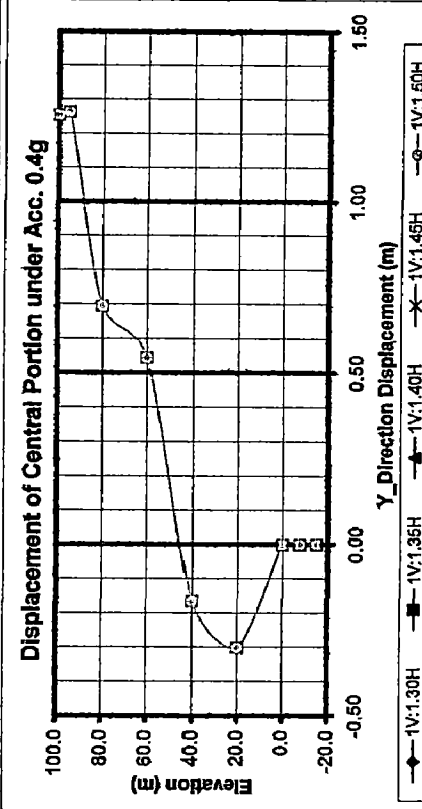
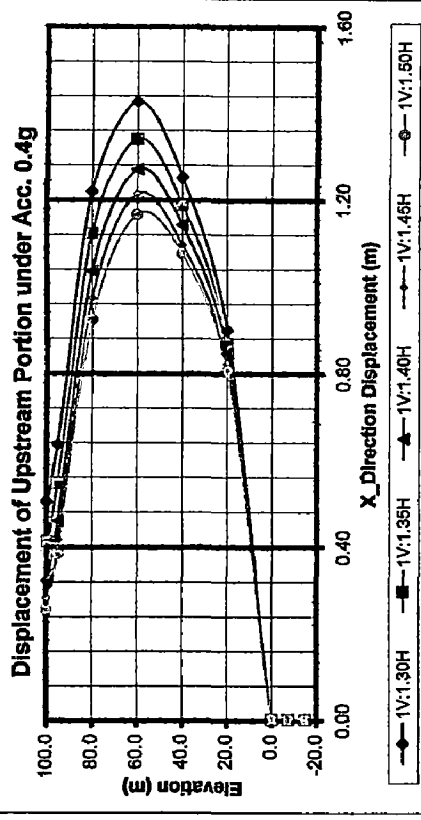
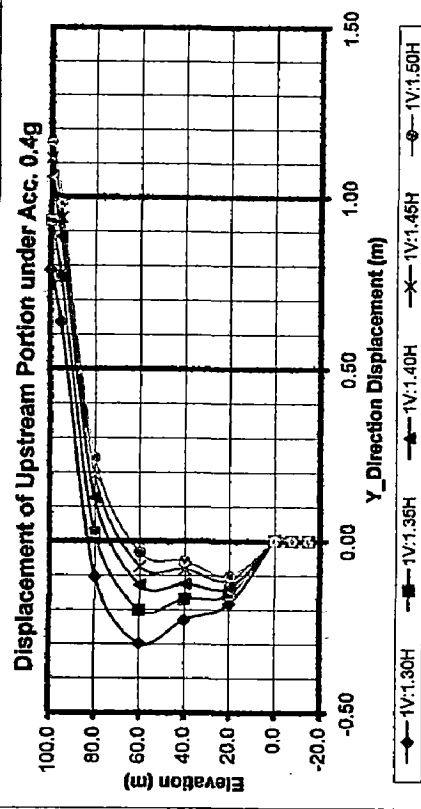
APPENDIX B : Figure B. 7 : Horizontal and Vertical Displacement of CFRD 100 m under Seismic Load 0.2g in Slopes Variation



APPENDIX B : Figure B. 8 : Horizontal and Vertical Displacement of CFRD 100 m under Seismic Load 0.3g in Slopes Variation



APPENDIX B : Figure B. 9 : Horizontal and Vertical Displacement of CFRD 100 m under Seismic Load 0.4g in Slopes Variation



APPENDIX B : Figure B. 10 : Horizontal and Vertical Displacement of CFRD 100 m under Seismic Load 0.5g in Slopes Variation

